Quantitative Ultrasound Image Analysis of the Gastrocnemius Muscle for Injury Evaluation

Thesis submitted to Cardiff University for the degree of
Doctor of Philosophy

Mahdi Alqahtani

Cardiff University

Ph.D. Thesis

2010

UMI Number: U518501

Dissertation Publishing

Declaration / Statements

Declaration

This work has not previously been accepted in substance for any degree and is not concurrently submitted in candidature for any degree.

Signed .... Date ...\15 / \11 / 2010

Statement 1

This thesis is being submitted in partial fulfilment of the requirements for the degree of PhD.

Signed .... Date ...\15 / \11 / 2010
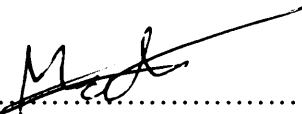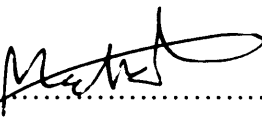
Statement 2
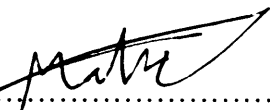
This thesis is the result of my own independent work/investigation, except where otherwise stated. Other sources are acknowledged by explicit references.

Signed .... Date ...\15 / \11 / 2010

Statement 3

I hereby give consent for my thesis, if accepted, to be available for photocopying and for inter-library loan, and for the title and summary to be made available to outside organisations.

Signed .... Date ...\15 / 11 / 2010

Abstract

Rupture of the gastrocnemius muscle is a common injury of the calf muscles. There are a number of studies describing different treatment techniques, however, only a few clinical trials have been published testing the effectiveness of these treatments. The aim of this study is to develop a non-invasive method based on quantitative ultrasound image analysis for the evaluation of muscle injury. The method needs to be sufficiently sensitive to detect possible changes in the muscle in order to monitor muscle injury repair and assist in gauging efficacy of treatment modalities. The gastrocnemius muscle was used to develop the method as this muscle constitutes a typical site for muscle injury. A three dimensional ultrasound sweep was performed on the gastrocnemius muscle of 25 healthy subjects and 5 patients with injured muscle using a 3D linear array transducer. Four slices were extracted from the 3D data set from the middle part of the muscle at different sites. Texture parameters include gray level, variance, skewness, kurtosis, co-occurrence matrix; run length matrix, gradient, autoregressive (AR) model and wavelet transform were extracted from the images. The coefficient of variation (CV) and intra-class correlation coefficient (ICC) were calculated for each texture parameter and used to test repeatability and reproducibility. The effect of varying the gain and the dynamic range setting on the texture features were also investigated. Four texture parameters were then used to obtain a reference set for normal gastrocnemius muscle. The four parameters were tested to ensure that there was no effect from the varying depth or size of ROI. These parameters were then tested against abnormal muscle. The texture parameters AR model and gradient were found to be the most sensitive parameters for differentiating healthy muscle from injured muscle and may be used as a tool to monitor the healing process.

Acknowledgements

First of all, I would like to express my appreciation to my supervisor Professor Len Nokes for his guidance and continuous support during my research.

I am deeply grateful to Dr Neil Pugh for his detailed and constructive comments, and for his support throughout this work.

I wish also to express my warm and sincere thanks to Dr Declan Coleman for his invaluable assistance and support during the course of this PhD.

Thanks to all my family and friends who all contributed to my thesis through the support and assistance.

Mahdi Alqahtani

Contents

Chapter 1: Introduction

Chapter 2: Literature review

Chapter 3: Data acquisition and Image analysis

Chapter 4: Influence of Depth and Size of Region of Interest (ROI) on Texture Features

Chapter 5: Influence of Ultrasound Settings on Texture Features

Chapter 6: Repeatability and Reproducibility

Chapter 7: Reference set of normal gastrocnemius muscle

List of Figures

Chapter 4

X

Chapter 5

XIV

List of Tables

Abbreviations

3D	Three-Dimensional
ANOVA	Analysis of Variance
AR	Auto-regressive
CV	Coefficient of variation
CT	Computerised tomography
DOMS	Delayed onset muscle soreness
ICC	Intra- Class Correlation
MRI	Magnetic resonance imaging
RF	Radio frequency
ROI	Region of interest
TGC	Time gain compensation
US	Ultrasound

Chapter 1 Introduction

1.1 Introduction

Muscle and soft tissue injuries account for approximately half the injuries that occur during sports related activities (Shellock et al 1994). They are most prevalent in individuals who participate in contact sports such as rugby and football. The most common muscular injuries are present within the lower extremities; these include the hamstring, the quadriceps and calf (gastrocnemius) muscle groups (Blankenbaker and De Smith 2004, Orchard 2002, Orchard 2001). The rupture of the medial gastrocnemius muscle has been demonstrated as a routine traumatic injury of the calf (Kwak et al. 2006a, Kwak et al. 2006b, Bianchi et al. 1998). It is generally associated with the presence of fluid collection called haematoma, and is diagnosed through the observation of abnormal echogenicity in sonographic images. Rupture of the gastrocnemius muscle typically occurs when there is forceful plantar flexion of the foot with simultaneous extension of the knee (forceful push-off with the foot), which produces active contraction and passive stretching of the gastrocnemius muscle (Miller 1977). Clinical examination of the muscle reveals a diffuse palpable mass, acute pain and localized soreness in the middle portion of the calf, and the patient is unable to walk without feeling pain (Mcclure 1984, Liu and Chen 1989, Flecca et al. 2007).

Following a literature review, Smith et al (2006) concluded that, although a large amount of literature is available describing treatments for muscle injuries, only few trials assessing the effectiveness of treatments have been published. Furthermore, this limited evidence base is plagued with numerous methodological weaknesses, making it very difficult to arrive at a conclusion as to which physiotherapy treatment modality is most

efficient for the treatment of muscle haematomas. On closer examination of the literature, one major shortcoming evident is the lack of an accurate and objective method to monitor the healing process of muscle injury. This in turn results in the inadequate measurement of outcomes to determine the most effective management regime. Therefore, there is significant motivation and need to develop an objective measurement method to monitor recovery to specific physiotherapy treatments. The possibility of being able to quantify muscle injury and monitor recovery objectively will certainly help decide which treatment protocols are most effective.

The aim of this study, taking into account the literature published on this issue, is to develop a non-invasive method based on quantitative image analysis for the evaluation of muscle quality. This method should be sufficiently sensitive to detect possible changes in muscle injury in order to monitor repair and to assist in testing the effectiveness of therapeutic modalities. In the calf muscles, specifically the gastrocnemius muscle constitute a typical site for muscle injury with regards to sport and other activities (Kwak et al. 2006a, Kwak et al. 2006b, Bianchi et al. 1998).Therefore, this muscle was used to develop the aforementioned method of muscle analysis.

1.2 General Objectives

Ultrasonography has been widely applied in the imaging of muscle, due to its cost effectiveness and the lack of risk associated with ionising radiation (Wong 2005). Medical applications of the texture analysis of tissues provide a quantitative means of analyzing and characterizing properties of tissues (Harrison et al. 2008). In clinical radiology, texture analysis of medical images provides more information on tissues than the human eye (Harrison et al. 2008). Ultrasonic evaluation of human muscle has been

performed in numerous studies and in many anatomical regions including the quadriceps muscle group, arm, low back, and facial muscles (Kiliaridis et al. 1995, Eisele et al. 1998, Scholten et al. 2003). A majority of studies have used a subjective evaluation method in terms of visual inspection of the images or measurement of muscle thickness. However, few studies have used quantitative ultrasound analysis to characterize the various components of the muscle tissue (Nielsen et al. 2000, Nielsen et al. 2006, Schedel et al. 1992, Eisele et al. 1998, Sipila and Suominen. 1996, Hicks et al. 1984).

Currently, the healing process of muscle injury is largely assessed by the subjective evaluation of changes of echogenicity in repeated sonographic images. To make an interpretation of the images more accurate and reproducible there is a requirement to develop an objective method to quantify changes in echogenicity that develop over time. There are no studies describing methods that quantify and diagnose the amount of muscle damage and reports that predict an accurate prognosis for recovery.

Following the analysis of the aforementioned literature, it may be hypothesised that the application of texture analysis techniques can provide information from ultrasound images, which can aid in the detection of subtle changes in the muscle, during early stages of injury and in turn monitor the healing process.

In order to fulfil this hypothesis, the general objectives are as follows:

(1) To characterize and quantify muscle tissue texture.

(2) To develop and validate a method based on quantitative ultrasound image analysis.

(3) To objectively analyse and characterize ultrasound images of the gastrocnemius muscle.

(4) To develop and apply tissue characterization techniques in evaluating ultrasound images, to measure the amount of muscle damage and ultimately make a better prediction of recovery.

(5) To use image texture analysis to detect small degrees of muscle damage that cannot be detected with subjective evaluation.

The post-processing of ultrasound images to provide objective tissue characterization to quantify the amount of damage to muscle was attempted within this research thesis. These techniques could be utilised to monitor the rate of the healing process over time assisting in testing the effectiveness of different therapeutic modalities enabling us to make a decision on the best treatment.

1.3 Specific objectives

In order to fulfil the broadly based aims as depicted above, objectives that are more specific are as follows:

(1) To investigate the suitability of a computer assisted echo texture analysis for analysing ultrasound images.

(2) To evaluate the accuracy of the texture analysis technique of the ultrasound image in diagnosis of muscle injuries.

(3) To investigate the influence of depth on textural features.

(4) To investigate the influence of size of region of interest (ROI) on textural features.

(5) To evaluate the effects of the settings of the ultrasonic scanner on the textural features.

(6) To test the repeatability and reproducibility of the scanning method.

(7) To compare texture features between right and left leg.

(8) To compare texture features between gastrocnemius muscle (leg) and biceps brachii muscle (arm).

(9) To investigate the texture analysis technique in monitoring the healing process of soft tissue injuries over time.

1.4 Thesis Structure

In order to demonstrate the importance and significance of the research carried out, this thesis has been structured in the following manner as shown in figure (1.1):

Chapter 1: Introduction, including general and specific objectives of the thesis and the thesis structure.

Chapter 2: Literature review, including muscle anatomy, muscle injury classifications, diagnosis of muscle injury, texture analysis techniques and their applications on medical images.

Chapter 3: Describes the general methodology of the research, data acquisition, and image analysis demonstrating the standard protocol in scanning the subjects and extracting texture features from images.

Chapter 4: Investigating the influence of depth and size of ROI on texture features and comparing between scanning sites along length of the gastrocnemius muscle.

Chapter 5: Investigating the influence of the ultrasound machine setting on texture features.

Chapter 6: Testing the repeatability and reproducibility of the scanning method. Testing short term and long-term repeatability (intra-operator) and reproducibility (inter-operator).

Chapter 7: Obtaining the reference set of normal muscle relying on specific texture parameters, comparing the right leg muscle to left leg, comparing gastrocnemius muscle to the biceps muscle and comparing healthy to injured muscles.

Chapter 8: General discussions, conclusions, and implications for future research.

```
Chapter 1  ────────▶  ┌─────────────────────────────┐
                      │         Introduction         │
                      └─────────────────────────────┘
                                    │
                                    ▼
Chapter 2  ────────▶  ┌─────────────────────────────┐
                      │       Literature review      │
                      └─────────────────────────────┘
                                    │
                                    ▼
Chapter 3  ────────▶  ┌─────────────────────────────┐
                      │   Data acquisition and Image │
                      │            analysis          │
                      └─────────────────────────────┘
                                    │
                                    ▼
Chapter 4  ────────▶  ┌─────────────────────────────┐
                      │     Influence of depth and   │
                      │    size of region of interest│
                      └─────────────────────────────┘
                                    │
                                    ▼
Chapter 5  ────────▶  ┌─────────────────────────────┐
                      │  Influence of ultrasound setting│
                      │       on texture features    │
                      └─────────────────────────────┘
                                    │
                                    ▼
Chapter 6  ────────▶  ┌─────────────────────────────┐
                      │      Repeatability and       │
                      │       Reproducibility        │
                      └─────────────────────────────┘
                                    │
                                    ▼
                      ┌─────────────────────────────┐
                      │    Reference set of normal   │
                      │    gastrocnemius muscle      │
                      └─────────────────────────────┘

Chapter 7  ◀───▶  ┌──────────────┐      ┌──────────────┐
                  │   Abnormal   │◀────▶│ Normal biceps│
                  │ gastrocnemius│      │              │
                  └──────────────┘      └──────────────┘
                                    │
                                    ▼
                      ┌─────────────────────────────┐
                      │  Monitoring the healing process│
                      │      of muscle iniurv        │
                      └─────────────────────────────┘
                                    │
                                    ▼
Chapter 8  ────────▶  ┌─────────────────────────────┐
                      │   General discussion and     │
                      │          conclusion          │
                      └─────────────────────────────┘
```

Figure 1.1 Showing the thesis structure

7

Chapter 2 Literature Review

2.1 Introduction

Fitness and athletic activities form a major part of the lives of people in the developed world. The obsessive focus on a healthy and fit lifestyle has found its way into top columns in most newspapers and magazines, on a regular basis. This current interest in sporting and related activities predisposes its participants to injuries. Statistical estimates suggest that several hundred million individuals involve themselves in regular exercise and structured sporting activities (Lieber and Friden 1999). This focus on fitness and health has led to a significant increase in the number of activity-related injuries. It is estimated that over 20 million American people per year have activity or sport related injuries that limit their activity in the workplace (Lieber and Friden 1999). Moreover, fitness and athletic activities in the context of rehabilitation is also increasing, both in the athletic and elderly population to speed up recovery after injury or hospitalization. However, in these cases, treatments to aid rapid recovery and restore muscle functions are the goal. In some sports, the risk of injury is high, because increased speeds and forces are encountered. It has been demonstrated that various levels of athletes, increased participation, intensity, demands and longer training hours increase the risk of injuries (Dreinhofer et al. 2007).

Furthermore, data from the European Union Injury Database illustrate that sport injuries accounted for about 20% of all accidents in 2002-2004. In Germany alone, two million sports injuries required medical attention and cost 4 billion Euros annually (Dreinhofer et al. 2007). Muscle injuries arising from sporting activities are more commonly observed with reference to rugby and football. Therefore, effective treatments are necessary to help

the recovery of these injuries and more importantly, to assess efficacy of treatments there is a pressing need for an objective and sensitive outcome measure.

2.2 Muscle structure and function

Muscles are designed to cater to the body's mobility requirements through providing joint movement and stability (El-Khoury et al. 1996). Muscles forces are similar to all other forces that are applied to the levers of the body to produce mobility and translatory components. Muscles take their origin from bones, dense connective tissue, or tendons; in turn, the two types of materials found in skeletal muscle are muscle tissue and connective tissue. In the human body the majority of muscles cross one joint, but many muscles cross two joints (Blankenbaker and De Smith 2004). The muscles that cross one joint are deep muscles and are concerned with stability, posture, and tone. They produce slow speeds of contraction but great strength. Usually, the muscles that cross more than one joint show an increased vulnerability to strain (Best and Garrett 1994, Blankenbaker and De Smith 2004). The muscles that cross two joints have greater adaptability for length change illustrating higher speeds of contraction; however, they produce reduced power throughout the range of movement (Best and Garrett 1994).

Muscle tissue demonstrates the properties of contractility and irritability. Skeletal muscle is composed of many thousands of muscle fibres and a single muscle fibre contains many fasciculi, which is a group of muscle fibres surrounded by layer of fibrous connective tissue. The smallest contractile unit of a muscle fibre is called a sarcomere. The individual muscle fibres are surrounded by connective tissue called the endomysium, and groups of muscle fibres are covered by connective tissue called the perimysium. The endomysium and the perimysium are continuous with the outer connective tissue sheath

called the epimysium, which envelopes the entire muscle (Holsbeeck and Introcaso 2001, Fornage 1995, Peetrons 2002).
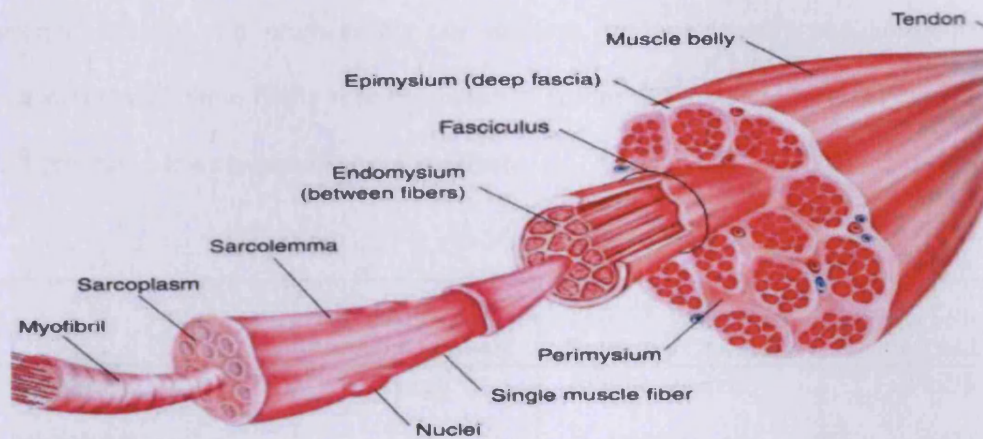
Figure 2.1 A schematic cross sectional view of the connective tissue in a muscle shows how the perimysium is continuous with the outer layer of epimysium. (http://www.biologycorner.com/anatomy/muscles/notes_muscles.html)

Fascicule, are muscle fibre groups, and similarly to the length of muscle fibres, they vary among the entire muscle. The fasciculi may be parallel, spiral or at an angle to the long axis. Muscles that show a fibre arrangement oblique to the muscle's long axis are termed unipennate, bipennate or multipennate with a central aponeurosis (Holsbeeck and Introcaso 2001). In a bipennate muscle such as the gastrocnemius, the fasciculi are obliquely set on both sides of a central tendon. Numerous studies suggesting that a decreased force at the tendons in pennate muscles is present (Maganaris et al. 1998, Kawakami et al. 1998). However, this loss is compensated through the pennate muscles, which typically have a large number of muscle fibres due to increased packing, thus increasing the cross sectional area. Therefore, despite the loss of force due to pennation, a pennated muscle, such as the gastrocnemius, is able to transmit a large amount of force to the tendon to which it is attached.

There are three principal versions of muscle fibres: Type I, Type II, and Type IIb. These

fibres can be differentiated from each other histochemically, metabolically,

morphologically and mechanically. In addition, different names and nomenclatures

associated with these fibres have been utilised within different texts and literature, Table

2.1 presents a few characteristics of the fibres.

	TypeIIb –Fast twitch Glycolytic	Type II- Fast-twitch Oxidative Glycolytic	Type I-Slow-twitch Oxidative
Diameter	Large	Intermediate	Small
Myoglobin content	Low	Intermediate	High
Speed of Contraction	Fast	Fast	Slow
Rate of fatigue	Fast	Intermediate	Slow
Muscle colour	White	Red	Red

Table 2.1 Characteristics of Skeletal Muscle Fibres –Adapted from (Staron 1997).

The Type II muscle fibres are demonstrated mainly within muscles that cross two joints,

they are best suited to activities that require a short energy burst (El-Khoury et al. 1996,

Steinbach et al. 1997). In turn, the muscles with a higher proportion of Type II fibres are

more susceptible to injury (Garrett 1996).

2.3 Muscle injuries

The most frequent injuries in the context of sport are muscle injuries, which account for approximately 10-55% of all sustained injuries (Jarvinen et al. 2005, Beiner and Jokl 2001). The muscles commonly involved are the rectus femoris, biceps femoris, semitendinosis, hip adductors and medial head of the gastrocnemius (El-Khoury et al. 1996, Steinbach et al. 1997, Garrett 1996, Ehman and Berquist 1986, De Smet and Best 2000, Nguyen et al. 2000, Varela et al. 2000). Muscle strain injury is not only the result of contraction, but may also be the consequence of stretch on a muscle while the muscle is in contraction (Garrett 1996). Therefore, two joint muscles are more prone to injury as the stretch does not only occur through one joint, but an increased stretch occurs via two joints. Muscle injuries may be instigated through various factors such as contusions, strains or lacerations (Jarvinen et al. 2005, Beiner and Jokl 2001, Garrett 1996, Huard et al. 2002). It is estimated that over 90% of sports related injuries are strain or contusions whereas lacerations are particularly rare and uncommon (Jarvinen et al. 2005).

2.3.1 Mechanisms of Injury

Sports injuries can occur because of many factors, such as overuse, which may cause injury to tendons, ligaments and muscle. Injuries to soft tissue may be instigated through direct or indirect trauma. Direct trauma refers to an injury occurring from a blunt or a sudden force overload .The cumulative effects of repetitive forces can potentially lead to indirect trauma resulting from repeated sub maximal loading. This triggers an inflammatory reaction, which results in swelling. The stages of both types of injuries can be divided into acute, sub acute and chronic.

2.3.2 Classification of muscle injuries

The classification of muscle injuries are based on the mechanism of injury, which may be divided into direct or indirect trauma. Direct trauma injuries are further subdivided into contusion and laceration. Delayed onset muscle soreness and muscle strains are inclusive of indirect injuries (Wong 2005).

2.3.2.1 Delayed onset muscle soreness

Delayed onset muscle soreness (DOMS) is a particular type of muscle pain and stiffness; numerous people have experienced it at some point in their lives. With DOMS, the muscles involved in this condition can ache for several days following the onset of intense activity (Boutin et al. 2002). DOMS often typically presents with soreness and swelling after unaccustomed exertion such as the initiation or resuming of training in athletes after a period of rest (Boutin et al. 2002). The DOMS begins 1 to 2 days subsequent to exercise and reaches a peak 2 to 4 days following exercise and resolves with conservative management usually by 7 days. Sonographic images of muscle experiencing DOMS may appear normal or show hyperechogenicity (Wong. 2005).

2.3.2.2 Muscle strain

Muscular strains are the most common type of injury in athletes who engage in track, field sport and football (Nguyen et al. 2000). These forms of muscular damage are induced by forces that may potentially be passive, internal or external forces. The risk of strain injuries is greater where there have been previous muscular strain problems. Previous injury has been suggested to be a strong risk factor where addictive strains on previously injured muscles make them more prone to damage (Orchard 2002). Overuse

and overstretching may also be the causative factor for strain injuries, which present in the muscle typically with loss of function, stiffness and pain. These injuries can be clearly illustrated in the hamstrings, hip adductors and medial head of gastrocnemius (Steinbach et al. 1997). The muscle tissue suffers a partial or full thickness tear when it is directly overloaded or repetitive stress causes it to reach its breaking point (Nguyen et al. 2000, Deutsch and Mink 1989). The clinical method to differentiate partial from full thickness tears pose a challenge, as pain often limits a full physical examination of the injury (Blankenbaker and De smith 2004).

2.3.2.3 Haematoma and contusion

A Haematoma is created when injury to soft tissue occurs, resulting in the breakage of capillaries and leakage of blood. Following the damage to the soft tissues, the blood from the capillaries may trickle under the skin causing that particular area to swell and bruise (Fig.2.2).

a)   b)
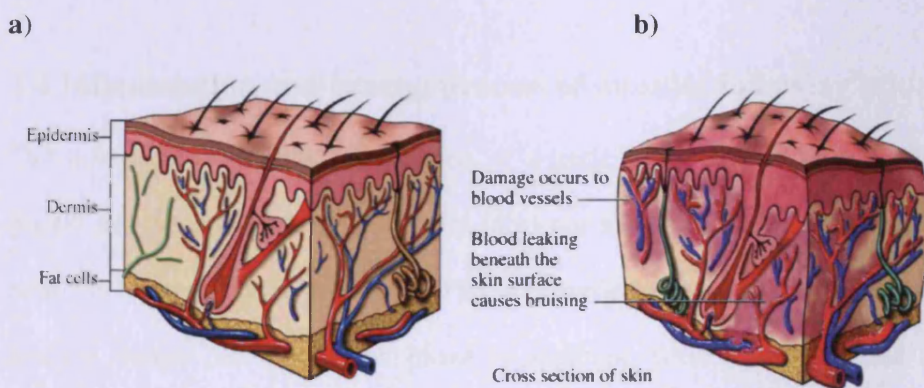
Figure 2.2 a) Normal tissue   b) Injured tissue-showing haematoma
(Adapted from **www.nucleusinc.com**)

Haematomas in muscle can result from different types of forces namely direct, blunt and compressive. In sport related injuries, this form of damage is largely common and usually

14

involves the quadriceps and gastrocnemius muscles (Kneeland 1997). Sportspeople who

participate in high speed and impact contact sports such as, rugby and football are highly

susceptible to muscle haematoma mainly within the lower limbs (Rothwell 1982).

The classification of haematomas are based on their location, they are classified as intra

or inter muscular. An intramuscular haematoma is the collection of blood within the

surrounding muscle sheath, which results in an increase in intramuscular pressure. The

symptoms include pain; swelling, which is more pronounced during the primary three

days and major loss of muscle function due to decreased extensibility and contractility

(Klein 1990). In the context of intermuscular haematoma, this results from the tearing of

muscle and an area of the surrounding sheath, therefore allowing the blood to spread

between the muscles and fascia. The symptoms with reference to this form of injury

include bruising and swelling which appear distal to the injured area, the other symptoms

are similar to the intramuscular haematoma (Klein 1990).

2.4 Inflammation and healing process of muscles following injury

The inflammation and healing process of muscle injury appear to follow a standard

pattern irrespective of the type of injury (direct or indirect) (Jarvinen et al. 2007). Hurme

et al. (1991) and Kalimo et al. (1997) have identified three phases with reference to this

process. Firstly, the destruction phase is apparent, whereby rupture and subsequent

necrosis of muscle fibres have been demonstrated. The formation of a haematoma

between the ruptured muscle fibres and the accompanying inflammatory reaction has also

been noticed. The second stage within this repair phase is where phagocytosis of the

necrosed tissue occurs. Following this there is a regeneration of the muscle fibres,

formation of scar tissue and growth of new capillaries into the injured area. Finally, in the remodelling phase, maturation of the regenerated fibres, reorganisation of the scar tissue and restoration of the function of the muscle occurs. The stages of injury, inflammation and healing are depicted in figure (2.3) below.
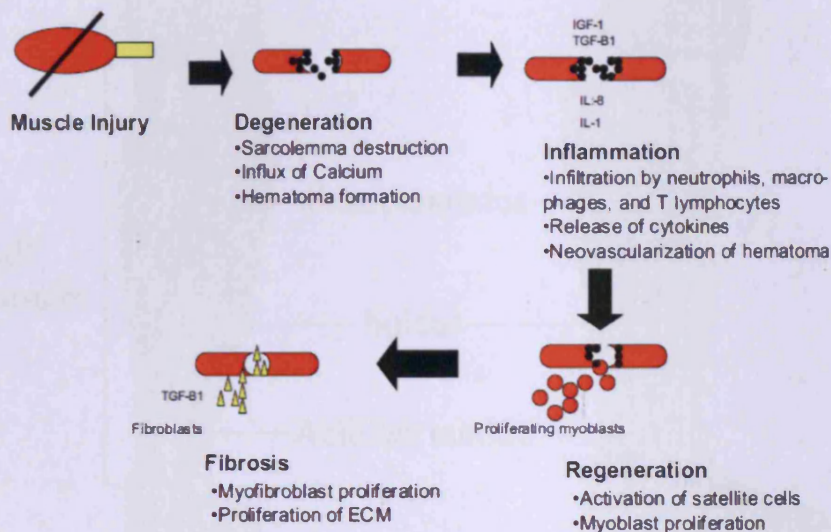
Figure 2.3 Stages of muscle healing after injury (Gates and Hurad 2005).

2.5 Anatomy of the gastrocnemius muscle

The gastrocnemius consists of two heads the medial and the lateral head as illustrated in Figure (2.4). The medial head is larger than the lateral head and originates from the posterosuperior depression on the medial condyle of the femur and the capsule of the knee joint (Drake et al. 2009). The lateral head arises from the lateral surface of the lateral femoral condyle and the capsule of the knee joint. The tendon of the gastrocnemius fuses with the tendon of the soleus to form the Achilles tendon, which is inserted into the middle third of the posterior surface of the calcaneum. (Drake et al. 2009) The gastrocnemius induces plantar flexion of the foot and produces some flexion at the knee. The gastrocnemius is also stated to contribute to stability of the knee

16

(Saglimbeni 2009). It also provides an important role to play in the gait cycle and is essential for walking and running (Drake et al. 2009).
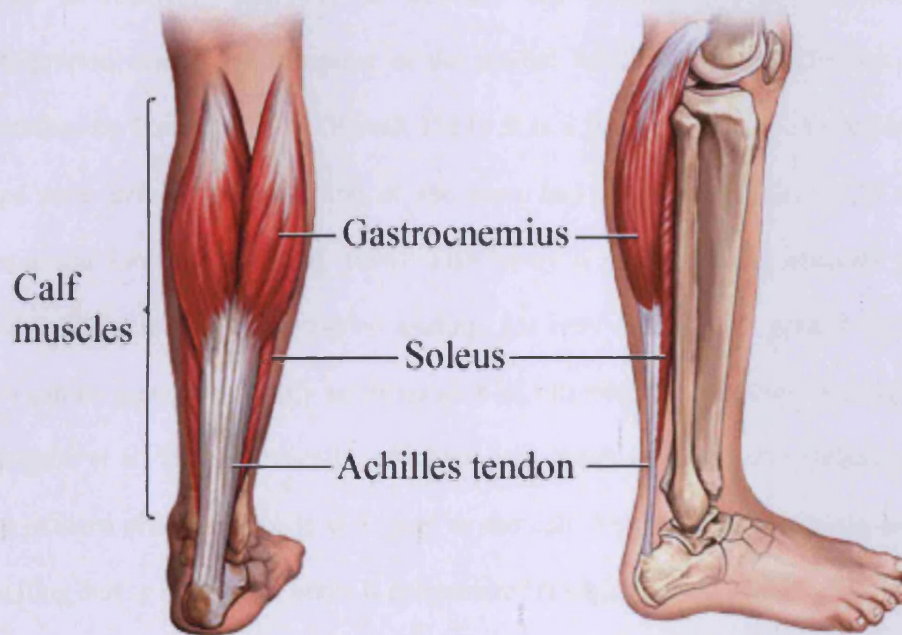
Figure 2.4 Gastrocnemius muscle anatomy (Adapted from www.tomahawknation.com).

The gastrocnemius is a bipennate muscle within which the fasciculi are obliquely set on both sides of the central tendon (Levangie and Norkin 2001). The gastrocnemius contains a high proportion of the fast-twitch type II muscle fibre that produces rapid strong movements that occur during running and jumping (Walmsley et al. 1978, Herzog et al. 1993). The soleus muscle on the other hand, contains twice as many slow twitch type I fibres as type II fibres. The soleus produces slow movement and is able to carry on sustained activity without fatiguing easily (Hyatt et al 2006).

2.5.1 Injury of the gastrocnemius

Rupture of the medial gastrocnemius muscle is a common injury associated with the calf muscles (Kwak et al. 2006a, Kwak et al. 2006b, Bianchi et al. 1998). The incidence of injury is relatively prevalent in athletes who perform sudden acceleration and deceleration manoeuvres. Rupture of the medial head of the gastrocnemius was first described by Powell in 1883 (Powell 1883). It is a frequent injury occurring in middle-aged men induced by extension of the knee and forceful dorsiflexion of the ankle (Froimson 1969, Gilbert et al. 1996). This injury is mainly occurs when the muscle is overstretched in uneven or sudden loading, not only during sport related activities but also can be generated in daily activities such as, climbing the stairs and running downhill (Delgado et al. 2002). Clinically, a sudden pain is felt in the middle portion of the calf and patients often describe it as a 'pop' in the calf. Following this, significant pain and swelling during the first 24 hours is encountered (Delgado et al. 2002).

Injury to the medial gastrocnemius muscle typically occurs when forceful plantar flexion of the foot is induced with simultaneous extension of the knee (forceful push-off with the foot), which produces active contraction and passive stretching of the gastrocnemius muscle (Miller 1977).The injury of the gastrocnemius during the gait cycle is well known. In addition, the injury of the gastrocnemius following a tennis serve during the push off movement was described more than 40 years ago (Froimson 1969).

2.6 Imaging muscle injury

The clinical assessment of muscle injury always begins with taking a careful history of the trauma. Following this, a clinical examination consisting of inspection and palpation of the involved muscles is carried out with muscle testing both with and without

resistance (Jarvinen et al. 2007). However, the history together with the physical examination of the patient may only generate restricted information about the extent of the injury, as often testing is limited due to pain and/or swelling. In these situations, diagnostic imaging tools such as computerised tomography (CT), magnetic resonance imaging (MRI) and ultrasound (US) can be utilised for the diagnosis of muscle injuries (Chen et al. 2009).

Low cost and availability often makes US the tool of choice for the initial assessment of muscle injuries, follow up and monitoring (Wong 2005). However, MRI is very useful when the region of interest is extensive and when underlying joint or bone pathology is suspected (Wong 2005). Table 2.2 outlines the advantages and different characteristics of these three imaging techniques.

	Ultrasound	CT scan	MRI
Availability	Readily available	Readily available	Increasing
Relative cost	Inexpensive	Expensive	Very expensive
Portability	Portable	Fixed	Fixed
Soft tissue contrast	Fair	Good	Excellent
Muscle	Fair	Good	Very good
Safety	Non Ionizing	Ionizing radiation	Non Ionizing
Repeatability	Yes	Limited	Yes

Table 2.2 Characteristics of muscle imaging techniques. Adapted from (Clague et al. 1995).

Ultrasound has been the method of choice for the diagnosis of muscle injuries (Kwak et al 2006a, Flecca et al 2007). In turn, the advantages of applying US in imaging muscles are as follows:

- US form a part of real time cross section imaging techniques.

- Non-invasive examination and acutely ill patients may be examined painlessly without any special preparation.

- Scanning can be facilitated in virtually any body plane section with the patient in any position.

- No hazards of ionising radiation or contrast materials.

- Good and excellent resolution.

- High specificity and sensitivity rates.

- Very useful in evaluation of changes of the pathology with time i.e. monitoring the healing process of muscle injury.

- Widely available and low cost procedure.

- With the development of newer 3D technology, volume scans of muscle can be measured.

- Proved to be successful in the evaluation of muscle trauma, including partial and complete muscle ruptures.

The disadvantages of utilising US in imaging muscles are as follows:

- Lower resolution than MRI and CT scans.

- Operator dependent.

Ultrasound is commonly employed for the assessment of sports injuries. In the evaluation of muscle, trauma ultrasound may be performed in both the acute setting and during rehabilitation. Ultrasound can be applied to grade injury, identify the muscle groups involved, help predict rehabilitation time, monitor the healing process, evaluate scar

tissue formation and the other complications of muscle rupture (Campbell and Wood 2002).

2.6.1 Physics of ultrasound imaging in biological tissue

Ultrasound provides a non-invasive method of observing the internal components of the body. Medical US uses pulses of high frequency sound waves (2-20 MHz) generated by a transducer that are sent to the patient. The pulse of US produces echoes at organ boundaries and within tissues. The echoes then return to the transducer where they are detected and displayed on the US machine.

The US transducer (probe) works on the principle of the piezoelectric effect. It is a crystalline, substance such that when a voltage is applied to the crystal, the molecules are deformed and a mechanical sound wave is produced. The frequency of the sound wave is mainly dependant on the size of the crystal. This sound pulse is sent to the body and an echo generated which returns to the transducer. This sound wave echo causes the crystals in the transducer to alter and a voltage is produced.

The amplitude of the returning echo will determine the size of the voltage produced due to reflection at organ boundaries, whereby large acoustic impedance is formed between the different structures. Smaller low amplitude echoes will occur due to scattering within tissues. The energy that reflects from a tissue aids in the generation of an image of its boundaries, and the transmitted sound allows for penetration into deeper structures for further echo delineation. Thus, ultrasound is capable of mapping both superficial and deeper layers of tissue. However, structures like bone or air where they are very large

differences in acoustic impedance, do not allow for passage of significant incident sound through these medium.

The creation of an image from echoes is based on sophisticated computer analysis of the returning echoes. However, due to the attenuation of the sound pulse with depth of penetration, the amplitude of the returning echoes is affected. The more delayed (more distant) echoes need to be amplified to compensate for the energy attenuated by the extra distances they travel. This adjustment is termed time-gain compensation and is an integral part of image generation (Kremkau 2002, Riley 1996). There is a necessity for these returning echoes to be amplified, compressed, and subtracted in order to formulate images.

The resolution of the ultrasound is directly proportional to the frequency of the incident sound, but the depth of penetration is inversely proportional to this frequency (Kremkau 2002, Riley 1996). Therefore, with higher frequency probes, structures that are more superficial may be studied in detail than deeper structures (Walker et al. 2004).

2.6.2 Ultrasound imaging of the healthy muscle

Muscle generates fewer echoes than other bodily structures as they have a very highly structured internal arrangement consisting of cytoplasm and repeating links of identical proteins (Ferrell et al. 1989, Heckmatt et al. 1988c). During axial plane viewing, most of the muscle is weakly echogenic, with numerous punctuate and curvilinear echoes that generate a mixed appearance to muscle. In the longitudinal plane, these echogenic structures appear to be the normal fibrous fat septa of the perimysium that surrounds muscle fascicles (Walker 1996). These fibrous tissues vary in thickness and intensity

throughout the muscle (Walker et al. 2004).. In the anterior tibialis muscle, as in various other muscles, the most prominent echo is generated through its central fibrous aponeuroses. Fibrous tissues, containing randomly distributed and oriented collagen fibrils, are more echogenic because they differ structurally (and acoustically) from the highly organized muscle architecture. The sonographic image of muscle is unique, allowing the examiner to differentiate muscle from adjacent fat, tendon, bone, or endocrine/apocrine tissue (Walker et al. 2004).

The inclusions of sections that contain other tissues, to provide a reference for assessing the echogenicity of muscle are often particularly helpful for routine imaging (Walker 1996, Walker 1998). The bone tissue typically generates a bright echo that defines its outer edge, as almost all sound is reflected at this point: as a result a shadow occurs below this edge as no further sound penetrates to create echoes from deeper structures (Walker et al. 2004). Including identifiable bony landmarks (e.g. tubercles) in an image is useful during comparative studies applying the opposite extremity or concerning serial studies.

It can be very challenging to image individual muscles in areas where multiple muscles overlap, because the selective activation of individual muscles may not be possible. In addition, the proportion of fibrous tissue varies from muscle to muscle and therefore, may appear more or less echogenic from one to another (Walker et al 2004). For instance, the triceps muscle is typically less echogenic than the biceps (Walker et al 2004).

Strength training and muscles that are subject to regular exercise will also vary in echogenicity. For instance, hypertrophic muscles post-exercise may appear hypoechoic due to a volume effect, which is due to an increase in myocyte size as compared to

fibrous tissue volume or it may be stated, the selective depletion of fibrous layer (Walker and Jackson. 1997). In addition, increased subcutaneous fat can reduce the overall echogenicity of muscle through absorbing increasing amounts of the sound energy (Reimers et al. 1993a, Reimers et al. 1993b).

2.6.3 Ultrasound imaging of the injured muscle

In the assessment of muscle injury ultrasound may be performed in both the acute phase and during the rehabilitation phase. Ultrasound possesses many uses in injury observation, it can be used to identify the muscle/muscle groups injured, grade the injury, predict prognosis, monitor the healing process or monitor the response to treatment and detect other complications of muscle rupture (Campbell and Wood 2002). The structural changes associated with muscle rupture are reflected in ultrasound images through the loss of brightness (echogenicity) or homogeneity or both, in the transverse image, and the loss of axial alignment of the echoes in the longitudinal image (Van Shie et al. 2001). However, the extent of these changes may vary depending on the severity of the injury.

The most important criteria for the ultrasonic assessment of muscle injuries over time are changes in echogenicity and size (Smith et al. 1994). The echogenicity and size can be measured either qualitatively or quantitatively (Van Shie et al. 2001). The qualitative method is based on an estimation of the intensity of the echoes (image brightness etc), but because of their subjectivity these methods are not very accurate or quantifiable and therefore not ideal to monitor healing.

Ultrasound is the imaging tool of choice for gastrocnemius rupture, as the echo from the fluid collected will enable to distinguish and visualise clearly the location, haematoma and local inflammation (Bianchi et al. 1998).

2.7 Healing process of the Haematoma

Ultrasound can identify a haematoma after the first few hours post injury. The ultrasound examination may be implemented between 2 and 48 hours after injury (Peetrons 2002). The haematoma containing clotted blood undergoes a process of liquefaction and through a phase of absorption, during which the haematoma develops a very heterogeneous appearance on ultrasound with areas of reflective matter (Fornage 1995).

Ultrasound imaging carried out at regular periods during the healing process reveals the reorganization of muscle structure (Fornage 1995). The resolution of the haematoma may potentially take anything from 3 weeks to 4 months, which is dependant on the extent of the initial trauma (Peetrons 2002). The regions in which repetitive rupture or injury granuloma and fibrous tissue has occurred, may impede the regeneration of normal muscle fibres, leading to a permanent scar, which in turn will limit function. The risk of recurrent rupture is proportional to the extent of residual scar tissue within the muscle (Campbell and Wood 2002).

In sports injuries, ultrasound assessment and examination is a poor predictor of outcome and is unable to provide an insight into the optimal time required to engage in limited athletic activity (Campbell and Wood 2002). However, it has been suggested that clinical assessment is a better predictor of recovery with regards to muscle testing and range of movement, although engaging in full scale athletic activity should be delayed until a normal echo through ultrasound is confirmed (Fornage 1995).

2.8 Treatment of Muscle injury

During the last decade, the progress in invasive, biomedical technology and intensive rehabilitation programmes has greatly improved treatment success of muscle injuries. The treatment protocols vary greatly and appear to generally depend on the severity of injury, however, there is little consensus on the optimal treatment for muscle injuries (Jarvinen et al. 2000, Crisco et al. 1994, Kasemkijwattana et al. 2000).

Physiotherapeutic treatment modalities such as therapeutic ultrasound, cryotherapy and electrical stimulation have been used in the treatment of common muscle injuries. The application of hot packs, ice, ultrasound therapy and electrical nerve stimulation are among the most commonly used modalities for the treatment of muscle injuries. One of most frequently used treatment modality in routine clinical practice is therapeutic ultrasound (Reef et al. 1993).

In clinical practice, effective markers for the resolution of muscle haematomas are reduction in pain, decreased swelling; improvement in muscle function and appearance of diffused coloration. On the other hand, persistent swelling between 24-72 hours, increased pain and restriction of movement range are efficient indicators of the severity of injury and lack of progress of the healing process (Klein 1990, Smith et al. 2006). Therefore, the treatment of haematomas depends particularly on how they present clinically and respond to early treatment.

Most assessments of acute muscle injury are subjective and the experience of the clinician appears to play a vital role in the selection of treatment modalities. One of the reasons for the non-consensus of treatment protocols may be due to the subjective nature

of the assessment of haematomas and muscle injuries, which highlights the importance for the requirement of objective measurement methods.

2.9 Subjective ultrasound assessment of muscle injury

The significance of ultrasound imaging as a tool in assessing the extent and severity of muscle injury is well established. Currently the ultrasound interpretation of the extent, size of injury and the progress of the healing process are largely subjective and qualitative. Many grading systems for assessing muscle injury have been described (Fornage 1995, Holsbeeck and Introcaso 2001, Peetrons 2002). Levine and Colleagues et al. (2000) suggested that muscle strains might be divided into three grades: grade I, grade II and grade III. The incidence of grade III is less when compared to grade I, which are also referred to as low grade strains.

A - Grade I

In a low-grade strain, the muscle tissue is stretched beyond its elastic point, and microscopic rupture to the muscle fibres is present, with less than 5% of the fibres damaged. Significant pain ensues initially, however rapid recovery with conservative management has been demonstrated. Ultrasound images for this grade illustrate normal, increased focal or generalised echogenicity as depicted in figure 2.5 (Wong 2005).
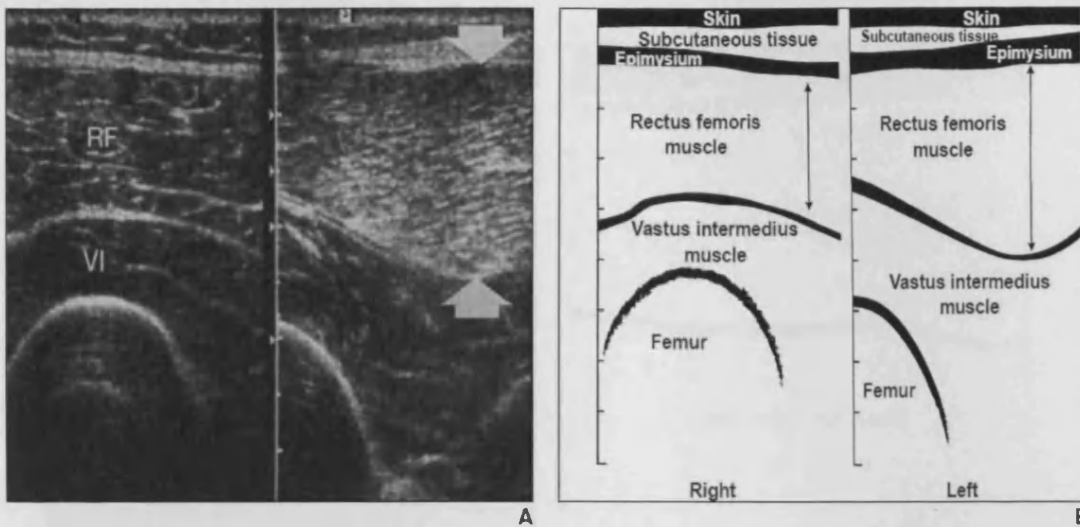
Figure 2.5 A) Ultrasound image and B) schematic diagram (right and left thigh) (A) Right thigh normal and left thigh image where the left rectus femoris muscle shows inflammation (width indicated by arrows). Adapted from (Lee and Healy 2004)

B - Grade II

A grade II strain, will demonstrate more pronounced symptoms than grade I, due to partial disruption of the muscle as in a small detachment or discontinuity. Acute pain, swelling and loss of function are presented. The partial detachment in the grade II strain may also include detachment from the adjacent fascia or aponeurosis, which occurs commonly when the gastrocnemius muscle detaches from the aponeurosis of the soleus muscle during racquet sports and running activities (Bianchi et al. 1998).

The forming of the haematoma in the muscle tendon junction is characteristic of grade II strains (Palmer et al. 1999). The ultrasound images of the grade II strain vary and depend on the severity and the acuteness of the partial rupture. Sonographically, it appears as an area of discontinuity of muscle fibres characterised by echogenic perimysial striae as depicted in figure 2.6. The cavity created by retracted torn muscle fibres is filled with blood and the sonographic appearance of the haematoma varies with the time from the trauma (Wong 2005).
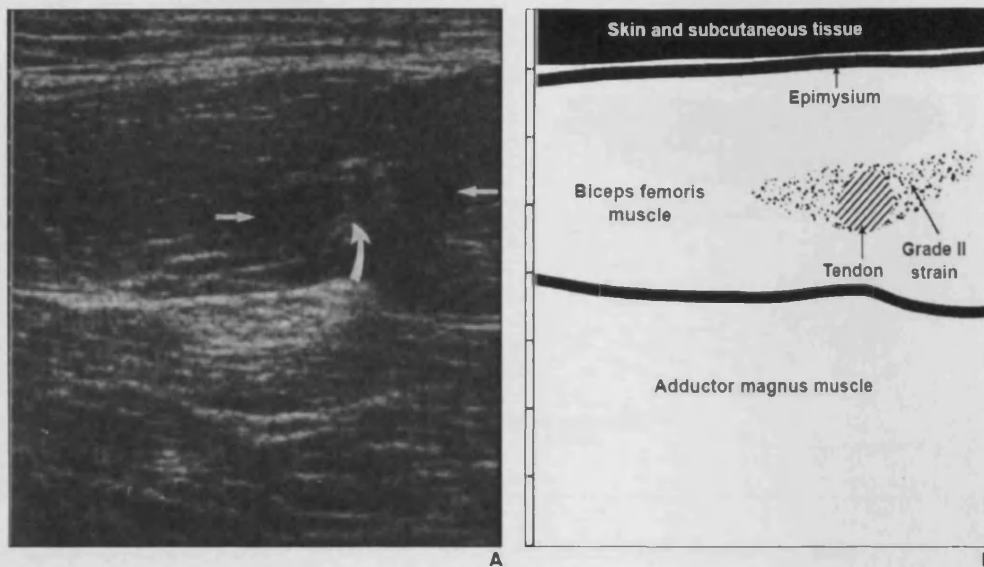
Figure 2.6 A) Ultrasound image of grade II strain of biceps femoris B) Schematic diagram of the grade II strain.
A) Shows partial disruption of the biceps femoris muscle indicated by arrows and explained with corresponding schematic diagram B. Adapted from (Lee and Healy 2004)

C - Grade III

Grade III muscle strain is characterised by complete muscle disruption with or without the retraction of the muscle. It usually occurs due to forceful contraction against a strong resistance to muscular activity (Wong 2005). On imaging, discontinuity of muscle fibres is apparent, which is mostly accompanied by muscle laxity (Wong 2005). On the ultrasound, the image appears hyper echoic due to the presence of fibrosis, muscle degeneration and chronic inflammatory cells (Temple et al. 1998). The muscle gap is usually filled by haematoma and effusion as illustrated in fig 2.7.
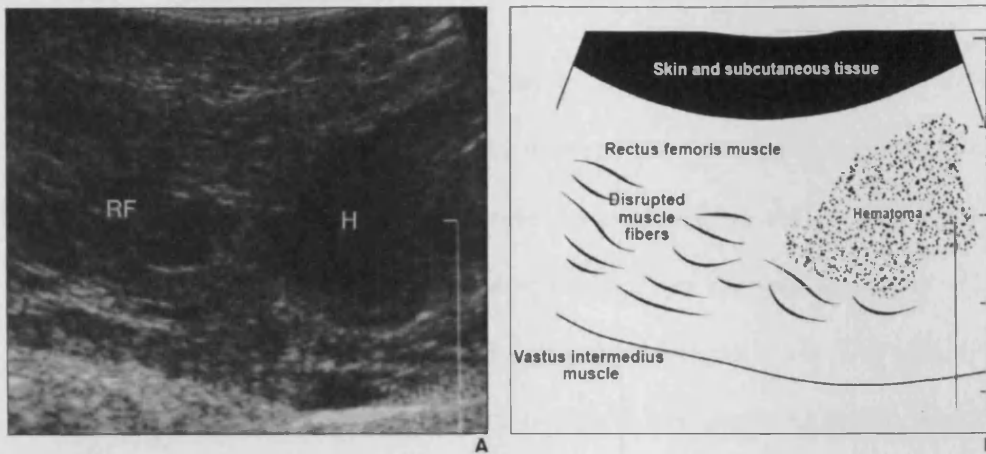
Fig 2.7 A) Grade III rectus femoris muscle strain. B) Schematic diagram
A) Ultrasound image showing grade III rupture of the rectus femoris muscle- rounded area H showing haematoma and disrupted of muscle fibres (RF) which is hypoechoic of rectus femoris. Adapted from (Lee and Healy 2004)

The formation of haematoma is a characteristic feature of muscle rupture. A haematoma forming between the medial gastrocnemius and soleus muscles is a frequent finding in patients. Kwak et al (2006a) reported that tennis leg (TL) was associated with fluid collection between the gastrocnemius and soleus muscles in 19 of 22 (90.2%) of their patients. They reported that 7 of the 22 patients were diagnosed with a partial rupture, and the remaining 15 patients with complete rupture of the medial head of the gastrocnemius. Flecca and colleagues (2007) have reported 24 individuals showing partial rupture out of 34 TL patients, with nine cases presenting with complete rupture. In 80% of cases, a haematoma was present. Delgado et al. (2002) also reported 141 patients demonstrated TL whereby, 89 (63%) had fluid collection between the medial head of the gastrocnemius muscle and the soleus muscle. The collection of fluid between the

gastrocnemius and soleus muscles was also reported by Yilmaz et al. (2008) in 11 out of 14 (78.5%) patients.

In these studies (Kwak et al. 2006a, Kwak et al. 2006b, and Flecca et al. 2007), the authors measured the haematoma forming between the gastrocnemius muscle and soleus muscle as the distance of separation between the two muscles. Following this, the degree of fluid collection after partial or complete rupture was analyzed during the follow up period. Kwak et al. (2006a) also reported that the thickness of the fluid collection was significantly greater in those patients with complete gastrocnemius medial head ruptures (mean 9.7 mm) compared to those of the individuals with partial tears (6.8 mm).

The authors participating in ultrasound based studies (Kwak et al. 2006a, Kwak et al. 2006b, Delgado et al. 2002, Yilmaz et al. 2008, and Flecca et al. 2007) concluded that ultrasound is a useful imaging modality for the diagnosis and follow-up of patients with ruptures of the medial head of the gastrocnemius. In addition, Reef et al. (1993) measured the length of the lesion and the cross-sectional area damaged. Genoverse et al. (1990) linked this cross-sectional area and used it to qualitatively grade lesion echogenicity and express them as severity of injury.

Therefore, there are numerous methods to grade muscle tears by utilising systems that describe ultrasound abnormalities, varying from normal through to complete severe tears with retraction (Holsbeeck and Introcaso 2001, Fornage 1995, Peetrons 2002). However, the clinical meaningfulness of these grading systems, and inter and intra-rater validity is questionable and studies which have been implemented to test these systems are minimal (Campbell and Wood 2002).

The different degrees of experience and visual judgment lacking a systematic approach are also known to contribute to the relatively high rates of inter and intra observer variations for visual evaluation (Krupinski 2004). Moreover, manual scoring and measuring size of muscle injury is subjected to bias and errors, which are inevitable with human decision-making. The experience of the operator will have an effect (Shamir et al. 2009)

It is also important to note that muscle fascicles can provide a strong or weak reflection on imaging, which is dependant on size and direction making it difficult to detect small abnormalities. In addition, the change in the US setting of the imaging device may lead to muscles appearing brighter and cause errors in diagnosis (Pillen et al. 2006).

In clinical practice, the most important aim is to identify the presence of significant muscle bundle tears and haematomas. The diagnosis is simplified when a typical history of muscle contusion or strain is accompanied by objective evidence of swelling and/or ecchymosis distal to the lesion (Jarvinen et al. 2007). Haematomas that are small in size and those deep within the muscle belly may be more difficult to diagnose clinically (Jarvinen et al. 2007).

Echo intensity can be evaluated visually, but assessment using this approach is rather subjective and depends on the experience of the observer (Pillen et al. 2006). Moreover, muscle echo intensity increases with age and differs with muscle groups (Reimers et al. 1993a, Reimers et al. 1996a, Pillen et al. 2006, Scholten et al 2003). This delineates difficulty in assessment visually, whether a gray value is pathologically increased or still

within the normal range for a given age (Pillen et al. 2009). Therefore, to effectively evaluate muscle injury and study the process of healing, it is essential to be able to quantify the injury at the different stages objectively.

2.10 Objective ultrasound assessment of muscle injury

Diagnostic ultrasound has been used for several years to evaluate the extent of the muscle damage that has occurred. With the help of diagnostic ultrasound, clinicians can see the evidence of muscle fibre disruption, but they still do not have a method for objectively quantifying the full extent of the damage or offer an accurate prognosis for recovery. Nicoll et al. (1992) evaluated injury by measuring the mean gray-level of the image area for obtaining a more quantitative assessment. However, there is a strong potential and possibility of extracting additional information from ultrasound images applying second order texture analysis algorithms.

Texture analysis has demonstrated its usefulness in many medical applications. Quantitative ultrasound methods have been introduced to evaluate tendon injury through measurements using gray scale analysis, including measurement of mean gray level or mean echogenicity (Micklethwaite et al. 2001). A wealth of studies examining the application of texture analysis to evaluate muscle pathology. Many studies have applied texture analysis methods to investigate neuromuscular disorders (Heckmatt et al. 1988a, Heckmatt et al. 1988c, Fischer et al. 1988, Heckmatt et al. 1989, Pillen et al. 2003, Maurits et al. 2003, Maurits et al. 2004).

The advantages of a more objective method of analysing the degree of healing of a muscle injury also include the identification of an endpoint of the healing, when

treatment may be discontinued. There is a clear requirement for the regular monitoring or treatment of muscle injury, testing the efficacy of different treatments in speeding recovery. Therefore, there is a definite need for more measurable assessment tools or techniques to aid accurate diagnosis and to prescribe the best treatment method available.

2.11 Texture analysis

The requirement for robust quantitative measures in medical imaging has driven the development of texture analysis techniques. The main purpose of carrying out an imaging procedure is for the definition of tissue features and characteristics (Lerski et al. 1993). The term texture analysis simply means procedures for analysing gray zones in images. This is of particular significance when a clinician needs to determine whether pathology is present and to what extent the pathology has progressed.

As discussed earlier within the thesis, the typical method of image analysis conducted by the radiologist is largely qualitative in nature and can lack sensitivity. Therefore, the necessity for methods in processing images is vital for accurate diagnosis, monitoring and treatment for different clinical conditions. The information of textures from the image has been ascertained to be a particularly sensitive feature for the assessment of different pathologies (Lerski et al. 1993). Since the visual assessment of texture can be subject to bias, and from previous studies it is known that human analysis of texture properties has limited accuracy and sensitivity, therefore mathematical analysis of texture aims to address these shortcomings. The remainder of this chapter aims to present and explain the mathematical approaches towards texture analysis.

Texture in an image refers to the distribution of brightness and darkness within the image and to concepts such as coarseness, linearity, and regularity (Castellano et al. 2004, Lerski 1993). Texture can also be defined as the pattern on a surface or object (Srinivasan and Shobha 2008). Texture analysis is used to define the variations of gray zones in an image (Lerski 1993). In simple terms, the evaluation of the relationship of pixels and the gray level intensity in images is the principle of texture analysis (Castellano et al. 2004).

2.12 Texture analysis techniques

Texture analysis techniques are applied to characterize the spatial distribution of gray level variations within an image (Haralick et al. 1973, Lerski 1993). They are used to quantify the complexity of an image linked to the extent, frequency, and spatial arrangement of these variations. This measurement of complexity may provide information on the structure of the object being imaged. It is worth noting that these techniques can provide information that is not visible to the human eye (Julesz 1975).

Texture analysis applications provide advanced non-visible information on tissues of interest (Harrison et al. 2008). Tissue characterization by means of texture parameters alone or in combination with clinical staging or other imaging findings may progress to new clinical methods for diagnosis, treatment planning and follow-up (Harrison et al. 2008). According to the basis of the interaction of the pixels texture analysis methods may be classified as structural, statistical, model based and transform. (Materka and Strzelecki 1998).

2.12.1 Structural approach

The structural approach addresses the principle of presenting texture by the means of well defined microtexture (primitive) and the arrangement of macro texture (spatial arrangement) of those primitives (Haralick 1979). Structural approaches provide a symbolic representation of the image (Castellano et al. 2004). In order to describe texture features using the structural approach, defining the primitives and placement rules are necessary (Materka and Strzelecki 1998). These methods are not highly developed, particularly in the case of medical imaging and pose challenges with regards to computation.

2.12.2 Statistical approaches

The statistical approach uses the information gained from the spatial distribution of gray values and analysis these values by computing local features at different points in the image, and then derives a set of statistics from the distribution of these features (Ojala and Pietikainen 2004). The statistical methods are considered to be the most widely used method in medical image analysis (Holli et al. 2010). The statistical approach may potentially be further sub divided into first order, second order and higher order statistics .First order statistics are the analysis of single pixels, second order statistics analyses two pixels and higher order statistics define three or more pixels (Ojala and Pietikainen 2004).

2.12.2.1 First order statistics

First order statistical analysis is the most common method used for image feature computation. The histogram is computed from the intensity of pixels, without taking into

consideration any spatial relations between the pixels within the image. In other words, they depend only on individual pixel values and not on the interaction of neighbouring pixel values (Castellano et al. 2004, Srinivasan and Shobha 2008).

In this study, four first order textural features were calculated namely: the gray levels values, variance, skewness and kurtosis. The gray level of the histogram measures the mean gray level value of the image, providing an indication to the brightness and darkness of this image. The permissible gray level values of a pixel range from 0 to 2^b -1, where b is the number of bits of the image. With regards to most digital images, 8 bits are sufficient and in this context, the gray level values range from 0 to 255. The lowest value is attributed to dark pixels and higher values to the bright pixel (Castellano et al. 2004). Fig 2.8 depicts an example of a 3 bits digital image with 5*5 pixels and the gray level for each pixel individually.

The variance is a measure of how far from the mean the gray-level values in the image are distributed. The skewness measures the deviation of the gray levels from a symmetric distribution. The kurtosis describes the shape of the histogram peak, the sharper the peak the higher value of kurtosis. The shape of the histogram provides many clues to the characteristics of the image. For example, a narrowly distributed histogram indicates a low-contrast image (Srinivasan and Shobha 2008).

0	0	0	0	0
4	1	6	4	2
3	1	3	2	7
5	1	2	7	7
4	2	7	7	7
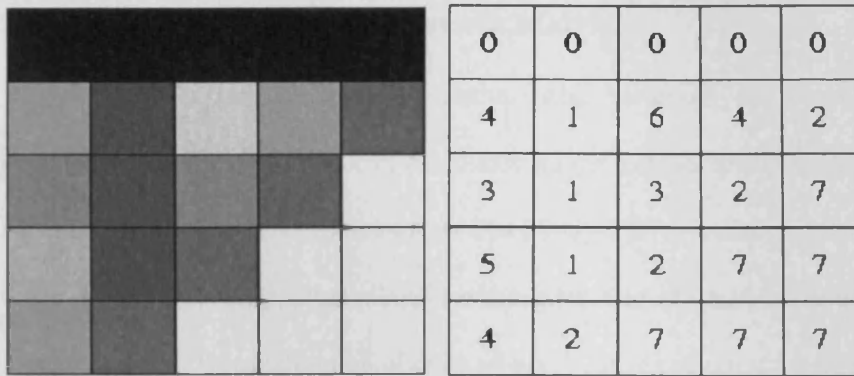
A   B

Fig 2.8 A: image with 5*5 pixels with gray level values ranging from 0 (black) to 7 (white) B) numerical representation on the image (from Castellano et al. 2004).

The main limitation of a first order statistics is that it fails to provide any information regarding the relationship with other adjacent pixels (Srinivasan and Shobha 2008). Moreover, the first order statistic parameters, especially the gray level and variance are highly dependant on the depth and gain setting of the US machine (refer to chapter 4 and chapter 5) and tissues affected by similar pathologies may demonstrate different properties (Basset et al. 1993).

2.12.2.2 Second order statistics

The second order statistic provides information on the features of two pixels and demonstrates information regarding the relationship between these pixels (Srinivasan and Shobha 2008). Co-occurrence matrix, gradient and run length matrix are second order statistic parameters.

2.12.2.2.1 Gray level co-occurrence matrix

Harliack (1979) was the primary author who proposed the co-occurrence matrix parameters. Co-occurrence matrix calculates image features and considers the interaction between two pixels (Srinivasan and Shobha 2008). The co-occurrence matrix is a second order statistical technique that allows for the extraction of statistical information from the image regarding the distribution of pairs of pixels. It is computed by defining a direction, a distance, and pairs of pixels separated by this distance, computed across the defined direction, which are analyzed (Singh et al. 1997, Beekman and Visser 2004). There may be many co-occurrence matrices computed for a single image, one for each pair of distances and directions defined. Normally a set of 220 co-occurrence matrices are computed, for five different pixels distances from 1 to 5 pixels, and four different directions ($\theta=0°$, 45°, 90° and 135°) as shown in figure (2.9).
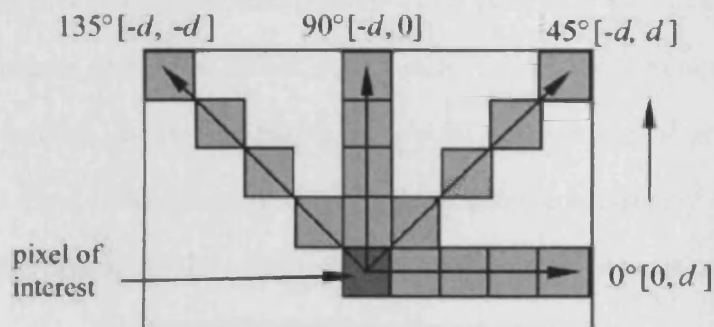
Figure 2.9 Showing computation of co-occurrence matrix with pixel of interest (Lu et al. 2006).

The co-occurrence matrix is widely used for tissue characterisation as for each sample it estimates a set of features (Bassett et al. 2000).

2.12.2.2.2 Gray level run length matrix

Run length matrix is derived from a series of consecutive pixels of the same gray level intensity in a given direction. Castellao et al (2004) defined the run length matrix as a parameter that is used to measure the distribution of the gray level a cross a set direction, for the length of pixels having the same gray level value. The gray level run length matrix provides information related to the spatial distribution of gray level runs (i.e. pixel-structures of same pixel value) within the image. The run-length matrix measures each allowed gray-level value and how many times the runs occur (Castellano et al. 2004). The run length parameter can be calculated in four directions: horizontal, vertical and the two alternate diagonals.

2.12.2.2.3 Gradient

Haralick (1979) described gradient as the parameter that measures the intensity variation between each pixel and adjacent pixels, to identify directional patterns in gray levels. Therefore, in principle the region or point in the image the gray level changes from dark to white, indicates a high gradient at that point, consequently if it changes gradually from dark to light gray then that implies a lower gradient value (Castellano et al. 2004).

2.12.3 Model-based approaches

The principle of model-based texture analysis is the use of fractal and stochastic models to interpret an image by generating an image model and in turn analysing the associated parameters (Manjunath and Chellappa 1991, Strzelecki and Materka 1997). The advantage of using the model-based approach is that it may also synthesize the image in addition to the description of texture features. The theory states that these models function on the principle that the intensity of each pixel in the image depends on the

intensity of its adjacent pixels (Bharati 2004). An example of such a model-based texture descriptor is the autoregressive (AR) model, which has been applied to this study.

2.12.3.1 Auto-regressive model

The basis for the auto-regressive model is, the estimation on the principle that the relationship between pixels in the particular gray level value is the weighted sum of the gray-level values of adjacent pixels (Castellano et al. 2004). In other words, the definition of features within an image is based on patterns of interactions between adjacent pixels or groups of pixels through the method. This parameter may be used to characteristize an object as it assumes that these interactions and relations are unique for a particular type of pattern (shape) in an image (Castellano et al. 2004).

2.12.4 Transform methods

Transform methods are useful in calculating multi-scale features and time-frequency to describe texture in numerous resolutions (Srinivasan and Shobha 2008). The principle of transform methods is that the texture properties are represented in space where the co-ordinate system is closely related to the features of the texture, such as frequency and size (Materka and Strzelecki 1998). Daugman (1985) describes this principle within the Gabor method. Although the Gabor method is constructive and provides better localisation than its contemporary methods, it poses one major shortcoming, which is the inability to localize a structure in space with reference to natural textures (Srinivasan and Shobha 2008). Wavelet transforms overcomes these shortcomings, which allows for the most common type used for medical application.

2.12.4.1 Wavelet transforms

The wavelet transform function alters the resolution in space which allows it to present textures at the most suitable scale (Materka and Strzelecki 1998). Therefore, this allows for a wide range of choices for this function, and the user may select the most appropriate wavelet for the analysis of texture, for a given situation. It is also particularly helpful in texture segmentation (Castellano et al 2004). During this mode of analysis, each pixel is associated with a set of wavelet coefficients, which describe the frequency of the image at a point over a set of different scales; from these coefficients, one can compute texture parameters (Kociołek et al. 2001, Szczypiński et al. 2001).

2.13 Tissue characterization

It is evident from the available literature that visual inspection alone for the diagnosis of tissue pathologies can be prone to bias and can lack sensitivity and reliability. One main reason for this is that diagnosis largely depends on the sonographer, who observes tissue characteristics from the image and compares them with the image of different pathologies to arrive at a diagnosis. The other alternative to this method is the application of invasive methodologies, such as needle-guided biopsy. Although this is a very robust technique with less chance of error, being invasive in nature it is not necessarily the method of choice. To address this problem, researchers have developed quantitative criteria with the help of computer systems to aid diagnosis. The various mathematical methods described in this thesis attempt to address the shortcomings of subjective analysis and aim to provide texture analysis more power and reliability. As described in the section above (2.12), the commonly used texture analysis methods are based on gray level distribution of individual pixels and their relationship with adjacent pixels.

2.14 Ultrasonic tissue characterization

For over two decades, a method of analysing normal and diseased tissue has applied the use of ultrasound tissue characterisations (Allison et al. 1994). The ultrasonic signals contain information related to the absorption and scattering properties of the internal structures through which the ultrasound beam passes. In instances, where pathology changes tissue properties, the ultrasound echo provides useful information, which may be used for diagnosis of the pathological process.

The difference in scatter properties in tumour tissue has driven research to examine the correlation of texture and other signal parameters in tissues with other pathologies (Donohue et al. 2001). Research conducted regarding ultrasonic tissue characterization and analysis is usually divided into two main areas: the analysis of radio frequency data and analysis of B-scan echo texture analysis.

Numerous methods have been designed to analyze the returning RF data in order to estimate acoustic parameters, which may be used for tissue analysis. The advantages of this approach are the variability of the raw transducer data, with frequency resolution limited only by the sampling equipment. The main advantage of this approach differing to the alternative method is that it is operator independent and less likely to be biased via personal judgement (Maas 1994).

One parameter used in RF based tissue characterization is the relationship between attenuation and frequency. The phenomenon of the attenuation of tissue ultrasound is due to absorption and scattering and varies linearly with frequency. Therefore, the slope of attenuation to frequency relationship has been studied extensively. Many researchers

43

have analysed the slope of the attenuation coefficient versus frequency in the context of the characterizing parameters.

Although RF based techniques pose may advantages, one must be aware of the disadvantages, which are as follows:

- The returning RF signal must be sampled at a very high rate and requires a large storage space for the resulting data.

- RF based methods require specialized equipment not normally available in clinical studies (Maas 1994).

The alternative method of characterizing tissue in ultrasound images is the echo texture technique. The output of the US machine is used to analyse, study and correlate the physiological, histochemical and biochemical characteristics of tissues. The output consists of a two-dimensional matrix of pixels where each pixel has an x, y coordinate that specifies a location and a z coordinate which provides information regarding pixel intensity (Ginther 1995, Zagzebski 1996, Kremkau 2002). Various tissues at different times will exhibit certain characteristic appearances through the pixels on the output screen.

As suggested earlier, the analysis of texture characteristics appears to depend on the sonography. Moreover, in some pathological conditions the tissues give the impression of being very similar in their diagnostic criteria and induce difficulty for the sonographers. Therefore, with respect to visual examination a conclusive diagnosis cannot be drawn (Kadah et al. 1996).

The echo texture of an image is described via the use of the mean pixel intensity and the variance of the pixel values within the ROI on an image. In order for the computer to analyze analogue images, the analogue image information must be converted into a digital format. It is sometimes very difficult for the user to detect small changes in the pixel values without the committing errors. The computer-based method eliminates the subjective nature of the analysis allowing it to become more sensitive to changes in specific pixels values or the distribution of various pixel values. Singh et al (1997) and Pierson and Adams (1995) demonstrated that through utilising computer analysis one can also measure very specific areas of an image.

A vast amount of research has been conducted using various forms of echo texture. Beekman and Visser (2004) reviewed the capability of echo texture to evaluate the disorders of the nervous system. The review highlights the concept of echo texture, which can potentially differentiate normal from abnormal textures of peripheral nerves, differentiating muscles from nerves, and the possible therapeutic strategies. Therefore, echo texture analysis may be applied as a useful tool for effective quantitative diagnosis.

Ultrasound tissue characterization has been used to describe variouse anatomic structures, including the liver (Garra et al. 1989, Youssef and Sharawi 1990), kidneys (Rubin et al. 1988) breast (Garra et al. 1993) muscle (Nielsen et al. 2006) and eye (Romijn et al. 1991). The authors have demonstrated that the use of quantitative tissue characterisation could significantly increase the usefulness of ultrasound for the evaluation of tissue pathologies at various anatomical locations and tissue types. The liver and the breast were studied at a greater depth than other tissue structures

2.15 Ultrasonic characterization of muscle

The use of quantitative Ultrasonography appears to be very promising in clinical practice to differentiate tissue properties of disease muscles when compared to healthy muscle (Pillen et al. 2008). Fischer et al (1988) demonstrated computerised real-time US with computer programmes, which could be applied for specified tasks such as defining muscle interfaces and tissue composition. Cady et al (1983) illustrated the use of the texture analysis method to grade bright and dark areas in muscle tissue through quantification of the signal and suggested that small changes in muscle composition in dystrophic muscles can be detected. These changes were so subtle that they could not produce sufficient radiological density in order to be ascertained by CT. Heckmatt et al (1989) have also quantified echogenecity from computer-aided reconstructed muscle images and recorded marked differences between diseased and normal muscle. Although, the above studies have quantified ultrasound signal to differentiate abnormal from normal muscle, there is a gap in the information generated, as detailed quantification and analysis has not been performed (Bharathi et al 2004).

Nielsen et al (2000) developed a method based on first order statistics to characterize the supraspinatus muscle and concluded that first order statistical parameters are a sensitive and reproducible method for studying the muscle tissue. Moreover, Nielsen et al (2006) developed a novel method based on first and second order statistics to characterize properties between the supraspinatus and vastus lateralis muscle. The authors concluded that using higher order statistics developed a more complete description of the tissue composition in the muscle than just the mean gray-scale value. Several studies have indicated that quantitative muscle ultrasound is essentially useful in the initial evaluation of patients with symptoms of neuromuscular disease (Pillen et al. 2006, Pillen et al.

2008). In addition, with respect to tissue characterization it has been possible to differentiate between children, with and without a neuromuscular disorder with high sensitivity and specificity (Pillen et al. 2003, Heckmatt et al 1989).

Texture analysis of ultrasonic images can also be used for the characterization and the differentiation of the muscle structure between athletes and untrained individuals (Sipila and Suominen 1991). Basset et al (1994) depicted that with regards to ultrasonic images, the tiredness and fatigue of muscles may be revealed through the application of texture analysis.

Limited applications of ultrasonic tissue characterization on human muscles have been demonstrated. Moreover, the studies that did potentially use ultrasonic characterisation to identify muscle changes, these were implemented using methods of visual evaluation, which is very subjective and prone to bias. No reported studies were found in the literature regarding the use of quantitative ultrasound image analysis being used for the gastrocnemius muscle, which is one of the most commonly injuries muscle in sport injuries in the lower limbs. The aim of this study therefore is to develop a quantitative texture analysis method for the gastrocnemius muscle that may then be possible applied to similar injuries elsewhere in the body.

Chapter 3 Data acquisition and Image analysis

3.1 Introduction

The role of texture analysis of medically based images is gaining great importance in the field of diagnostic imaging. It has caught the interest of many researchers, who have focussed on assisting texture analysis through the development of computer aided diagnosis systems. These systems have the ability to enhance the precision and accuracy of image characterisation.

A computer aided quantitative evaluation system for muscle injuries may be divided into 5 parts:

1   Acquiring an image: A device such as MRI, CT or ultrasound can be used to generate the digital image. In this thesis, ultrasound system was used.

2   Defining a region of interest (ROI) within the image. A different size and shape of the ROI can be defined within the image.

3   Extraction of the texture features from the ROI defined in the image.

4   Determination of the most suitable texture parameters to analyze the image for the select purpose required.

5   Data analysis and classification of the texture features within the image.

Taking into account the importance of texture analysis, as well as the computerised system that has been developed to assist this mode of analysis, this research project focuses on the development of a process of determining a subset of texture features,

which are most suitable for characterizing normal muscle and quantifying muscle trauma. With regards to the hypothesis, identifying such characteristics will be useful in monitoring the healing process of a muscle injury. Figure 3.1 describes an overview of this research plan.

```
                    ┌──────────────────────────────────┐
                    │     Gastrocnemius Muscle         │
                    └──────────────────────────────────┘
                          │                    │
                          ▼                    ▼
              ┌──────────────────┐   ┌──────────────────┐
              │  Abnormal muscle │   │   Normal muscle  │
              └──────────────────┘   └──────────────────┘
                       │                      │
                       ▼                      ▼
              ┌──────────────────┐   ┌──────────────────┐
              │ Image acquisition│   │ Image acquisition│
              │   (Ultrasound)   │   │   (Ultrasound)   │
              └──────────────────┘   └──────────────────┘
                       │                      │
                       ▼                      ▼
              ┌──────────────────┐   ┌──────────────────┐
              │  ROI Selection   │   │  ROI Selection   │
              └──────────────────┘   └──────────────────┘
                       │                      │
                       ▼                      ▼
              ┌──────────────────┐   ┌──────────────────┐
              │ Texture features │   │ Texture features │
              │    extraction    │   │    extraction    │
              └──────────────────┘   └──────────────────┘
                       │                      │
                       │                      ▼
                       │            ┌──────────────────┐
                       │◄───────────│ Optimizing texture│
                       │            │     features      │
                       │            └──────────────────┘
                       │                      │
                       ▼                      ▼
              ┌────────────────────────────────────────┐
              │       Reference set of normal          │
              │       gastrocnemius muscle             │
              └────────────────────────────────────────┘
                              │
                              ▼
              ┌────────────────────────────────────────┐
              │     Differentiate and monitor          │
              │       the healing process              │
              └────────────────────────────────────────┘
```
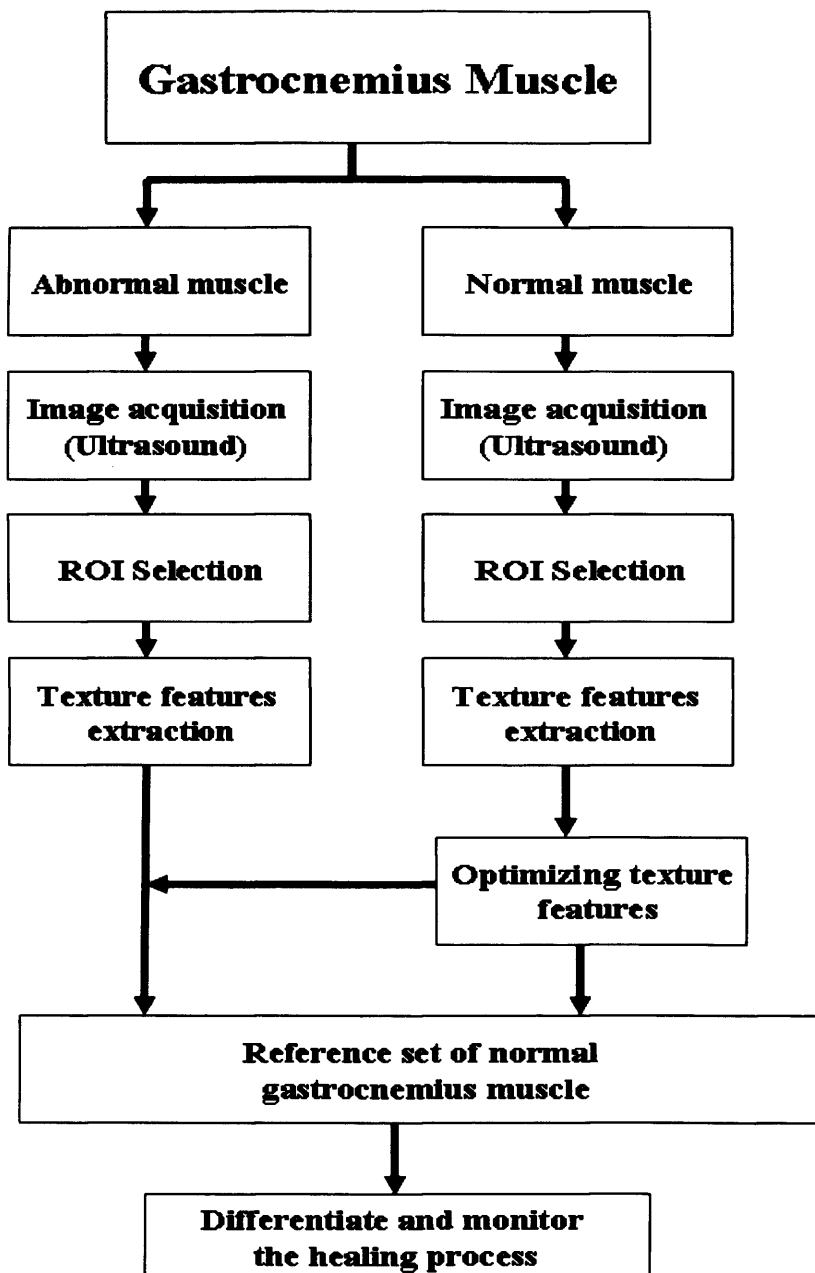
Figure 3.1 Overview of research plan

49

3.2 Image acquisition

For the purpose of this study, ultrasound was performed on Aplio ultrasound system (Toshiba medical system, Europe) using a 3D linear array transducer (Model PLT-1204MV) working on an 8.5MHz frequency with a 192 transducer element array. Figure 3.2 illustrates the probe used in the study.

Figure 3.2 The 3D ultrasound probe used in the study.

3.3 Three-dimensional ultrasound

Three-dimensional ultrasound was developed to address some of the limitations of 2D ultrasound and to enable the clinician to view the anatomical region of interest in three dimensions (Kim and Choi 2007). Moreover, 3D can provide better ultrasound guidance for various invasive procedures such as biopsies and image guided surgeries. It is also very useful in the context of minimally invasive surgery (Kim and Choi 2007). The incorporation of 3D ultrasound has only recently been included in routine clinical practice for certain procedures, although it has been readily available for nearly 25 years

(Kim and Choi 2007). The main reasons for this are that the affordability and speed have only currently been improved in order for it to be utilised in routine practice.

As suggested earlier 2D US has its limitations, it was identified that with respect to the 2D ultrasound, the analysis of the images were primarily of a subjective nature and relied on the experience of the examiner. Furthermore, the examiner must create a mental image and reconstruct a 3D impression of the pathological or anatomical structure (Lee et al. 2002). This shortcoming is overcome in the 3D US system, whereby the transducer motion is removed from the examiner's possession and is replaced through mechanical means: the 3D reconstruction is handled by the computer system (Hamper et al. 1999, Rankin et al. 1993, Elliot et al. 1996). This greatly reduces the subjective based analysis of images, particularly after the user has become more familiar with and has mastered interpreting of the images. 3D US enables images to be viewed in different planes, any number of times, thereby increasing the accuracy and consistency of the findings, thus aiding in a more definitive diagnosis (Fenster and Downey 1996, Fornage 1999).

With 3D ultrasound, the user is required to hold the probe at the angle and position of choice over the anatomical area of interest. This enables the operator to select the required view and orientation and allows for great manoeuvrability over complex anatomical areas. However, to enable correct reconstruction of the image, the exact angulations and position of the ultrasound probe must be known for each image (Kim and Choi 2007).

The 3D transducer method is an alternative method to the free-hand acquisition method and addresses some of its limitations (Kim and Choi 2007). This method involves the process of, obtaining the 3D volumetric data through mechanical movement of the transducer, which generates 2D US images at predefined spatial intervals sampling the volume in question properly, without missing any regions. However, the main disadvantage of this technique is the bulkiness and weight of the 3D transducers in use today, as compared to conventional 2D transducers. The 3D transducers house both the motor and transducer, making it more difficult to handle (Won et al. 2003).

The application of 3D array transducers is fast becoming the most common method of acquiring a 3D image. A motor contained within the automated transducer ensures consistent data acquisition. When the motor is active, the transducer elements automatically sweep through the selected ROI while the transducer is held stationary (Prager et al. 2010)

3.4 Ultrasound setting parameters

In the study all system-setting parameters were kept constant, the image depth was set to 4cm to allow the scanning of the gastrocnemius muscle. Initial studies were completed to determine the gain and dynamic range, and a value of 80 dB was selected (the results of these studies are discussed in detail in chapter 5). The time gain compensation swept gain setting was kept uniform thought the study.

The 3D sweep angle was set to 30 degrees, which was the maximum permitted. Table 3.1 shows the settings used in the study. These settings were saved as a group and stored on the ultrasound machine. This setting group was in turn utilised for all scanning

procedures in order to avoid the potential variations in the images, which may be caused

by different settings.

Setting	Value
Frequency	8.5 MHz
Depth of scan	4 cm
Gain	80 dB
Sweep gain	Central
Frame rate	22 fps
Focus point	Off
Post processing	Off
Type of scan setting	MSK
Dynamic range	80 dB
3D Sweep Angle	30 degrees

Table 3.1 Ultrasound settings parameters used in the study.

3.5 Data acquisition of the gastrocnemius muscle

Ultrasound scans were performed according to a standard protocol for all the subjects used in the study. During the ultrasound scanning procedure, the participants were asked to lie in a specific prone position on the scanning couch, adjusting the placement of their ankles, so that they are level with the end of setting of the scanning couch, it was ensured that their knees were fully extended.

The procedure of scanning the subjects is as follows:

1   The subject was to lay prone on the scanning couch.

2   A 2D scan using a 12 MHz linear probe was performed and this was used to mark the insertion of the gastrocnemius muscle at its origin. The 2D scan was used to locate the origin and insertion of the region of interest, as the 2D scan is quicker and easier to visualize the attachment point of the muscle etc. The proximal attachment was taken to be the posterior aspect of the capsule of the knee and the myotendon junction between the gastrocnemius and the Achilles tendon was taken as the distal attachment.

3   The length of the medial gastrocnemius was then measured.

4   A skin marker was then used to draw lines to distinguish the medial from the lateral of the gastrocnemius muscles.

5   To locate the area of interest in the gastrocnemius muscle, the underlying muscle was divided into 3 regions (proximal, central and distal) as shown in Figure (3.3). The distal region lies at the furthest end of the muscle where the muscle attaches to the Achilles tendon. The Central region covers the area between the proximal region where the muscle attaches to the knee and the distal region. The proximal region occupies the proximal end of the gastrocnemius muscle to the point at back of knee around the capsule, which is one of the origin locations.

The measured average length of medial gastrocnemius muscle of 10 subjects was 20.5cm. The length of the 3D probe is approximately 6.5cm, therefore this is the reason for the use of 6.5cm divisions of the distal and central regions: for ease in obtaining images with the use of one placement.

The point at which the gastrocnemius muscle attaches to the Achilles tendon was chosen as a reference point for measuring the length of the distal and central regions. These reference points were chosen because the proximal end of the gastrocnemius muscle is more difficult to visualize due to the complexity of the overlapping muscle and tendon that covers the posterior placement of the knee joint.

The central region (C) was chosen to be the region of interest (ROI) for this study, this was initiated, as the main aim of the study is to develop a non-invasive diagnostic method and once the methodology is developed and the hypotheses proved this method might be used for any region within the calf muscles.

A

6.5 cm

D C P
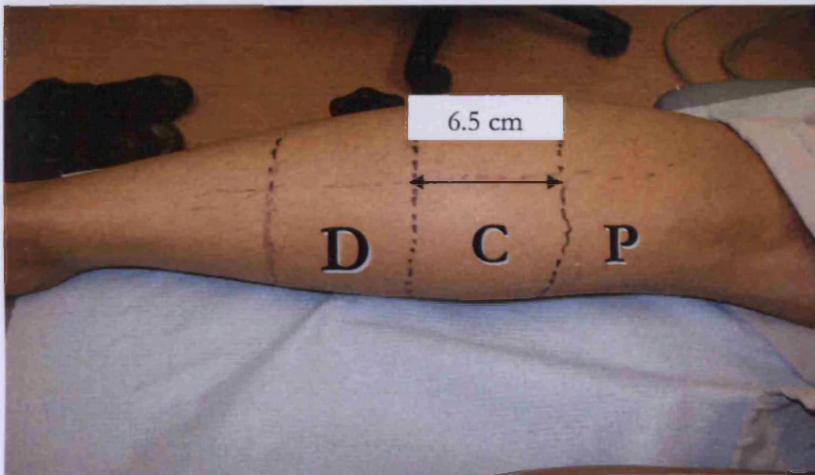
B

Figure 3.3 (A) Participant lying in the prone position (B) section divided 6.5 cm apart to determine the ROI , D: Distal region , C: Central region , P: Proximal region.

The probe was placed on the central region of the muscle (C) and a 3D ultrasound scan performed keeping the 3D probe in fixed position as shown in figure (3.4). The scan took approximately 2 seconds; care was taken during the scanning procedure to maintain the

same standard position of the participant and the placement of the transducer. The 3D

data set was consequently analyzed and a series of 2D cross-sectional ultrasound images

of the gastrocnemius were obtained from the set following processing. For the purpose of

analysis, four 2D image slices were extracted from the 3D set in the bitmap image

format. The distance between the image slices was chosen to be 10mm for consistency,

however the distance between slices is optional and may be selected from 0.2 mm up to

10mm.

Figure 3.4 Shows the manner in which the 3D probe was placed on the central region of the medial gastrocnemius muscle left leg.

Figure 3.5 depicts an example of a single 2D ultrasound image obtained from the 3D image set, from the central region of the gastrocnemius muscle. Figure 3.6 and 3.7 illustrate a schematic representation of the scanning method and the location of the 4 image slices.
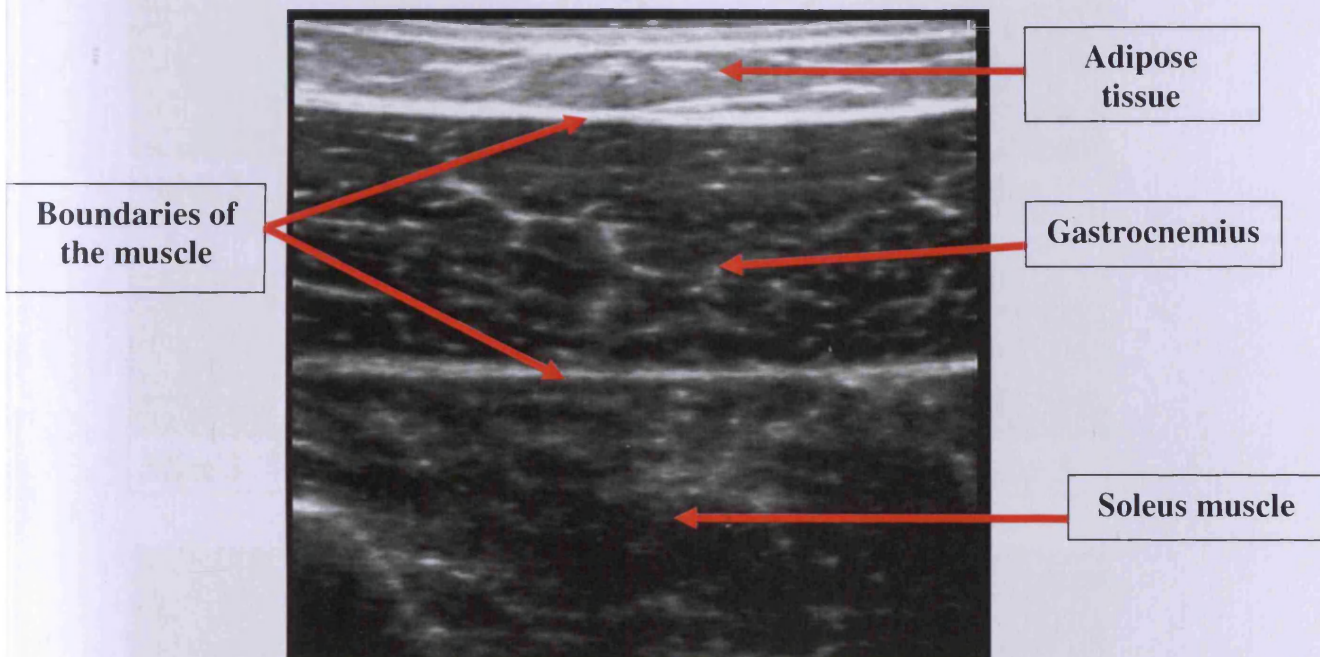
Figure 3.5 Ultrasound scan showing the cross section of gastrocnemius muscle
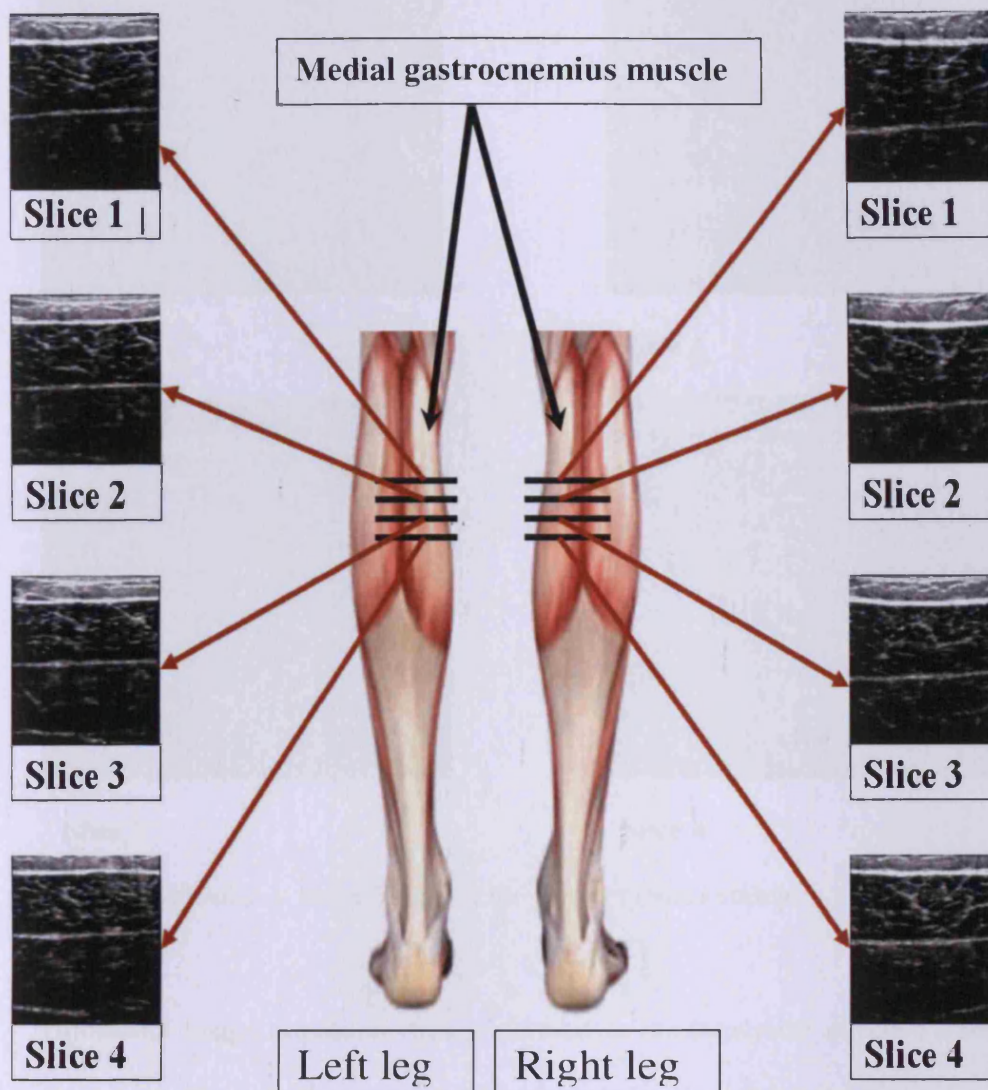
Figure 3.6 Shows the scanning sites and the four slices collected from left and right leg
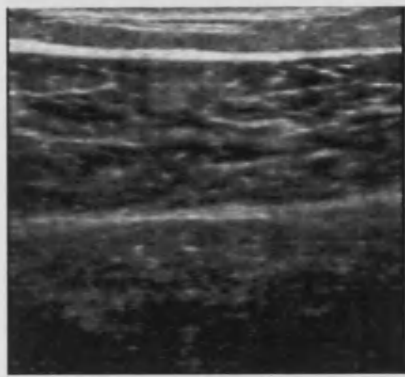
Slice 1   **Slice 2**
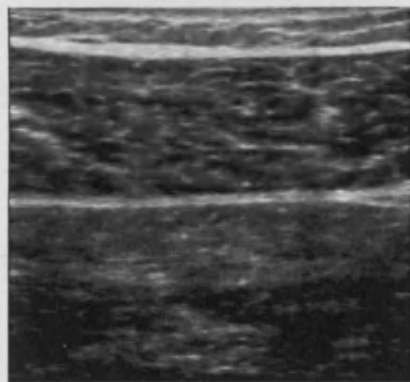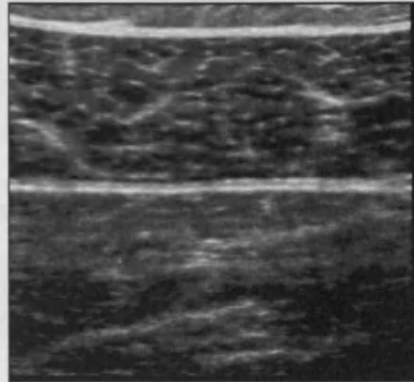
Slice 3   **Slice 4**

Fig 3.7 Four slices - series images of the gastrocnemius muscle

Ultrasound image acquisition was performed in the transverse direction covering the cross sectional area of the muscle. The longitude scan directions was not performed because a study by Nielsen et al (2000) found no statistically significant differences in the muscle tissue gray scale intensities between longitudinal and transverse scanning directions for any of the first order statistical parameters. There is a mark on the probe indicating the direction of the scan sweep, and this mark was used to ensure that the probe was placed in the same direction for all scans. The participants were asked to keep their muscle fully relaxed during the scan as contraction of the muscle may result in an increased muscle diameter and decreased echo intensity (Heckmatt et al. 1980, Heckmatt

et al. 1988b). The scan was repeated 10 times on each participant in order to obtain mean measurement values in the context of each leg, for each subject. A flow chart showing the image acquision and slice selection is detailed in figure (3.8).
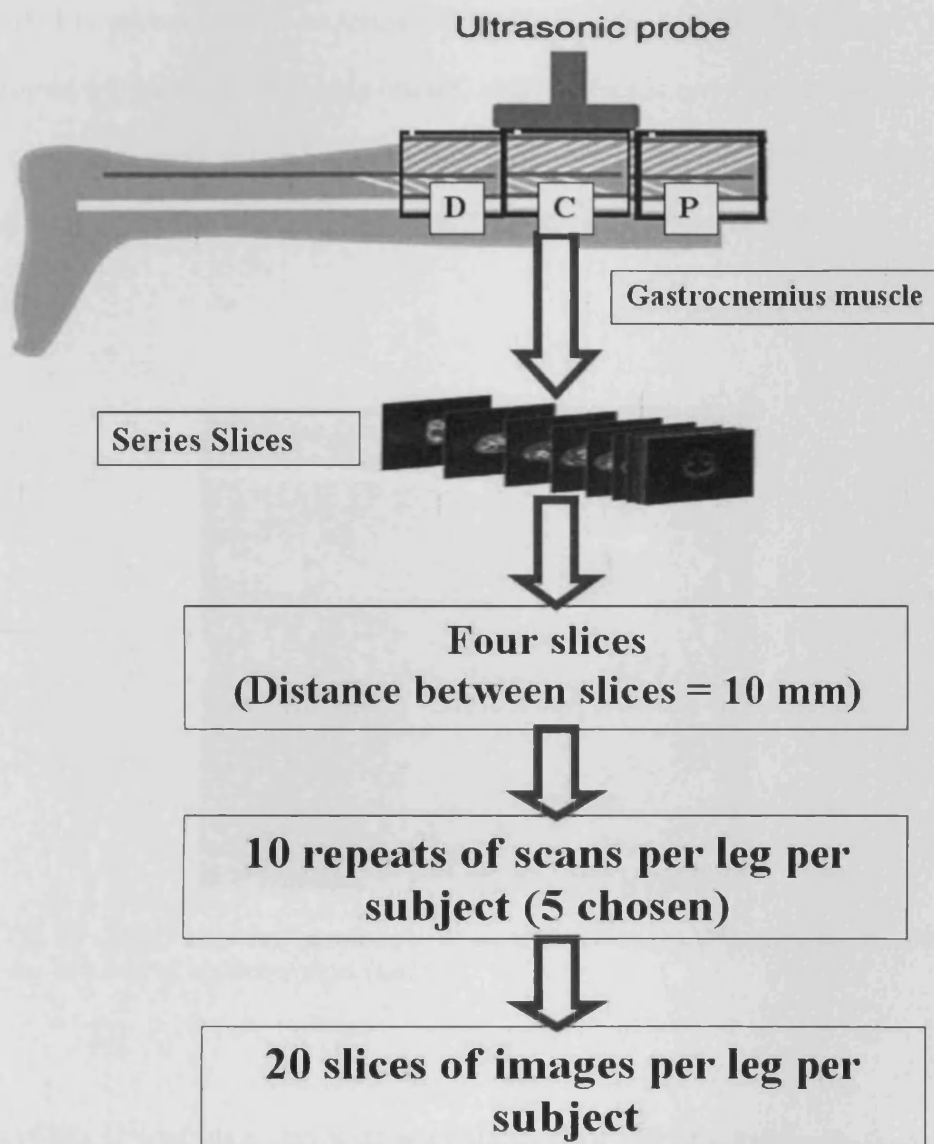
Figure 3.8 Flow chart showing the image acquisition methods (D: distal, C: central, P: proximal).

During the study, the participants were allowed to move and relax between each scan and the probe was repositioned to the standard position anew every time. All the scans were performed by the main investigator. In addition, five out of ten scans were selected to be included in the study by an experienced physicist at the Medical Physics and Clinical Engineering department, excluding images, which were not very clear due to artefacts or poor contact between the probe and the skin. Figure (3.9) shows an example of an image possessing an artefact due to the lack of application of the conduction gel.

Fig 3.9 Image showing an example of an air artefact at the transducer skin interface due to a lack of conductive gel (arrows).

The effects of artefacts within images are undesirable and may lead to misdiagnosis of the anatomical structure in question (Goldstein and Madrazo. 1981). One of the phenomenons that generate artefacts in ultrasound images is reverberation, which occurs

due to multiple reflections in the scanned subject or multiple reflections the region of interest and transducer (Angelsen 2000).

The extent to which these artefacts are presented is affected by the instrument and the instrument settings used (Lizzi et al. 2003). Image artefacts can occur for a number of reasons, and may lead to a more complicated interpretation procedure as important information may be lost(Angelsen 2000).

During the next stage of research, the texture parameters were extracted from the five images selected and the mean of each texture parameter was taken to reduce the impact of variation.

3.6 Image analysis

The 2D image slices were extracted from the 3D set on the ultrasound machine and stored in bitmap format in turn transferred to a personal computer for analytical purposes. Each 2D image extracted from the 3D set in the bitmap format was composed of 800x600 pixels, with gray scale values ranging from 0 to 255. The lowest value corresponded to the darkest, echo-poor area in the image, whilst the highest value (255) corresponded to the maximum brightness. The region of interest (ROI) for calculation was defined and marked manually with the aid of a computer mouse on each image within the border of the gastrocnemius muscle (the size of ROI selection will be discussed in more detail in chapter 4).

Texture analysis was performed using the software package MaZda 4.5 (Institute of Electronics, Technical University of Lodz, Poland), which allows for computation of

approximately 300 different parameters (see chapter 2 for more details regarding these parameters). The signal intensity of each ROI was normalized using the limitation of dynamics to $\mu\pm3\sigma$ (μ, gray-level mean; and σ, gray-level standard deviation) which is a feature option of the MaZda software (Szczypinski et al. 2009).

From each ROI the type of texture parameters extracted were as follows:

- First order statistics parameters including gray level, variance, skewness, and kurtosis (4 texture parameters).

- Second order statistics parameters including co-occurrence matrix, run length matrix, and gradient. With regards to the co-occurrence, 220 parameters (4 directions and 5 inter-pixel distances) were extracted from each ROI and the sum of these parameters was considered for analysis. With regards to the run length matrix, 20 parameters (5 run length- matrix-based features at 4 different directions each) were extracted from each ROI and the sum of these parameters was considered for analysis. With reference to gradient, 5 parameters were extracted from each ROI and the sum of these parameters was considered for analysis.

- Auto-regressive (AR) model parameters: 5 parameters extracted from each ROI and sum of these parameters was considered for analysis.

- Wavelets transform parameters: 12 parameters extracted from each ROI and sum of these parameters was considered and first, second and third scale parameter values were only considered. The MaZda software did not allow for the computation of the wavelet fourth, fifth and sixth scale parameter values from a small ROI. Therefore, these wavelet parameters were excluded from further feature selection. (For more details regarding these parameters refer to chapter 2).

3.7 MaZda Software

The MaZda software has been in development since 1998. The name of the program is an acronym derived from 'Macierz Zdarzen', which is the Polish counterpart for the English term 'co-occurrence matrix'. It was written for the research project titled "Quantitative Analysis of Magnetic Resonance Image Texture". The MaZda package enables calculation of almost 300 texture features (covering the basic texture parameters known from the literature) (Szczypinski et al. 2007). These features may be calculated for the entire image or with respect to defined regions of interest (ROI).

The program code has been written in C++ and Delphi TM with the use of OpenGL libraries. It has been compiled for computers that use Microsoft Windows 9x/NT/2000/XP operating systems (Szczypinski et al. 2007).

Typical steps of image texture analysis are described in the flowchart presented in figure (3.10).
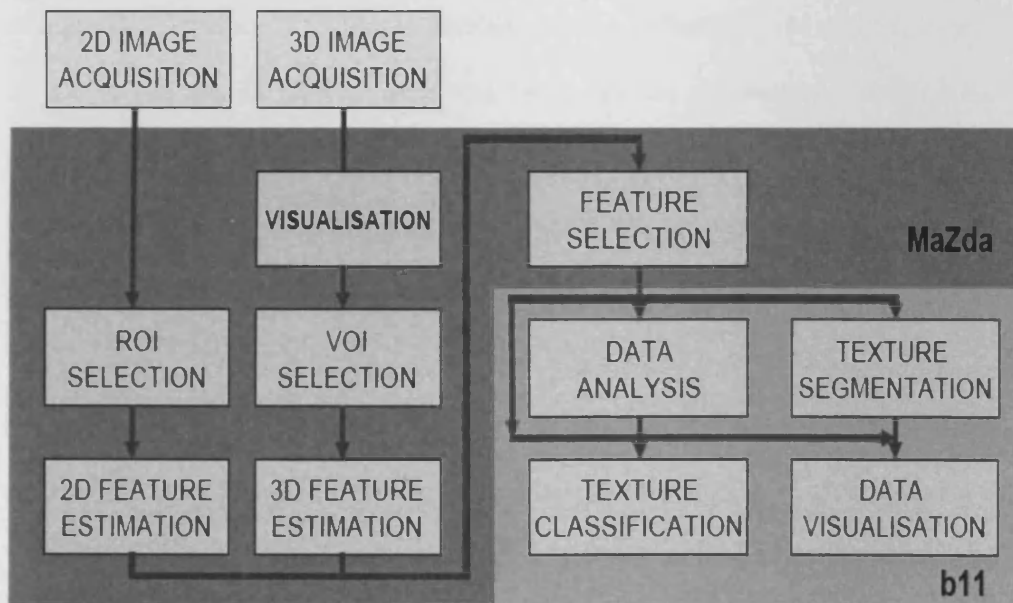
Figure 3.10 Main steps in texture analysis using the MaZda package (Szczypinski et al. 2007).

The first step of the program is image acquisition; any acquisition device, which generates a digital image, may be used as an input for the software such as an MRI scan, CT scan, or Ultrasound images. MaZda software can download images in the most popular imaging format such as Windows, bitmaps and DICOM formats. The next step is to draw the ROI, it is possible to draw a region of interest on the image or analyze the image as a whole. The software allows for definition of up to 16 ROI's within a single image. If more than 16 regions are required for analysis, they may be analyzed successively, ranging up to 16 at a time (Szczypinski et al. 2007, Szczypinski et al. 2009). Once these ROI's have been established, MaZda allows for the calculation of texture parameters available from a list of approximately 300 different definitions.

Features extraction is the first stage of image analysis. The results obtained from this stage are used for texture discrimination, texture classification or for tracing the texture changes in a sequence of images to monitor structural changes over time (Szczypinski et al. 2009). The MaZda software uses three computational approaches, namely: statistical, model based and image transform methods (Szczypinski et al. 2009). Statistical approaches represent the texture indirectly using the non-deterministic properties that govern the distributions and relationships between the gray-levels of an image.

The model-based texture analysis, using fractal or stochastic models, attempt to interpret an image texture using generative image models and stochastic models, respectively. Transform methods of texture analysis, such as Fourier, Gabor, or wavelet transforms (Cohen 1989, Bovik et al. 1990, Daugman 1988) represent an image in a space with a co-ordinate system, which is related to the characteristics of a texture.

The MaZda software was applied to identify and differentiate biomedical image areas with different textural features, as those that represent healthy and pathological tissue. The MaZda package is a reliable and robust tool for the analysis of image textures (Szczypinski et al. 2009).

Chapter 4   Influence of Depth and Size of Region of Interest (ROI) on Texture Features

4.1 Introduction

The affect of attenuation with depth of ultrasound, the size of the region of interest, gain, and dynamic range are important variables to consider as they can influence the analysis of texture features. These sources of variability have to be considered carefully when evaluating image texture as different settings might influence the resultant image. The influence of gain and dynamic range on texture features will be discussed in detail in Chapter 5. Ultrasound depth is an important parameter to consider, the strength of the ultrasound echo signal will weaken with depth due to the attenuation of the ultrasound signal by tissue.   In clinical B-scan ultrasound, the texture features of an organ or region is highly dependant on the distance between the tissue and the transducer. The texture features might not be the same from the top to the bottom of an image for the same tissue; this is due to the intervening tissue layers that are present between the transducer and the tissue layer of interest (Powis R and Powis W 1984). Moreover, the strength of the attenuated ultrasound signal decreases with depth, the returning echo from farther structures will be weaker than those returning from closer layers(Muzzolini 1996).The ultrasound machine attempts to compensate for this effect by using time gain compensation (TGC) to boost the level of the signal from deeper depth.

A study by Morris (1988) did not examine in detail the influence of depth on the correction of image. Morris (1988) used co-occurrence matrix to devise a simple

algorithm for deriving a correction factor for depth dependence using a foam phantom and demonstrated it is efficacy on placental data. Other studies by Fatemi and Kak (1980), Cloostermans, and Thijssen (1983) studies the formation of the ultrasound beam which they claimed could be used for a depth correction. This unfortunately means that these algorithmic programs need extensive calculation and are not readily useful. In normal practice, the analysis is confined to the ROI that has a set distance to the transducer (Raeth et al. 1985, Nicholas et al. 1986). In this way, the flexibility in the choice of size and location the ROI is reduced (Oosterveld et al. 1991). It was noted that most of the literature describing the analysis of texture features employ some corrections for the depth dependant properties of the sound beam, which if not carried out would influence the estimation (Cloostermans et al. 1986, Verhoef el al. 1985, Insana 1983, Fink and Cardoso 1984). The size and shape of the ROI are also important variables to consider when analysing ultrasonic tissue textures. There are number of studies (Brooke-Wavell et al. 1995 , Fournier et al. 1997 , Damilakis et al. 1998), showing that the differences in the size and location of the ROI can affect the reliability of quantitative ultrasound assessments. Although diagnostic ultrasound has been a useful tool for many years where researchers have used computerized algorithms to assist clinicians to diagnose diseases, the effects of size and shape of ROI in texture analysis have been poorly addressed and studied. This study investigates the texture features along the length of the medial gastrocnemius muscle at different sites and the effects of depth and ROI on the texture parameters to see which are influenced by depth and size of ROI

4.2 Participants

In this study, 10 healthy volunteers (8 male /2 female, mean age: 25 {range 18-38}) were chosen. The left medial head of gastrocnemius muscle for all subjects was scanned using the Toshiba ultrasound system with 3D transducer (for more details please see chapter 3). The left leg was chosen because no significant features were noted between the right and the left legs (see chapter 7 for more details). Informed consent was obtained from all participants after explaining the aim, protocol, and procedures in the study (see Appendix B). All volunteers declared having normal health, with no history of any musculoskeletal disorder. The study was approved by the local Ethics Committee. The 3D ultrasound sweep was performed in the central (middle) region of the muscle. Following this, four 2D images were extracted from the 3D data set with a distance of 10mm between them. All the scans were performed using the standard protocol described in Chapter 3.

4.3 Scanning sites along length of the gastrocnemius muscle

4.3.1 Method

On each ultrasound image slice, the largest possible rectangular shaped ROI with size of 250x 90 pixels that encompassed the gastrocnemius muscle was defined. The size and shape of the ROI were kept the same for all slices and subjects. The ROI was defined at the same level of depth for all subjects within the border of the gastrocnemius muscle and avoiding neighbouring structures.

4.3.2 Statistical analysis

The Shapiro- Wilko test was used to test the normality of the data due to the small sample size of the study (P >0.05 was considered normal distributed).One-way ANOVA test was used for the normally distributed data and the Wilcoxon- Mann Whitney test was used for the non –normally distributed data (P value less than 0.05 was considered statistically significant).The SPSS for Windows Version 16(SPSS inc., Chicago, Illinois, USA) was used for the statistical analysis.

4.3.3 Result

Figures 4.1 to figure 4.4 show the values of first order statistic parameters gray level, variance, skewness, and kurtosis. The figures 4.5 to 4.9 show second order statistic parameters co-occurrence matrix, run length matrix and gradient, autoregressive model and wavelet transforms at different scanning sites along the length of the gastrocnemius muscle (central region). The trends in these parameters were similar in all four image slices. The mean values for each parameter is shown in table (4.1), upper and lower confidence interval set at 95%. All four image slices showed no significant difference (p>0.05) in texture features along the length of the gastrocnemius muscle. This finding indicated that the middle part of the gastrocnemius muscle is homogenous and that is why a single one of the 2D image can be used.
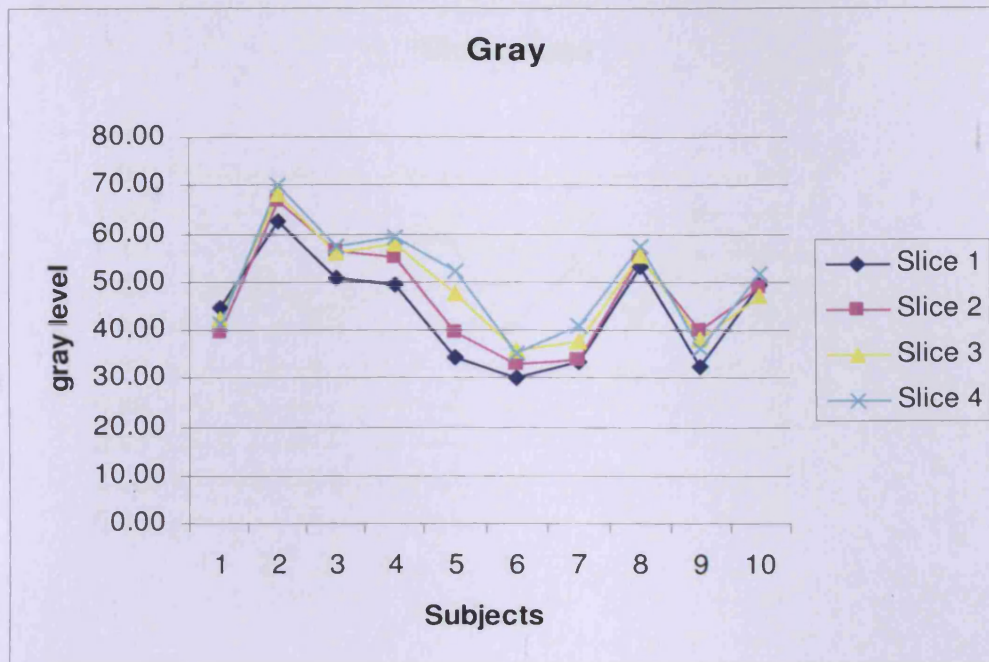
Figure 4.1 Line graph showing the dispersion of gray level values at different scanning sites along length the gastrocnemius muscle (slice 1 to slice 4 represent the scanning sites)
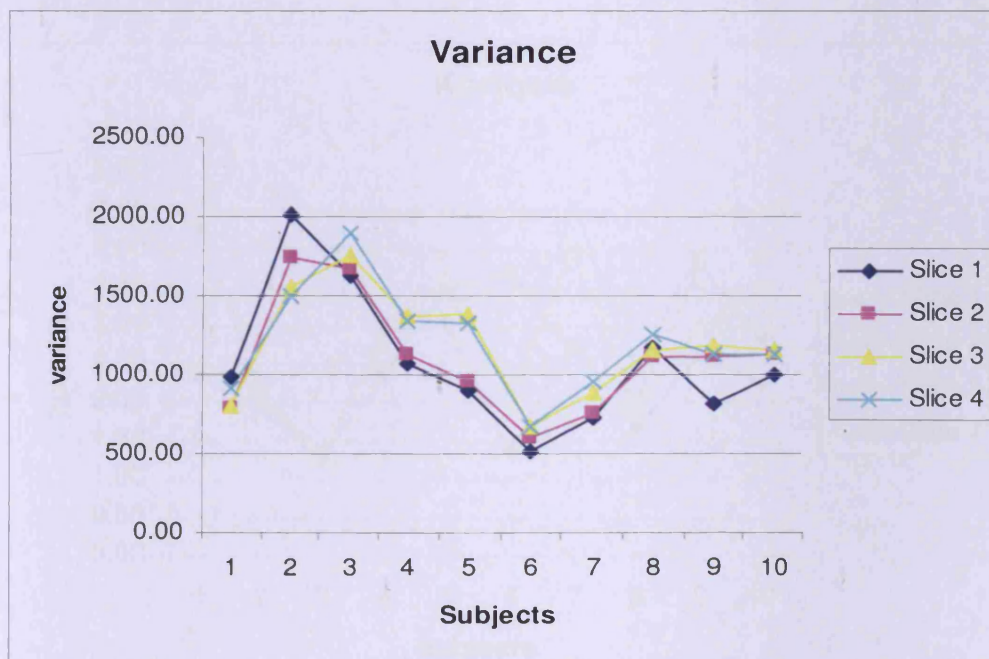
Figure 4.2 Line graph showing the dispersion of variance values at different scanning sites along length the gastrocnemius muscle (slice 1 to slice 4 represent the scanning sites)
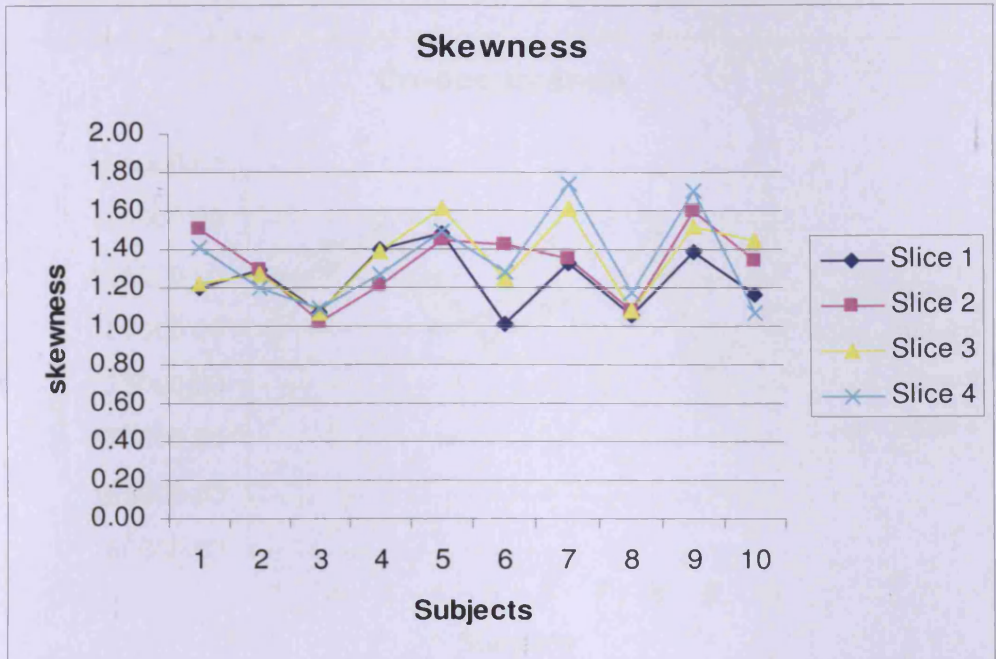
Figure 4.3 Line graph showing the dispersion of skewness values at different scanning sites along length the gastrocnemius muscle (slice 1 to slice 4 represent the scanning sites)
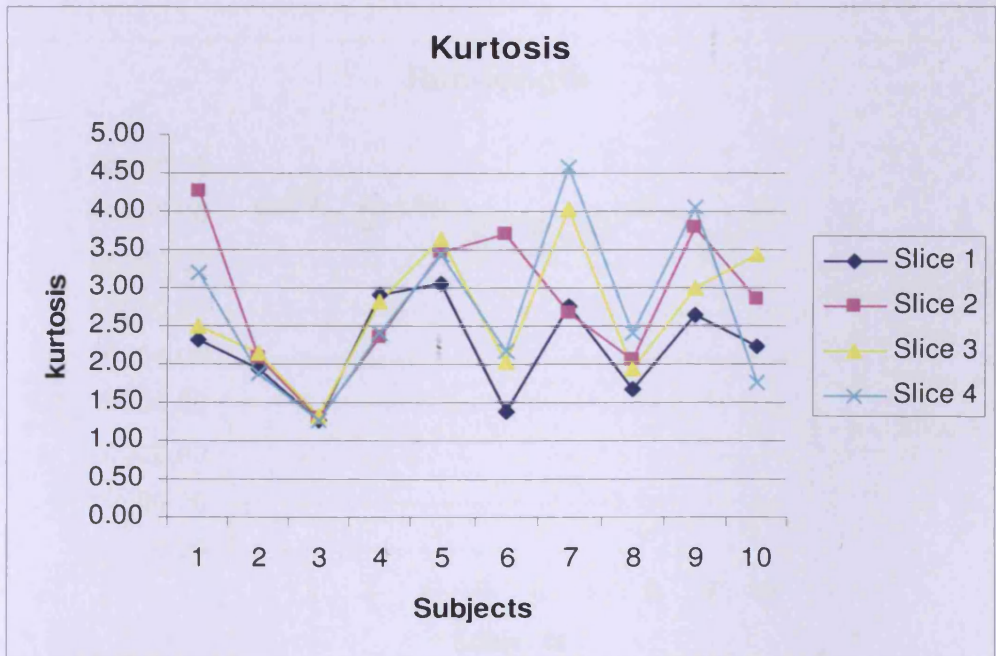
Figure 4.4 Line graph showing the dispersion of kurtosis values at different scanning sites along length the gastrocnemius muscle (slice 1 to slice 4 represent the scanning sites)

73
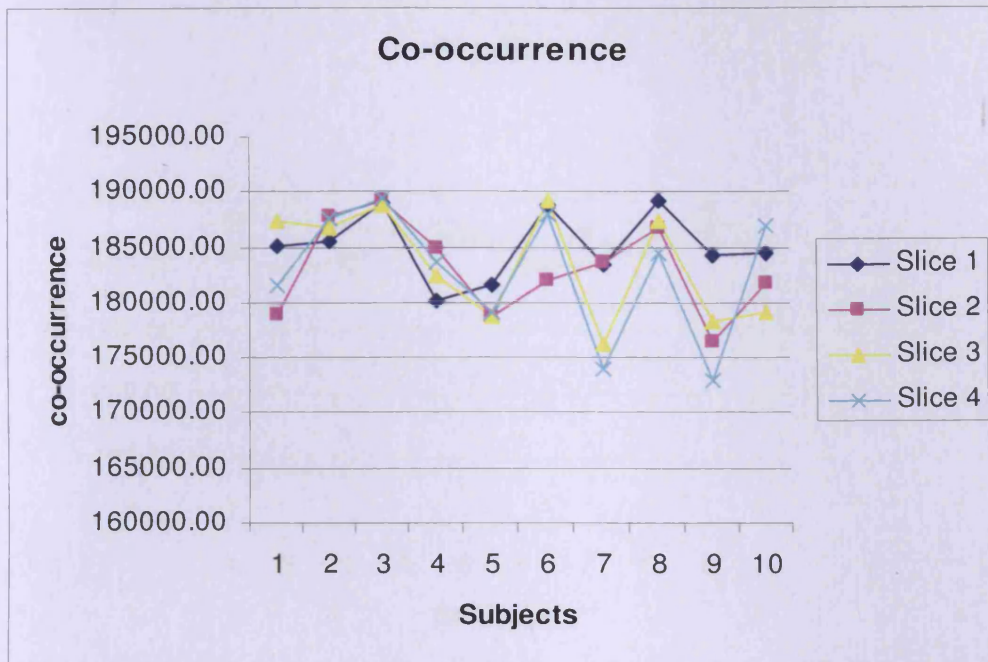
Figure 4.5 Line graph showing the dispersion of co-occurrence matrix values at different scanning sites along length the gastrocnemius muscle (slice 1 to slice 4 represent the scanning sites)
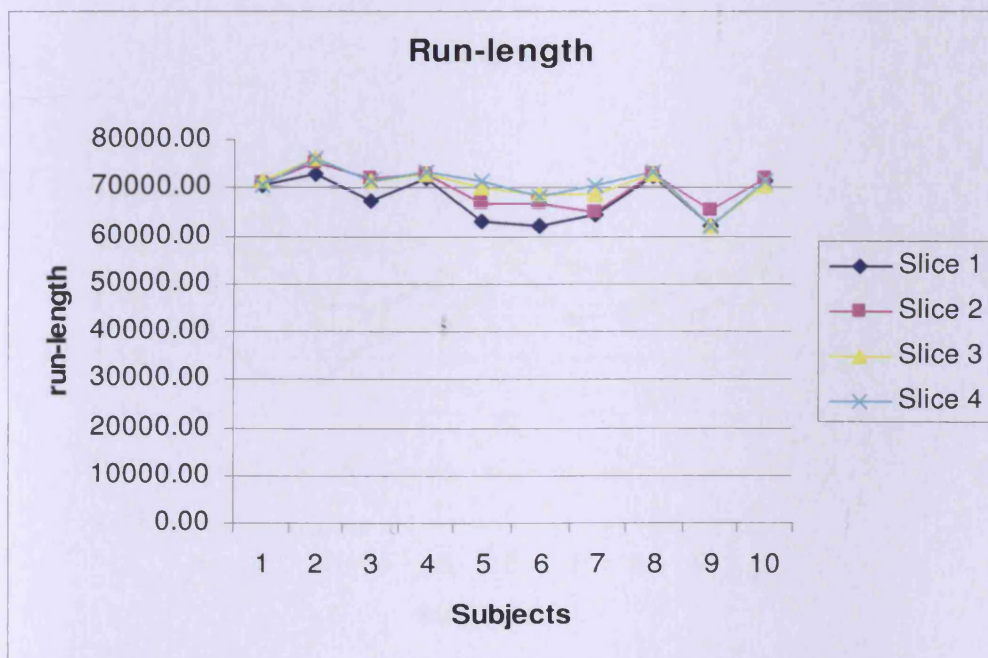
Figure 4.6 Line graph showing the dispersion of run length matrix values at different scanning sites along length the gastrocnemius muscle (slice 1 to slice 4 represent the scanning sites)
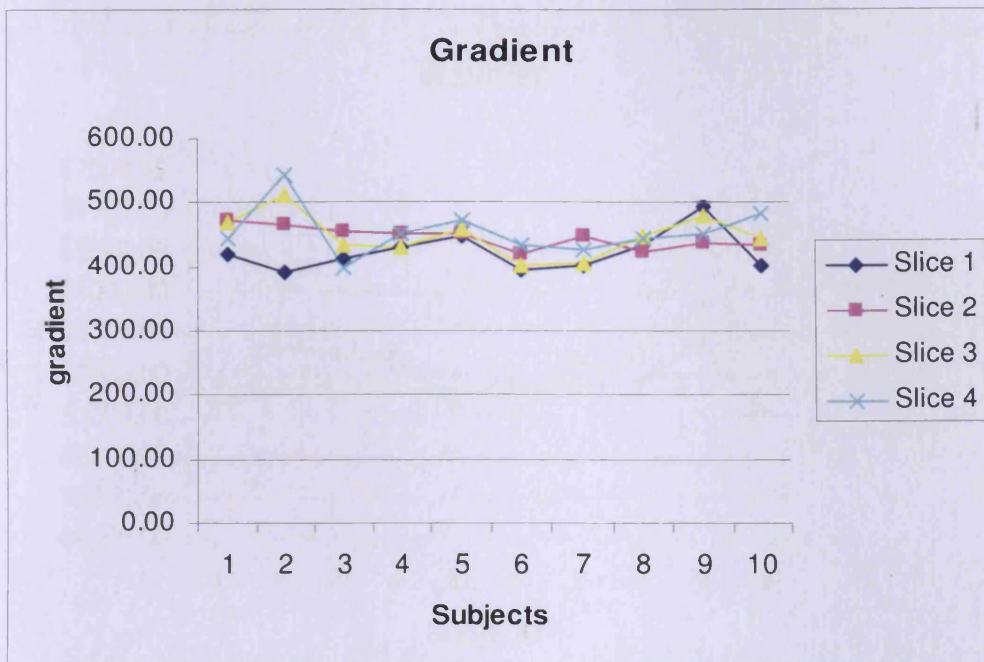
Figure 4.7 Line graph showing the dispersion of gradient values at different scanning sites along length the gastrocnemius muscle (slice 1 to slice 4 represent scanning sites)
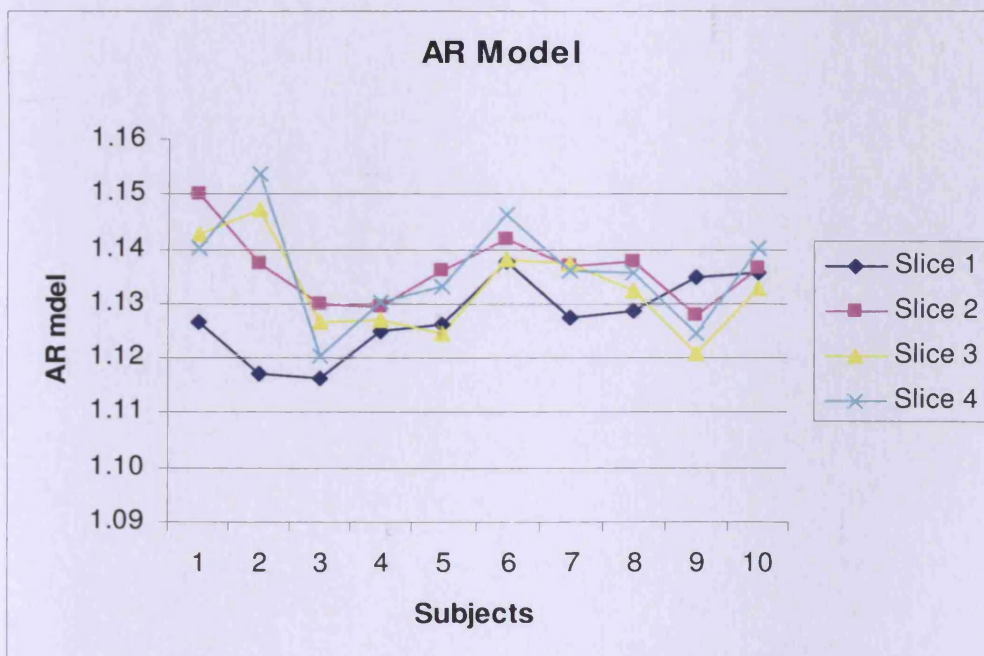
Figure 4.8 Line graph showing the dispersion of auto-regressive model values at different scanning sites along length the gastrocnemius muscle (slice 1 to slice 4 represent the scanning sites)
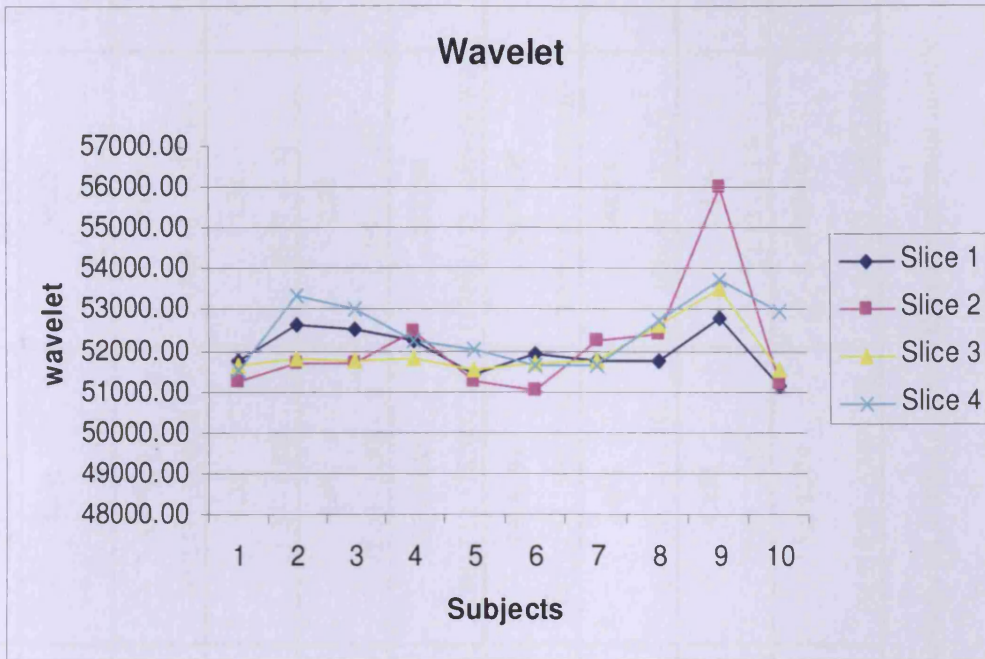
Figure 4.9 Line graph showing the dispersion of wavelet transform values at different scanning sites along length the gastrocnemius muscle (slice 1 to slice 4 represent the scanning sites)

Texture Parameters	Slice 1	Slice 2	Slice 3	Slice 4	p-value
Gray level	44.05 (36.28 - 51.83)	46.82 (38.74 -54.87)	48.61 (41.02 - 56.19)	50.22 (42.07 - 58.38)	0.636
Variance	1082.83 (768.28 - 1397.38)	1097.62 (832.66 - 1362.57)	1193.56 (950.41 - 1436.72)	1211.6 (967.10 - 1455.20)	0.821
Skewness	1.24 (1.12 - 1.36)	1.33 (1.20 - 1.46)	1.35 (1.20 - 1.50)	1.34 (1.17 - 1.51)	0.591
Kurtosis	2.23 (1.76 - 3.25)	2.85 (2.18 - 3.52)	2.67 (2.08 - 3.30)	2.72 (1.95-6 - 3.49)	0.420
Co-occurrence matrix	185193.06 (182960.98 - 187425.14)	183030.95 (180010.27 - 186051.63)	183425.63 (179849.12 - 187002.14)	182798 (178627.75 - 186968.90)	0.655
Run length matrix	67819.79 (64523.18 - 71116.40)	70053.22 (67464.24 - 72642.20)	70481.91 (67890.94 - 73072.88)	70972.95 (68343.87 - 73602.02)	0.298
Gradient	423.43 (401.22 - 445.64)	446.29 (434.11 - 458.47)	448.5 (424.51 - 472.49)	454.73 (426.80 - 482.66)	0.144
AR Model	1.127 (1.12 - 1.13)	1.136 (1.13 - 1.14)	1.133 (1.13 - 1.14)	1.136 (1.13 - 1.14)	0.075
Wavelet	51993.93 (51602.36 - 52385.50)	52135.07 (51097.57 - 53172.57)	51962.74 (51516.30 - 52409.16)	52486.67 (51922.17 - 53037.17)	0.573

Table 4.1 Mean values (upper and lower CI=95%) and p-values for texture parameters for all scanning sites in the gastrocnemius muscle

4.4 Depth Dependence

4.4.1 Method

The depth effect was tested by manually marking two regions A and B with varying depths using the computer mouse for each image. The regions A and B were defined within the muscle boundary as seen in figure 4.10. The size of both ROI's was 280* 20 pixels and the distance between region A and B was kept constant at 5 mm. The distance between the skin and region A was kept constant at 10 mm.
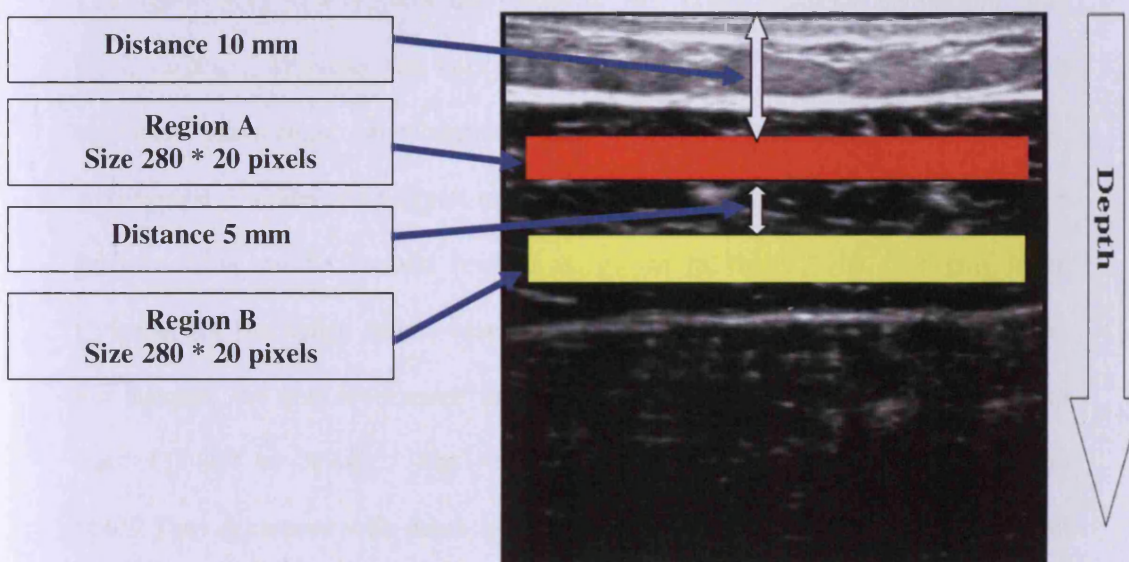
Figure 4.10 Region A and Region B (ROI's) are showing pixel size, distance between them and distance from skin. The ROI is shown within the border of gastrocnemius muscle.

4.4.2 Statistical analysis

The Shapiro- Wilk test was used to test the normality of the data due to the small sample size of the study (P > 0.05 was considered normal distributed). The paired t – test was used to test the depth effect for the normally distributed data and the Wilcoxon –Mann-Whitney test was used for the non-normally distributed data. (P value less than 0.05 was considered statistically significant).The SPSS for Windows Version 16(SPSS inc., Chicago, Illinois, USA) was used for the statistical analysis.

4.4.3 Result

The figures 4.11 to 4.14 show the values of first order statistical parameters: gray level, variance, skewness, and kurtosis. The figures 4.15 to 4.19 show second order statistical parameters: co-occurrence matrix, run length matrix and gradient, autoregressive model and wavelet transforms at two different depths A and B of the gastrocnemius muscle (central region) as shown in figure 4.10. The gray level, variance, and run length matrix were significantly lowered when the depth increased. For instance, the gray level mean value decreased from 53.54 to 34.38 and variance from 1374.19 to 789.46. The run length matrix decreased from 18175.71 to 16419.They decreased with depth as the strength of the ultrasound echo signal will weaken with depth due to the attenuation of the ultrasound signal by tissue. The other texture parameters showed similar values at different depth. The mean value for each texture parameter at both depths is shown in table 4.2 (upper and lower confidence interval 95%). All the texture parameters showed no significant difference between depths A and B (p > 0.05) except for gray level , variance and run length matrix (p < 0.05). This indicates that gray level, variance, and run length matrix are depth dependant.
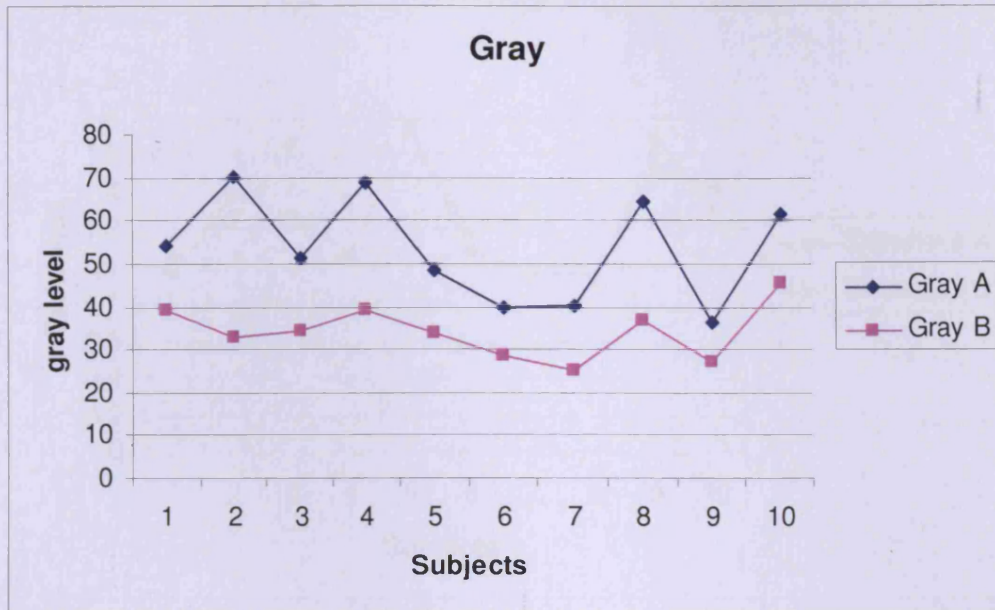
Figure 4.11 Line graph showing the dispersion of gray level values at depth A and depth B for the ten participants.

Figure 4.12 Line graph showing the dispersion of variance values at depth A and depth B for the ten participants.
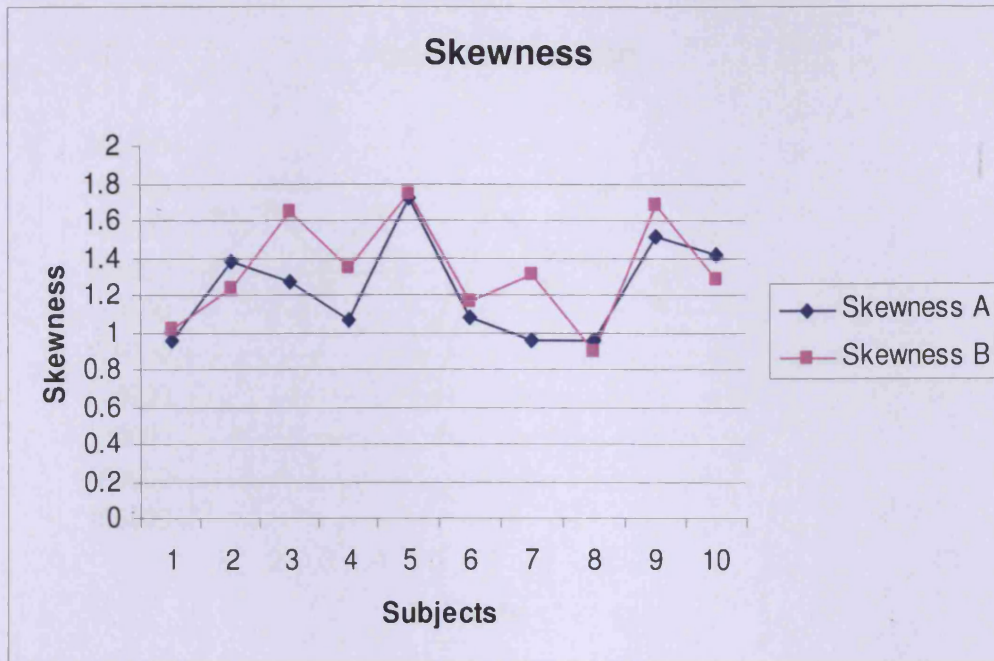
Figure 4.13 Line graph showing the dispersion of skewness values at depth A and depth B for the ten participants.
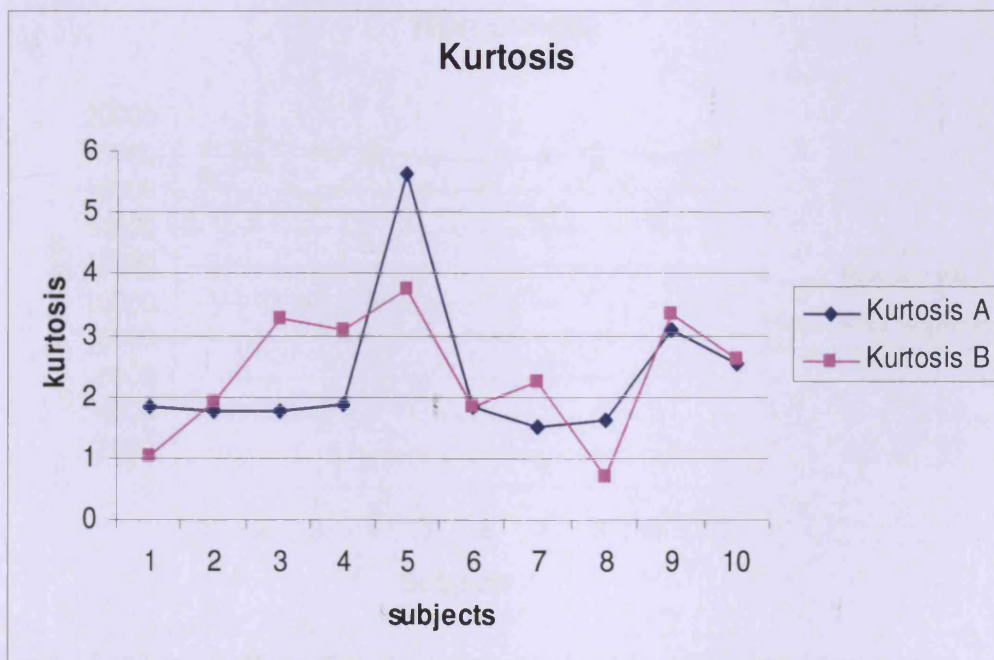
Figure 4.14 Line graph showing the dispersion of the kurtosis values at depth A and depth B for the ten participants.
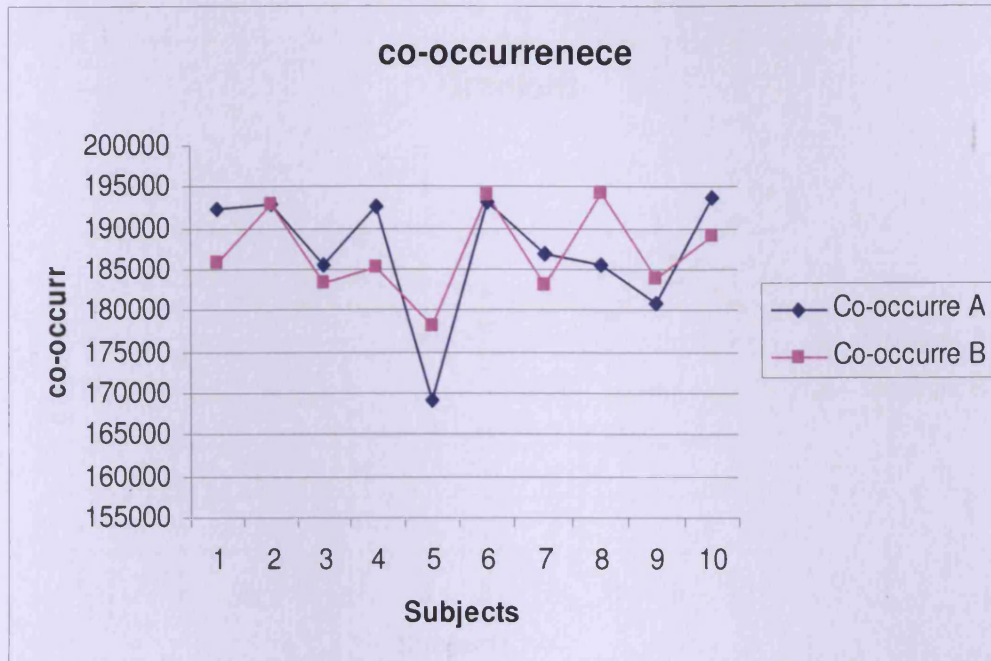
Figure 4.15 Line graph showing the dispersion of the co-occurrence matrix values at depth A and depth B for the ten participants.

Figure 4.16 Line graph showing the dispersion of the run length matrix values at depth A and depth B for the ten participants.
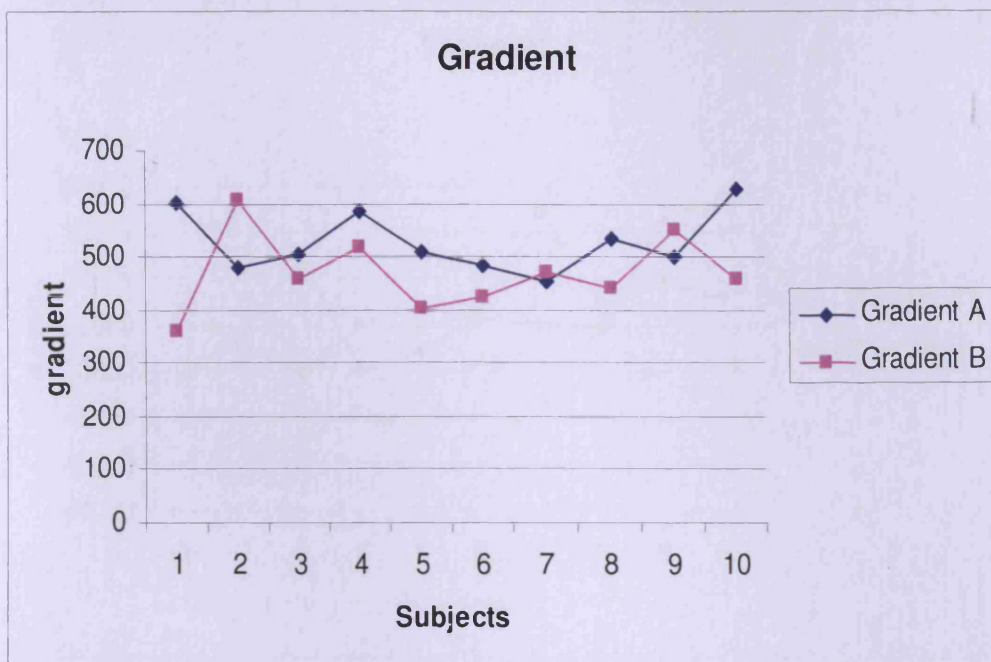
Figure 4.17 Line graph showing the dispersion of the gradient values at depth A and depth B for the ten participants.
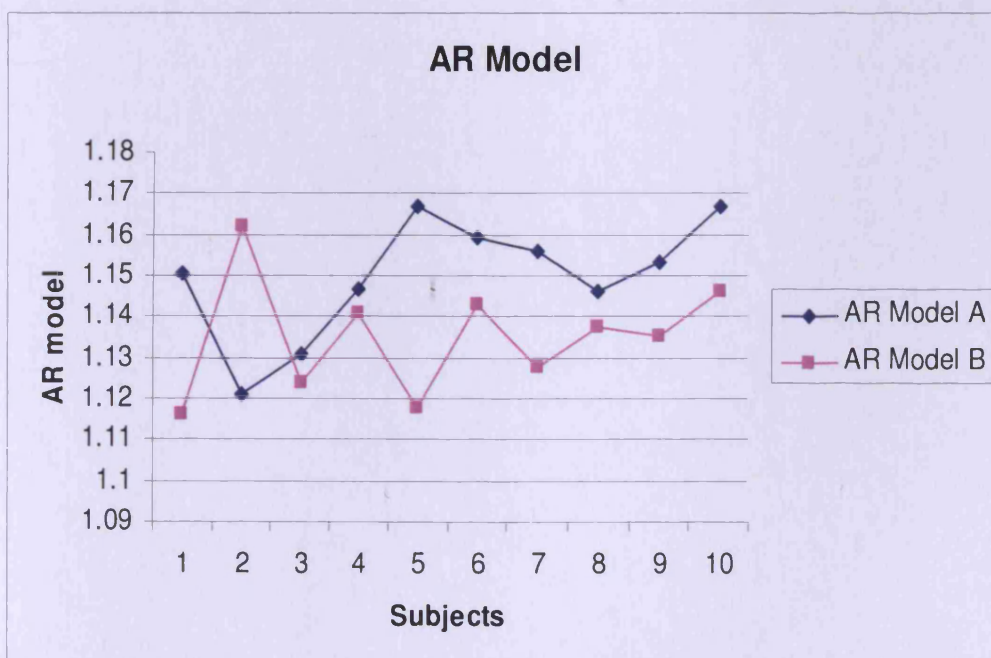
Figure 4.18 Line graph showing the dispersion of auto-regressive model values at depths A and depth B for the ten participants.
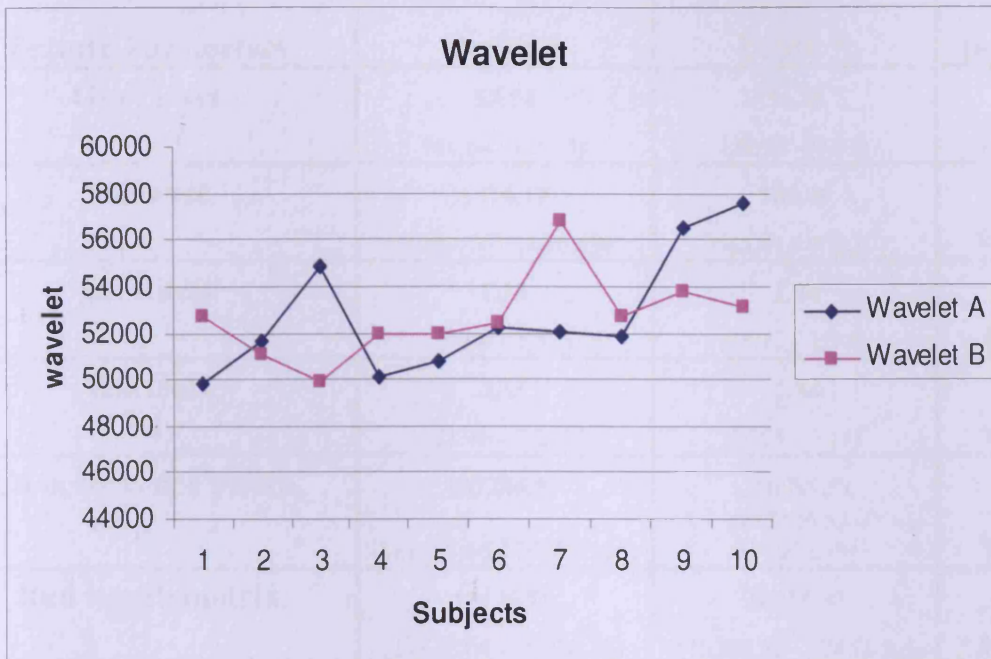
Figure 4.19 Line graph showing the dispersion of wavelet transform values at depths A and depth B for the ten participants.

Texture Parameters	Depth A	Depth B	p-value
Gray level	53.54 (44.64 - 62.45)	34.38 (29.93 -38.83)	0.000*
Variance	1374.19 (1069.76 - 1678.63)	789.46 (645.81 - 933.10)	0.002*
Skewness	1.23 (1.04 - 1.42)	1.34 (1.13 - 1.54)	0.118
Kurtosis	2.35 (1.46 - 3.24)	2.34 (1.65 - 3.11)	0.926
Co-occurrence matrix	187286.81 (181753.56 - 192820.06)	186999.52 (183126.54 - 190872.49)	0.880
Run length matrix	18175.71 (17840.64 - 18510.78)	16419.37 (15386.25 - 17452.50)	0.001*
Gradient	528.33 (486.64 - 570.01)	468.97 (416.85 - 521.08)	0.113
AR Model	1.135 (1.125 - 1.145)	1.497 (1.139 - 1.160)	0.082
Wavelet	52745.77 (50826.04 - 54665.51)	52639.72 (51335.23 - 53944.21)	0.918

Table 4.2 Mean values (upper and lower CI=95% of the mean) and p-values for texture parameters for depths A and B (* $p < 0.05$ Significant difference).

4.5 Size of Region of Interest (ROI)

4.5.1 Method

In order to investigate the influence of ROI on texture features, three groups of ROI were chosen with different sizes and shapes for investigation as shown in table (4.3).

First group

ROI was selected to be a rectangular window with size of 250*80 pixels then the ROI was reduced in horizontal and vertical direction(2 dimensional reduction) by approximately half to 125*40 pixels, 50*20 pixels, and 20*10 pixels respectively.

Second group

ROI was selected as rectangular window with size of 280*80 pixels then the ROI was reduced in the vertical direction to 280*40 pixels, 280*20 pixels and 280*10 pixels respectively.

Third group

ROI was selected as square window with size of 80*80 pixels then the ROI was reduced in horizontal and vertical direction by half to 40*40 pixels and 20*20 pixels

	ROI 1	ROI 2	ROI 3	ROI 4
Group 1	250*80	125*40	50*20	20*10
Group 2	280*80	280*40	280*20	280*10
Group 3	80*80	40*40	20*20	---------

Table 4.3 The three groups of ROI sizes, with initial pixel size and sizes after reduction. ROI 4 for group 3 was not included because 10 *10 was considered too small for the purpose of analysis.

Care was taken to define all the ROI having the same size at the same level of depth

on the same location for all subjects within the border of the gastrocnemius muscle,

avoiding muscle boundaries, or neighbouring structures.

4.5.2 Statistical analysis

The Shapiro- Wilk test was used to test the normality of the data due to the small

sample size of the study (P > 0.05 was considered normal distributed). One-way

ANOVA test was used for the normally distributed data and the Wilcoxon- Mann

Whitney test was used for the non –normally distributed data (P value less than 0.05

was considered statistically significant).The mean and standard deviation was

calculated for each texture parameter. The coefficient of variance (CV) was calculated

to evaluate the variation of texture parameters with different sizes of ROI. The CV is

the ratio of the standard deviation and the overall mean and is expressed as a

percentage. The SPSS for Windows Version 16(SPSS inc., Chicago, Illinois, USA)

was used for the statistical analysis.

4.5.3 Results

For group 1 where the size of ROI was varied, the figure 4.20 show the coefficient variation for first order statistics parameters. The first order statistical parameters gray level, variance, skewness, and kurtosis all showed a high CV of more than 19% at all sizes of ROI. The CV at size 20000 pixels for gray level shows 24.004 %, for variance 38.745 %, for skewness 19.375 % and for kurtosis 39.450 %. These coefficient variations were increased as the size of ROI decreased. Figure 4.21 shows the coefficient variation for second order statistics parameters, AR model and wavelet transform. The CV at size 20000 pixels for co-occurrence matrix 2.466 % , for run length matrix 6.626 % , for gradient 9.69 % , for AR model 0.822 % and for wavelet transform 0.89 %. This coefficient of variation increased when the size of ROI decreased, however most of texture parameters at size of ROI 5000 pixels show low CV .Therefore, a size of 5000 pixels as the minimum size of ROI for tissue characterization is taken for this study (this is shown in figure 4.21 and figure 4.22 as cut off point).

For groups 2 and 3, similar results were achieved (see Appendix A) suggesting that the shape of the ROI had no influence on the texture features. Table (4.4) shows the coefficient variations (CV) for each texture parameter in each group of ROI. When considering all groups (with different shape and size),most of texture parameters showed low variation except for gradient and run length matrix figure (4.22).
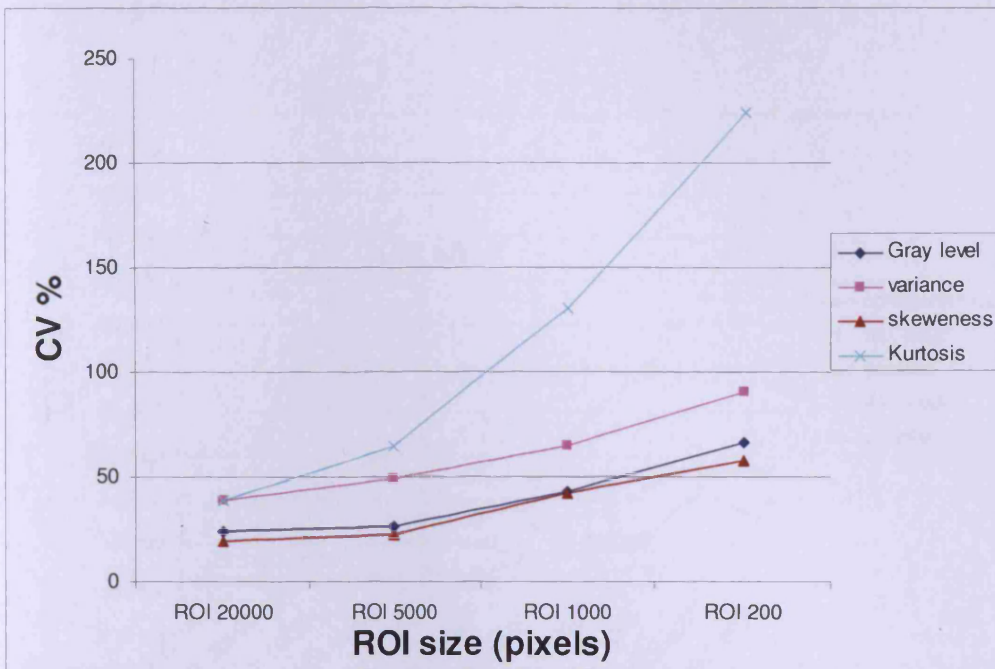
Figure 4.20 Coefficient of variation (CV %) of the first order statistic parameters for all sizes of ROI for group 1.
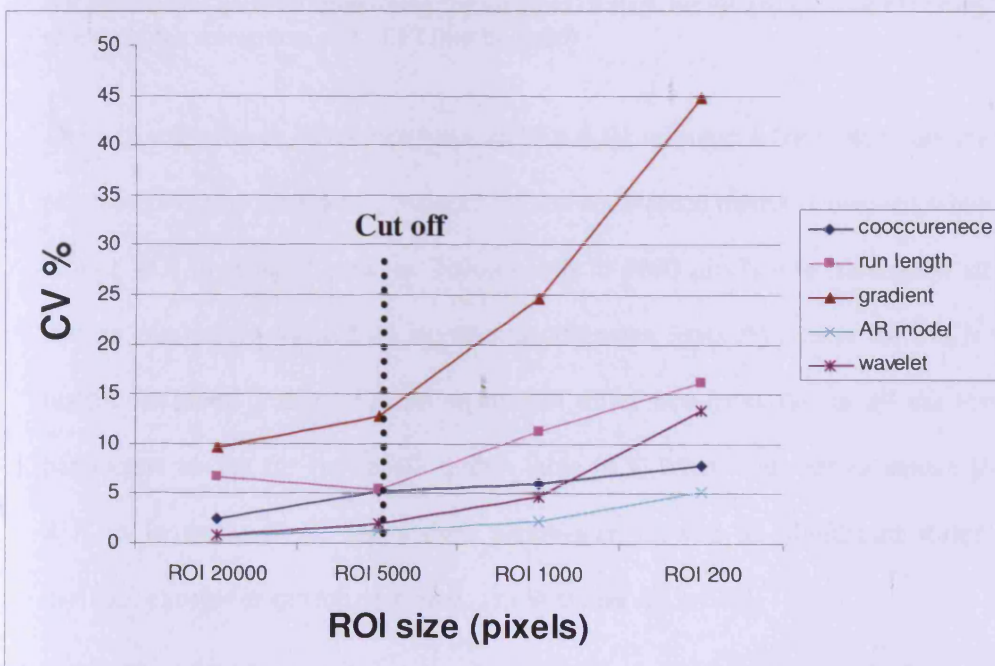
Figure 4.21 Coefficient of variation (CV %) of the second order statistic parameters AR model and wavelet transforms for all sizes of ROI for group 1 (cut off point represent the minimum size of ROI to be used)
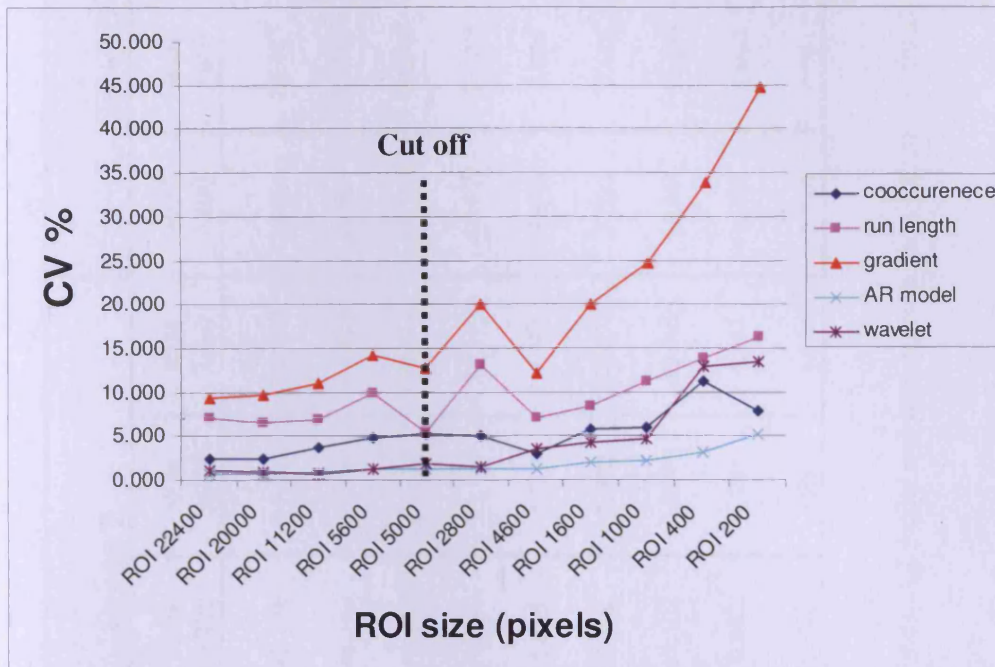
Figure 4.22 Coefficient of variation (CV %) for the second order statistic parameters AR model and wavelet transforms for all sizes of ROI for all groups (cut off point represent the minimum size of ROI to be used)

There is a significant difference between ROI sizes in-group 1 for most of the texture parameters except gray level, variance and co-occurrence matrix. However, when the size of ROI in group 1 between 20000 pixels to 5000 pixels was considered all the texture parameters showed no significant difference (p>0.05) except for run length matrix. In group 2 there was no significant difference (p>0.05) for all the texture parameters except for run length matrix table (4.5).When considering square shape ROI as in group 3, all the texture parameters showed no significant difference (p>0.05) except for run length matrix, gradient and AR model.

	Group 1				Group 2				Group 3		
	ROI 20000	ROI 5000	ROI 1000	ROI 200	ROI 22400	ROI 11200	ROI 5600	ROI 2800	ROI 6400	ROI 1600	ROI 400
Gray level	24.004	26.481	43.275	66.203	23.674	23.738	30.994	37.702	27.291	38.687	56.920
variance	38.745	48.925	64.568	90.243	37.741	39.742	46.168	46.924	44.868	62.853	94.288
skewness	19.375	22.984	42.290	57.636	19.021	19.452	22.626	28.744	24.119	32.500	52.023
Kurtosis	39.450	64.574	130.453	224.073	40.690	42.649	61.782	72.173	53.469	99.604	196.461
Co-occurrence	2.466	5.150	6.032	7.878	2.517	3.830	4.777	4.964	2.915	5.884	11.285
run length	6.626	5.397	11.217	16.258	7.088	6.918	9.902	13.077	7.033	8.468	13.843
gradient	9.690	12.809	24.636	44.800	9.361	11.102	14.243	20.022	12.241	19.991	33.871
AR model	0.822	1.239	2.251	5.193	0.741	0.989	1.247	1.241	1.242	1.993	3.233
wavelet	0.890	1.918	4.742	13.399	1.061	0.830	1.287	1.574	3.520	4.381	12.855

Table 4.4 Coefficient of variance (CV %) for first order statistics, second order statistics, AR model and wavelet transform parameters for all sizes of ROI, all groups.

91

	ROI 1 ROI 2 ROI 3 ROI 4		ROI 1 ROI 2 ROI 3			ROI 1 ROI 2		
	group 1	group 2	group 1	group 2	group 3	group 1	group 2	group 3
Gray level	0.71	0.76	0.33	0.82	0.88	0.29	1.00	0.71
Variance	0.20	0.94	0.94	0.94	0.36	0.65	0.76	1.00
Skewness	0.01	0.60	0.03	0.71	0.60	0.65	0.60	0.41
Kurtosis	0.00	0.94	0.01	0.88	0.15	0.26	0.94	0.26
Co-occurrence	0.82	0.26	0.02	0.29	0.20	0.11	0.60	0.23
Run length	0.00	0.00	0.00	0.00	0.00	0.00	0.00	0.00
Gradient	0.00	0.29	0.01	0.96	0.00	0.45	0.45	0.01
AR model	0.00	0.33	0.03	0.45	0.03	0.94	0.71	0.17
Wavelet	0.02	0.05	0.71	0.20	0.45	0.33	0.82	0.88

Table 4.5 P values for all texture parameters for all groups and all sizes of ROI. (p <0.05 considered significant difference)

The influence of the ROI size in second order statistic texture parameters, AR model, and wavelet transform for the three groups of sizes of ROI is illustrated in figures 4.23 to 4.27. Co-occurrence matrix, gradient, AR model and wavelet showed no significant difference (p>0.05) when considering the size of ROI varying from 22400 pixels to 5000 pixels with different shapes. Run length matrix shows a significant difference when the size and the shape of the ROI were varied from 22400 pixels to 5000 pixels.
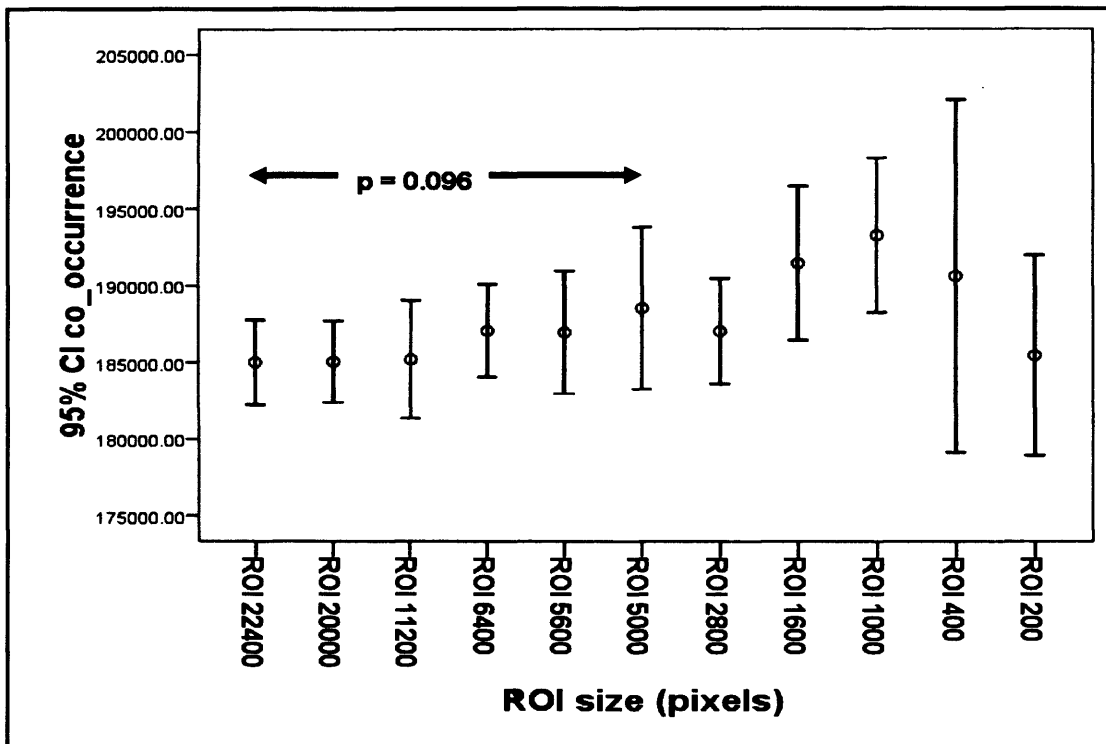
Figure 4.23 Error bar of mean and SD of co-occurrence matrix, error bar with 95 % confidence interval for different size and shapes of the ROI. P > 0 .05(no significant difference)
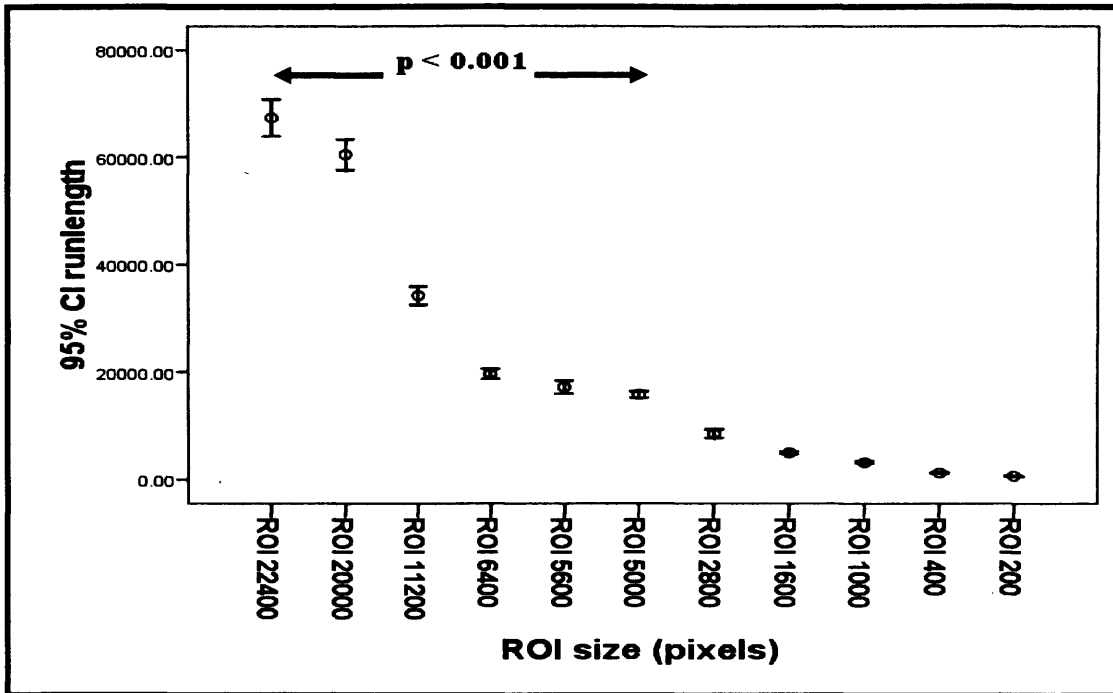
Figure 4.24 Error bar of mean and SD of run length matrix, error bar with 95 % interval confidence at different size and shapes of the ROI (p <0.05 : significant difference)
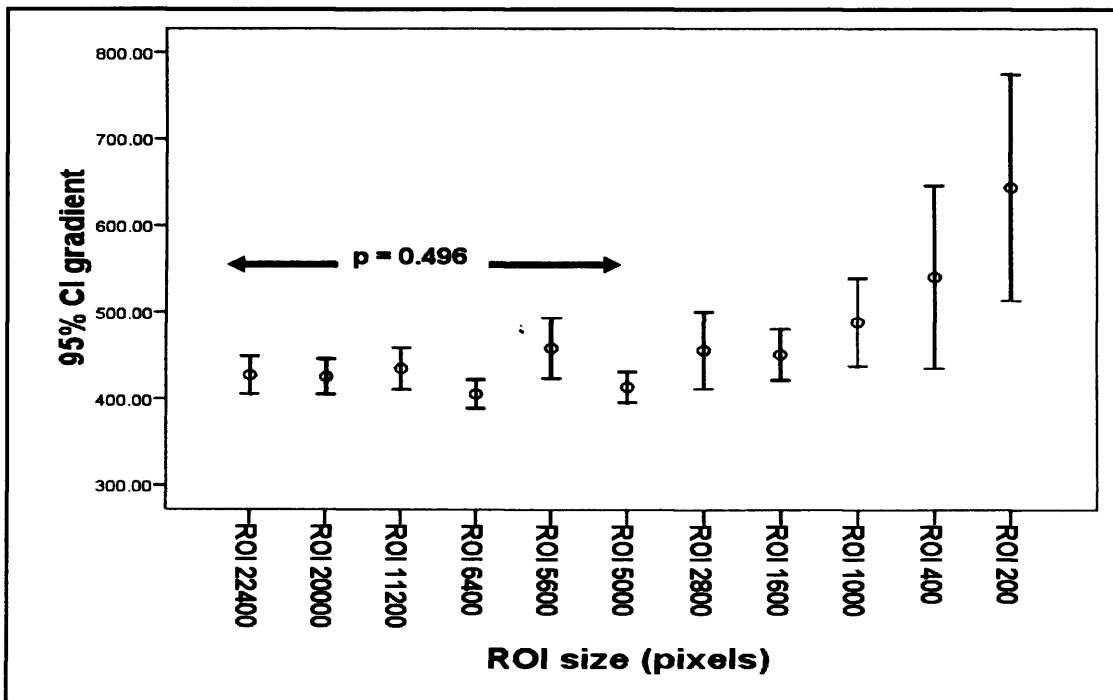
Figure 4.25 Error bar of mean and SD of gradient, error bar with 95 % confidence interval for different size and shapes of the ROI. (p > 0 .05: no significant difference)
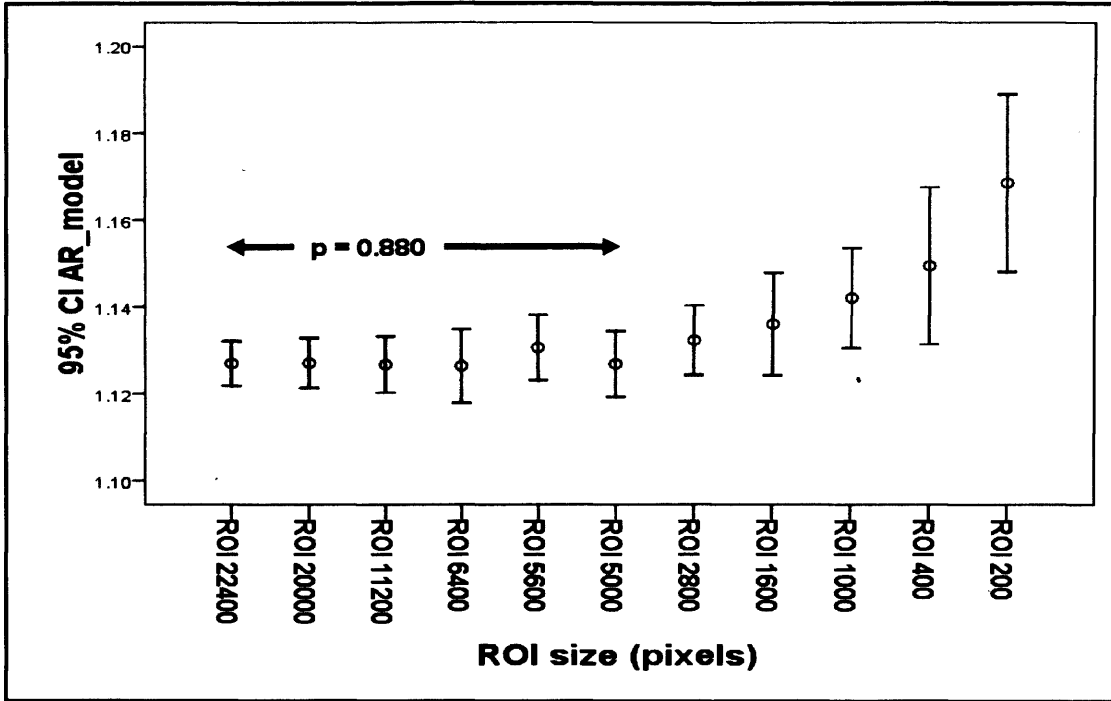
Figure 4.26 Error bar of mean and SD of AR model, error bar with 95 % confidence interval for different size and shapes of the ROI (p > 0 .05 : no significant difference)
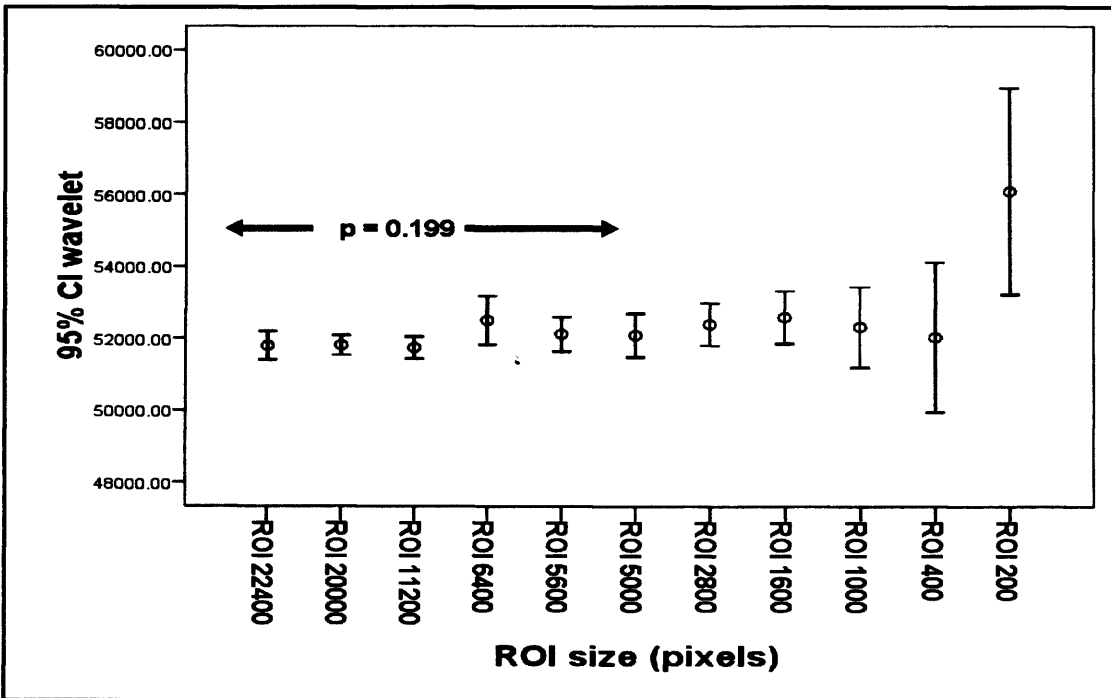
Figure 4.27 Error bar of mean and SD of wavelet transform, error bar with 95 % confidence interval for different size and shapes of the ROI (p > 0 .05 :no significant difference
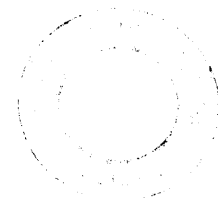
4.6 Discussion

The study showed that there are no significant differences in texture features between the different sites used in imaging the gastrocnemius muscle in this study. However, it must be noted that this does not necessarily mean the muscle is homogenous throughout its length. As described before in this study the four scanning sites were confined to the middle portion of the muscle. Nielsen et al. (2006) found no significant difference between scanning sites on the vastus lateralis muscle.

This study shows the importance of considering the influence of depth and size of ROI prior to making quantitative judgments about clinical significance of texture analysis results. With regards to the effect of depth on texture analysis, the first order statistic parameters: gray level , variance and run length matrix should be extracted for analysis using standardised depth levels; in other words for defining ROI on images to extract these parameters the depth must be kept constant. These texture parameters are depth dependant; this is due to the phenomenon of attenuation of the ultrasound signal. The ultrasound signal decreases with depth due to attenuation of the ultrasound beam by different tissue interfaces and therefore the echo returning from structures closer to the transducer head will be stronger than echoes returning from deeper structures. However, the other texture features showed no significant differences with depth A and depth B.

This study demonstrated the extent of influence that the size of ROI can have for tissue characterisation features. There was no significant difference found in second order statistic parameters co- occurrence matrix, gradient, AR model and wavelet transform when the size of the ROI was 5000 pixels and above. However, changes in the ROI size and shape resulted in run length parameter changes; when the size of

ROI decreased the value of the run length matrix decreased. The inference of these results suggests that the run length matrix when extracted from analysis should be done under standard ROI size, in other words the ROI size must be kept constant when extracting this parameter. In previous studies (Herlidou et al. 1999, Harrison et al. 2008) used texture analysis for diagnosis failed to acknowledge the influence of change of ROI size on the run length matrix parameter. The table (4.6) summarises the changes in texture parameters when altering the three variables of scanning site, depth, and size of ROI.

	Scanning Sites	Depth	Size of ROI
Gray level	Not affected	Affected	Not affected
Variance	Not affected	Affected	Not affected
Skewness	Not affected	Not affected	Not affected
Kurtosis	Not affected	Not affected	Not affected
Co-occurrence	Not affected	Not affected	Not affected
Run length	Not affected	Affected	Affected
Gradient	Not affected	Not affected	Not affected
AR model	Not affected	Not affected	Not affected
wavelet	Not affected	Not affected	Not affected

Table 4.6 The summary of effects on varying scanning site, depth, and size of ROI on texture parameters.

4.7 Conclusion

Based on the results and analysis the following inferences were drawn:

• No differences was found between scanning sites in the middle of the gastrocnemius muscle indicating the middle part of the muscle is homogenous.

• Gray level, variance, and run length matrix are depth dependant.

• Co-occurrence matrix, gradient, AR model, and wavelet are depth independent.

• A high variation in the first order statistic parameters and low variation in the second order statistic parameter, AR model, and wavelet transform was found when the size of ROI was kept constant between subjects.

• ROI size has a significant effect on the computed value of run length matrix.

• No significant difference was noted when the ROI size was varied from 5000 pixels and above for co-occurrence matrix, gradient, AR model, and wavelet

•Choosing bigger size of ROI seemed to give consistent and better results with low variation.

Chapter 5 Influence of Ultrasound Settings on Texture Features

5.1 Introduction

The technique of computerised B –mode image analysis appears as a complementary approach to improve the diagnostic accuracy of conventional US. The most common features extracted from digitized US images are derived from texture analysis. They have proved to be useful in the characterization of various organs or tissues, the few publications related to breast Ultrasonography (Garra et al. 1993, Goldberg et al. 1992) demonstrated promising results that have to be confirmed. In particular, in both studies, data was acquired using different variable settings of the US scanner, which could bias the results (Lefebbvre et al. 2000). Quantitative analysis of medical ultrasound images for diagnostic purposes may vary due to the changes of many factors besides the variation of the texture itself. For instance, a particular statistical parameter may change drastically under different scanner settings even though the same tissue is being studied (Chan and McCarty 1990). Therefore, before the effectiveness of statistical texture analysis in tissue characterization can be investigated, the effect of varying ultrasound setting needs to be considered.

To deal with the influence on texture features of variable scanner settings, various authors stress the importance of using standardized condition settings for all measurements (Hirning et al. 1989, Pohle et al. 1997, Sun et al. 1996, Kadah et al. 1996, Huynene et al. 1994). Other authors have adjusted the parameter setting for optimal visualization (Mailloux et al. 1986) or kept to values normally used in clinical practice (Dixon et al. 1997). However, using these methods has limitations when it

comes to practical clinical use. The fixing of the scanner settings severely restricts an ultrasound scanner's technical possibilities. It infers that the sonologist is now restricted from selecting those settings that allow for optimal visual diagnosis. Furthermore, it may be possible in all cases to achieve optimal signal conditioning for quantitative analysis. The aim of this study component is to investigate how the texture parameters behaves with the variation of the gain and dynamic range setting in the ultrasound machine and to find the optimal values of gain and dynamic range to be used.

5.2 Subjects and methods

5.2.1 Participants

Left medial gastrocnemius muscle of 5 healthy volunteers {4males/1 female, with a mean age of 24 years (Range: 18-38 years)} were subjected to scanning by ultrasound. All volunteers had normal health with no history of any musculoskeletal disorder. The approval of the local Ethics Committee was obtained and all participants were fully informed about the protocol and procedure before obtaining their consent.

5.2.2 Image acquisition

Ultrasound scans were performed according to the standard protocol used for all the subjects (chapter 3).Only one 2D slice was chosen for use in the investigation of the gain and dynamic range setting affect on texture features as a previous study on 10 subjects (see chapter 4) has shown the middle part of the gastrocnemius muscle is homogenous. The scanning was performed at different settings of gain and dynamic range. Imaging was repeated once with the dynamic range being constant and gain

range varying between 70 and 90 dB (70-75-80-85-90) and again with a constant gain setting while varying the dynamic range through the same values. Five images were captured at each sitting. When evaluating the effects of a given setting, all others settings were kept constant. All scanning procedures were performed by the same investigator.

5.2.3 Image analysis

On each Ultrasound image slice, A ROI with size of 250x80 pixels was defined. Size and shape of the ROI were kept constant for all subjects. The ROI was defined at the same level of depth for all subjects within the border of the gastrocnemius muscle avoiding muscle boundaries or neighbouring structures. The ROI for calculation was defined and marked manually with the aid of a computer mouse on each image

5.2.4Statistical analysis

Because of the small sample size (<50), the Shapiro-Wilk test was used to test the normality of the data(P>0.05 considered normal distributed). One-way ANOVA was then used to test for significant differences between the varying settings (P value less than 0.05 was considered statistically significant). The coefficient of variation (CV) was then calculated to evaluate the variation of texture parameters. Expressed as a percentage, the CV is the ratio of the standard deviation and the overall mean. SPSS for Windows version 16 (SPSS inc., Chicago, II, USA) was the statistical package used for statistical analysis.

5.3 Results

Figure 5.1 to figure 5.9 show the changes in texture features while varying the gain setting ranges from 70 to 90 dB. The variation due to the gain setting was found to be high for 6 of the texture parameters with the mean CV ranging from 32.26% - 70.51% (gray level 70.51%, variance 58.60%, skewness 41.18%, kurtosis 86%, run length 32.26%, gradient 35.03%). For the other 3 texture parameters the CV was low with values ranging from 1.34% - 5.30% (co-occurrence matrix 5.30%, AR model 1.34% and wavelet 2.13%) Table 5.1.
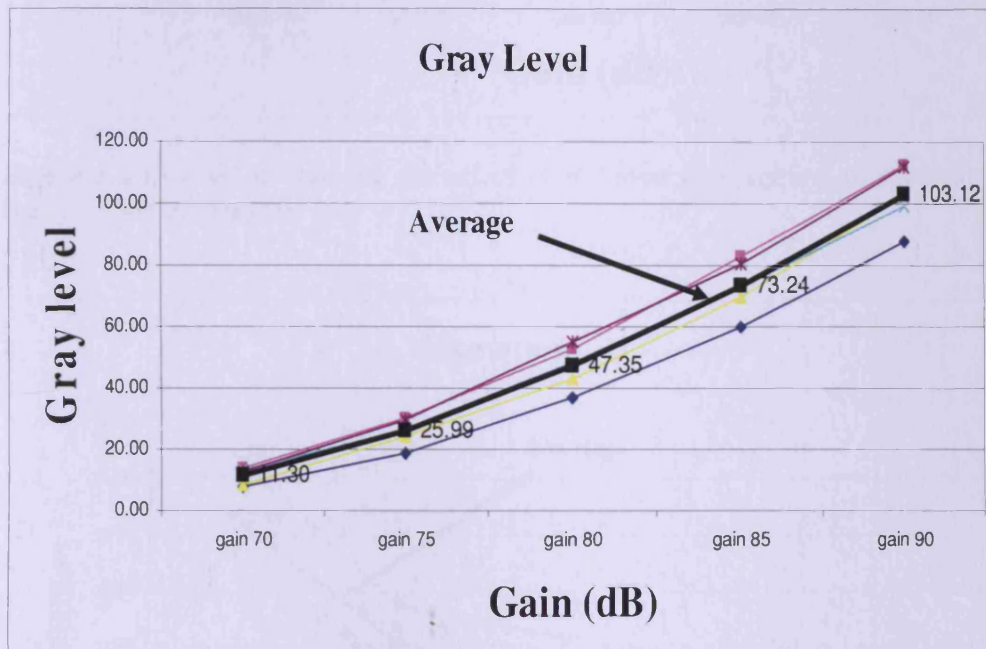
Figure 5.1 Line graph showing effect of different gain settings on gray level intensity (5 subjects and average).
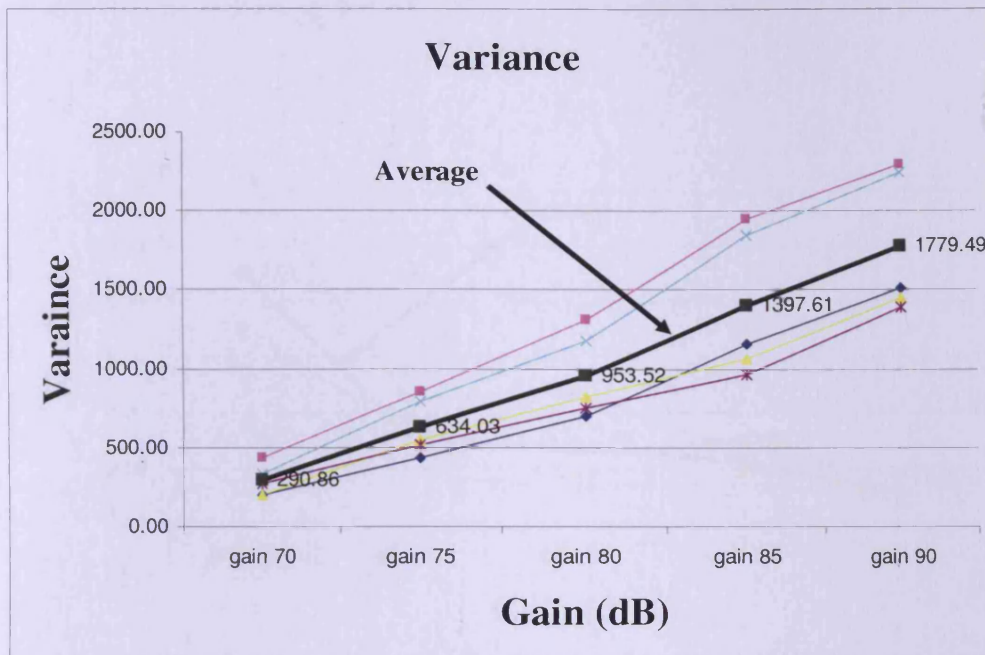
Figure 5.2 Line graph showing the effect of different gain setting on variance (5 subjects and the average)
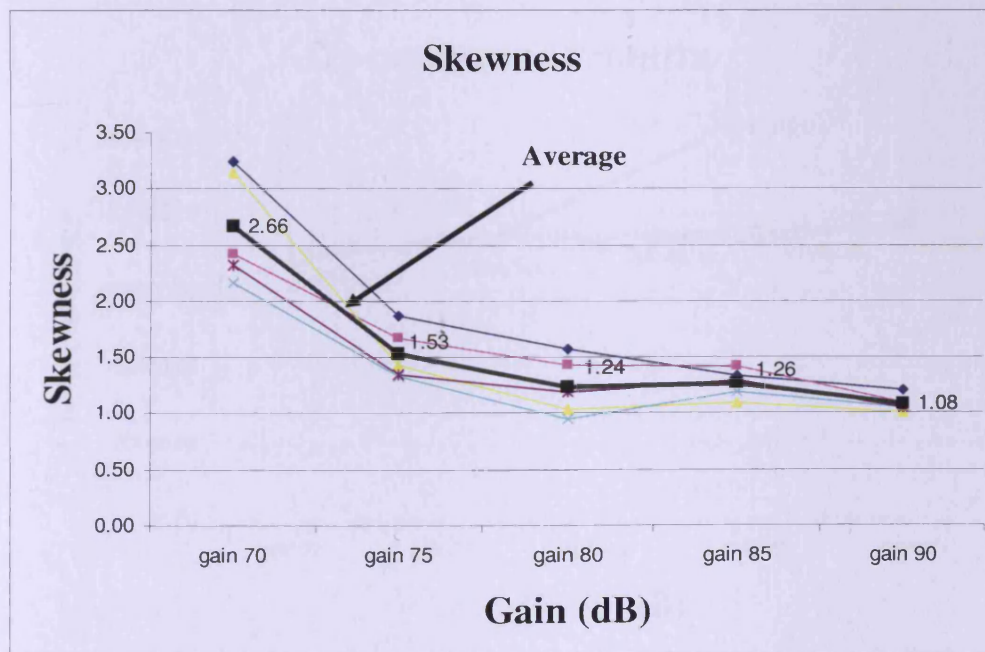
Figure 5.3 Line graph showing the affect of different gain setting on skewness (5 subjects and the average.
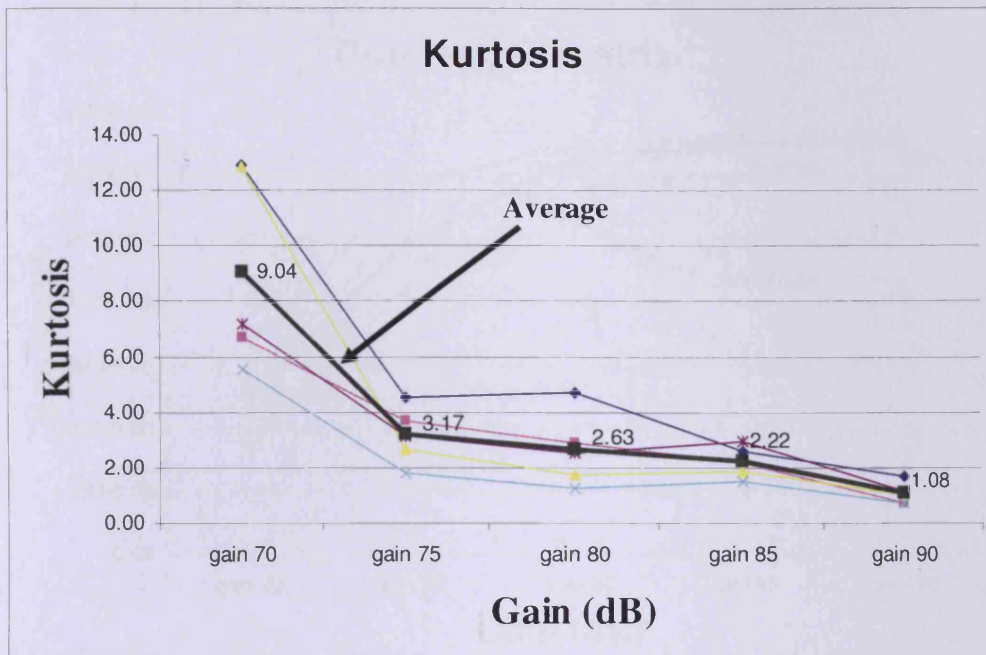
Figure 5.4 Line graph showing the effect of different gain setting on kurtosis (5 subjects and the average)
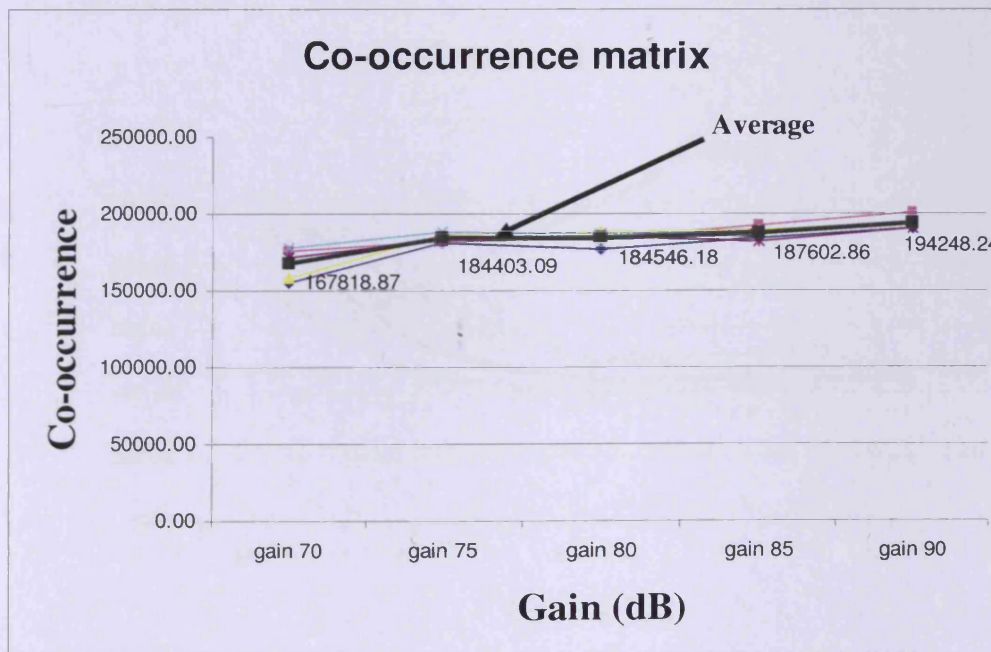
Figure 5.5 Line graph showing the effect of different gain setting on co-occurrence matrix (5 subjects and the average)
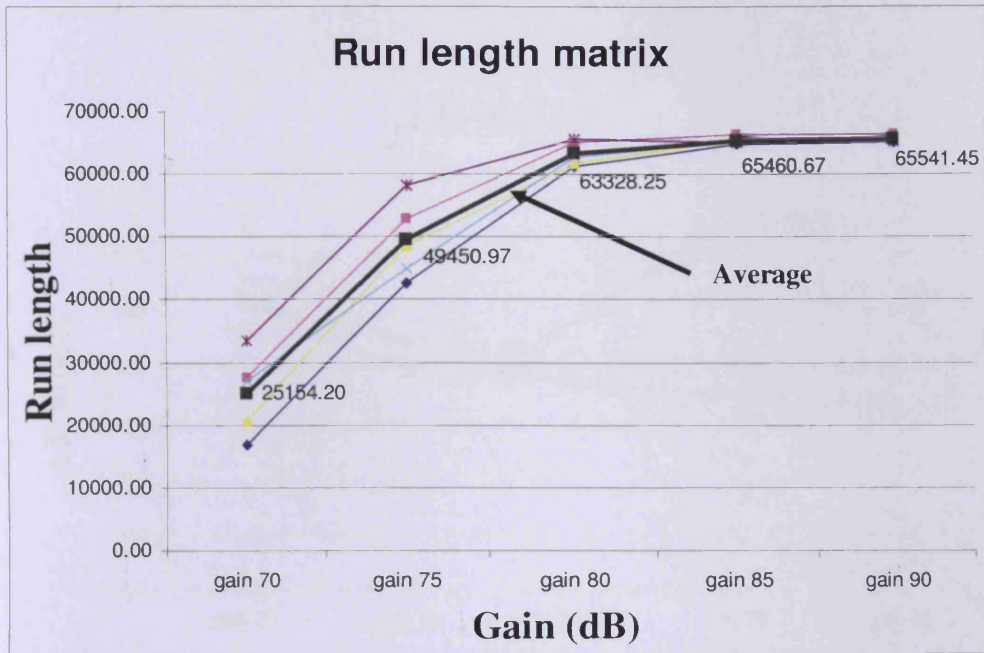
Figure 5.6 Line graph showing the effect of different gain setting on run length matrix (5 subjects and the average)
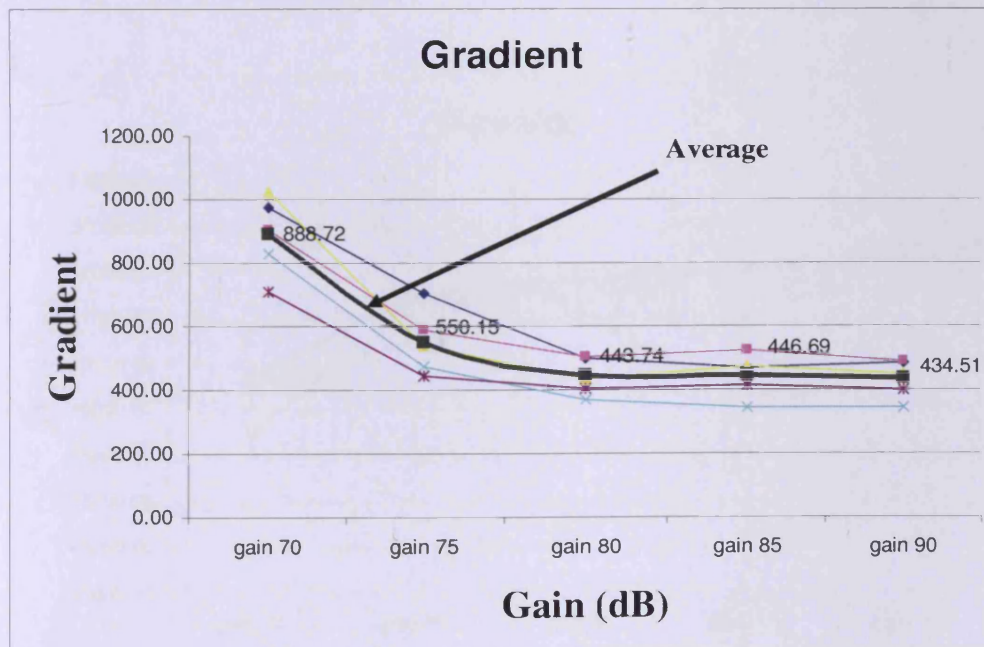
Figure 5.7 Line graph showing the effect of different gain setting on gradient (5 subjects and the average)
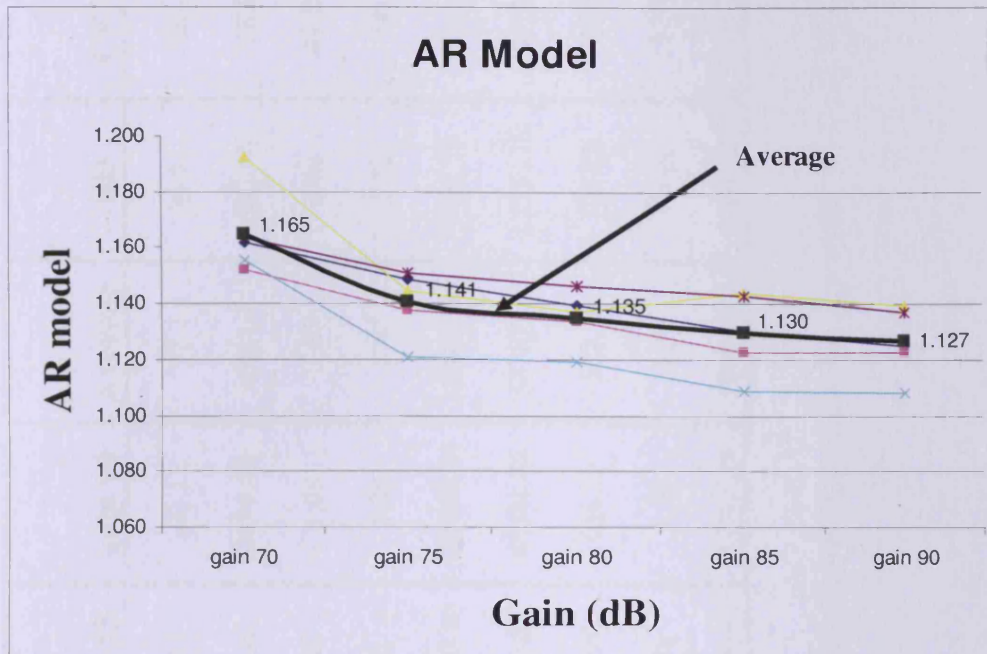
Figure 5.8 Line graph showing the effect of different gain setting on auto-regressive model (5 subjects and the average)
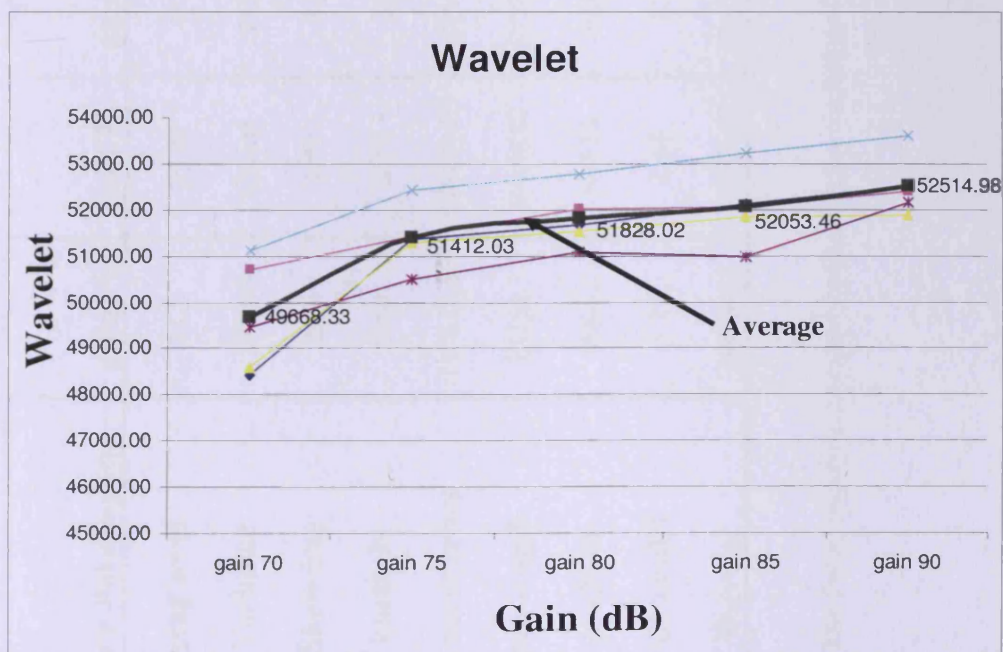
Figure 5.9 Line graph showing the effect of different gain setting on wavelet transform (5 subjects and the average)

Texture Parameters	gain 70	gain 75	gain 80	gain 85	gain 90	Average	SD	CV %
gray level	11.3	25.99	47.35	73.24	103.12	52.2	36.81	70.51
Variance	290.86	634.03	953.52	1397.61	1779.49	1011.1	592.46	58.6
Skewness	2.66	1.53	1.24	1.26	1.08	1.55	0.64	41.18
kurtosis	9.04	3.17	2.63	2.22	1.08	3.63	3.12	86
co-occurrence	167818.87	184403.09	184546.18	187602.86	194248.24	183723.85	9745.71	5.3
run length	25154.2	49450.97	63328.25	65460.67	65541.45	53787.11	17350.19	32.26
gradient	888.72	550.15	443.74	446.69	434.51	552.76	193.65	35.03
AR model	1.17	1.14	1.14	1.13	1.13	1.14	0.02	1.34
Wavelet	49668.33	51412.03	51828.02	52053.46	52514.98	51495.36	1096.21	2.13

Table 5.1 The mean, standard deviation and coefficient variation (CV %) for all texture parameters at different gain levels

All the texture parameters including first and second order statistics, AR model and wavelet showed significant differences when considering the gain varying from 70 to 90.dB (70-75-80-85-90).When considering gain varying from 75 dB to 85 dB , no significant difference was found for 6 of the 9 texture parameters , with the exception of gray level, variance and rung length as shown in table 5.2.

Texture parameters	Gain 70-75-80-85-90 dB (p value)	Gain 70-75-80-85 dB (p value)	Gain 75-80-85 dB (p value)
Gray level	0.000	0.000	0.000
Variance	0.000	0.010	0.011
Skewness	0.000	0.014	0.097 (NS)
Kurtosis	0.000	0.015	0.369 (NS)
Co-occurrence	0.000	0.004	0.380 (NS)
Run length	0.000	0.000	0.000
Gradient	0.000	0.087 (NS)	0.093 (NS)
AR model	0.001	0.34 (NS)	0.424 (NS)
Wavelet	0.000	0.132 (NS)	0.381 (NS)

Table 5.2 Variation of parameters with gain ranges, p value >0.05 no significant difference (NS = No significant difference).

Figure (5.10) to figure (5.18) show the changes in texture features while varying the dynamic range setting from 70 to 90 dB. The dynamic range setting did not appear to adversely affect the texture features with a mean CV of 6.98 % for the kurtosis parameter and for the other parameters was less than 5 %, ranging from 0.20% - 4.72% (gray level 1.90%, variance 4.72%, skewness 3.56% , occurrence matrix 0.36% , run length 0.67% , gradient 4.64% , AR model 0.20% and wavelet 0.27%) Table (5.3).
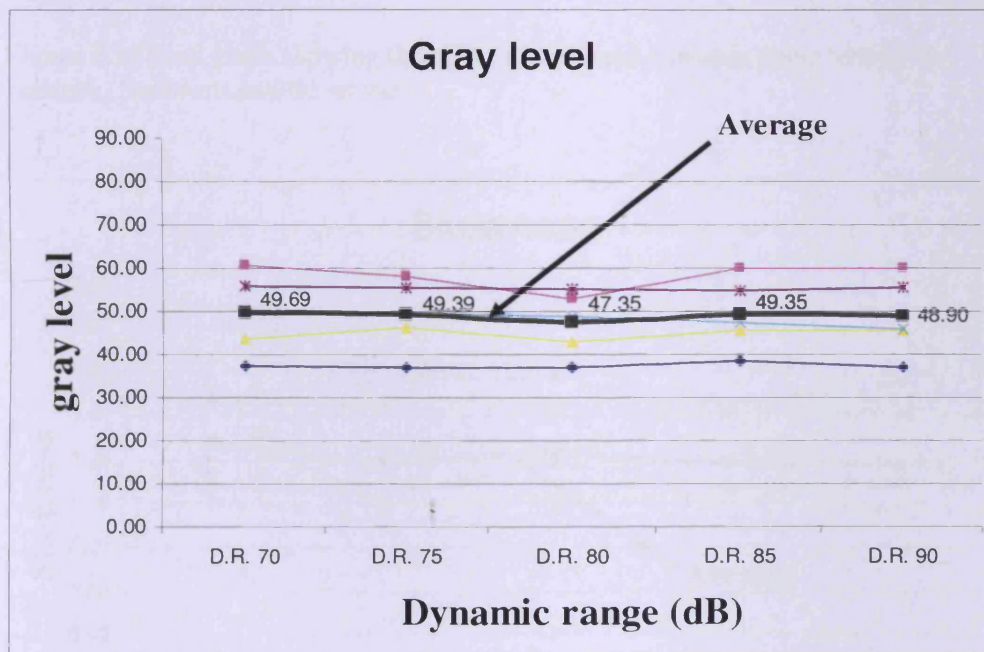
Figure 5.10 Line graph showing the effect of different dynamic range setting on gray level intensity (5 subjects and the average)

109
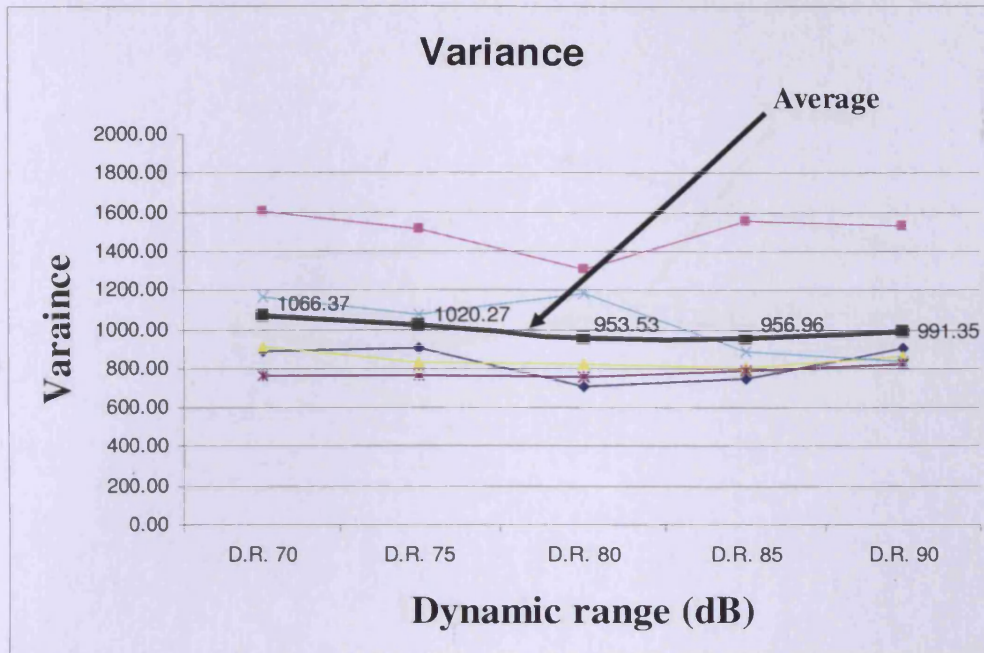
Figure 5.11 Line graph showing the effect of different dynamic range setting on variance (5 subjects and the average)
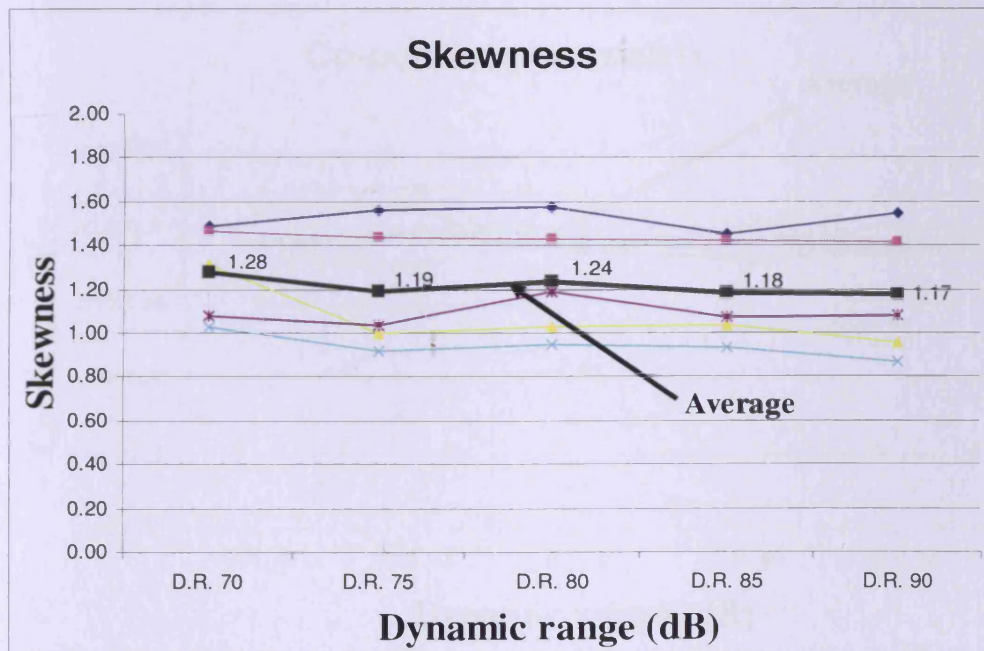
Figure 5.12 Line graph showing the effect of different dynamic range setting on skewness (5 subjects and the average)
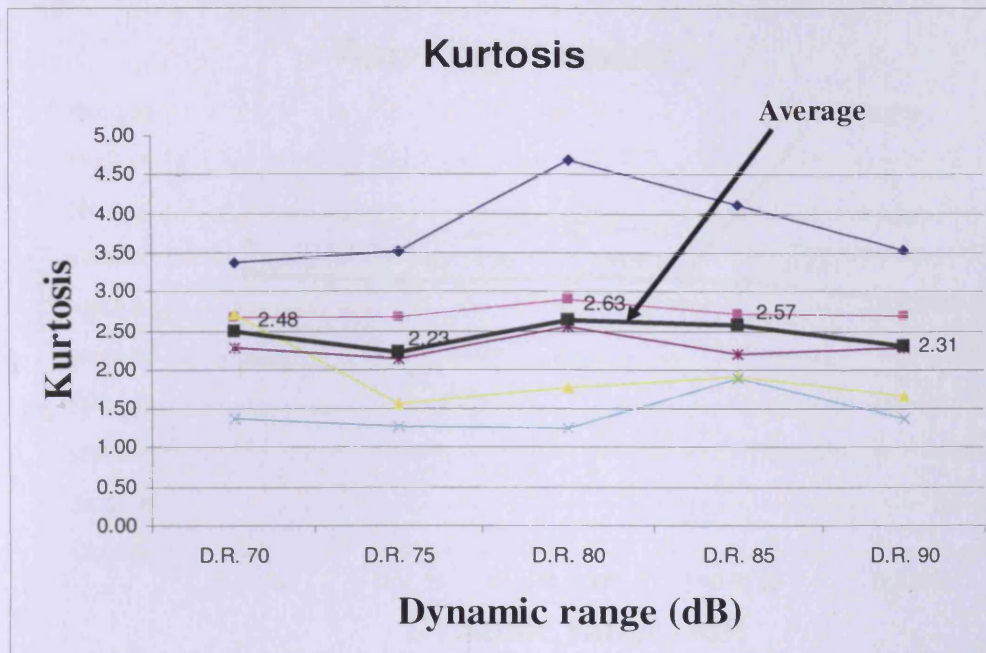
Figure 5.13 Line graph showing the effect of different dynamic range setting on kurtosis (5 subjects and the average)
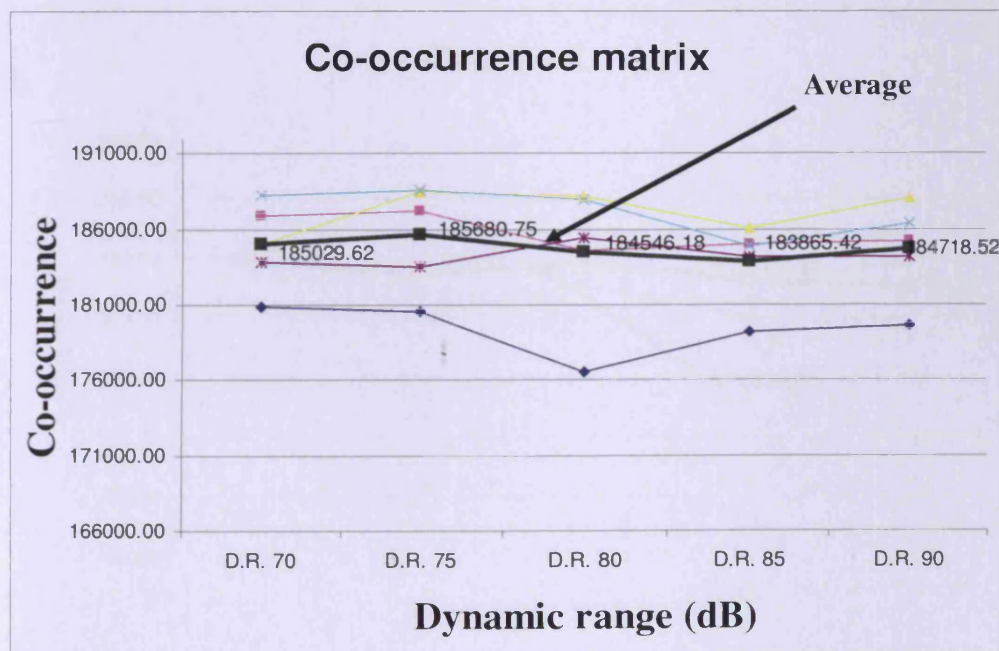
Figure 5.14 Line graph shows the effect of different dynamic range setting on the co-occurrence matrix (5 subjects and the average).
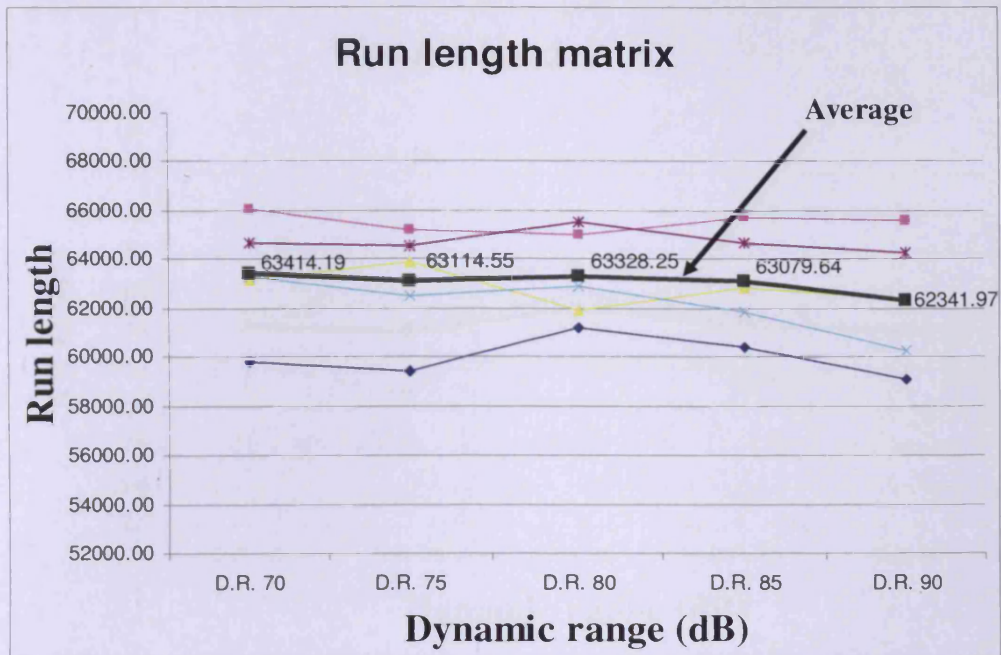
Figure 5.15 Line graph shows the effect of different dynamic range setting on the run length matrix (5 subjects and the average).
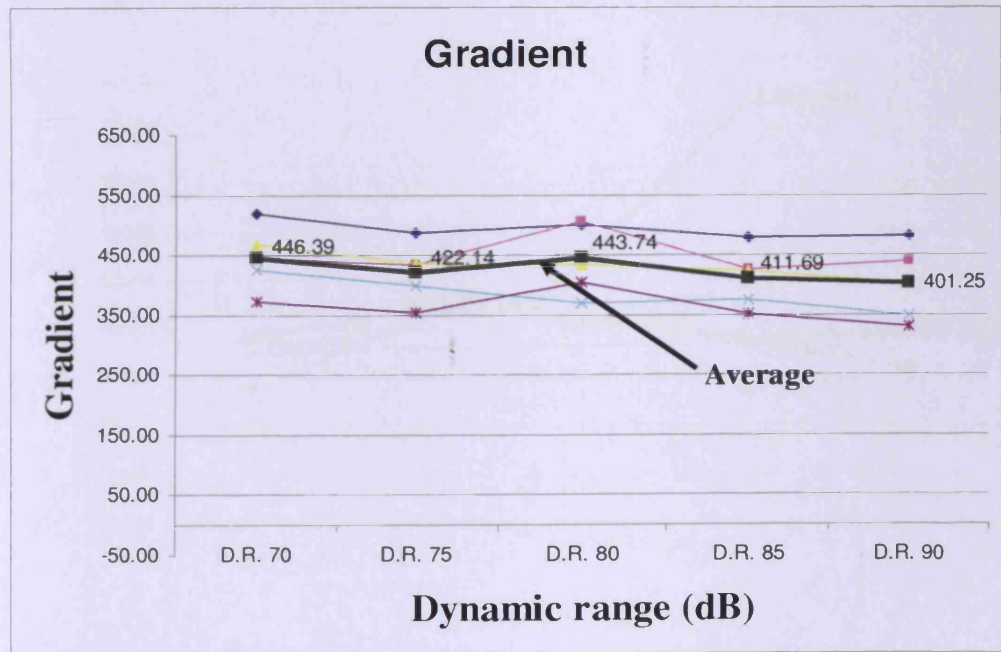
Figure 5.16 Line graph shows the effect of different dynamic range setting on gradient (5 subjects and the average)

112
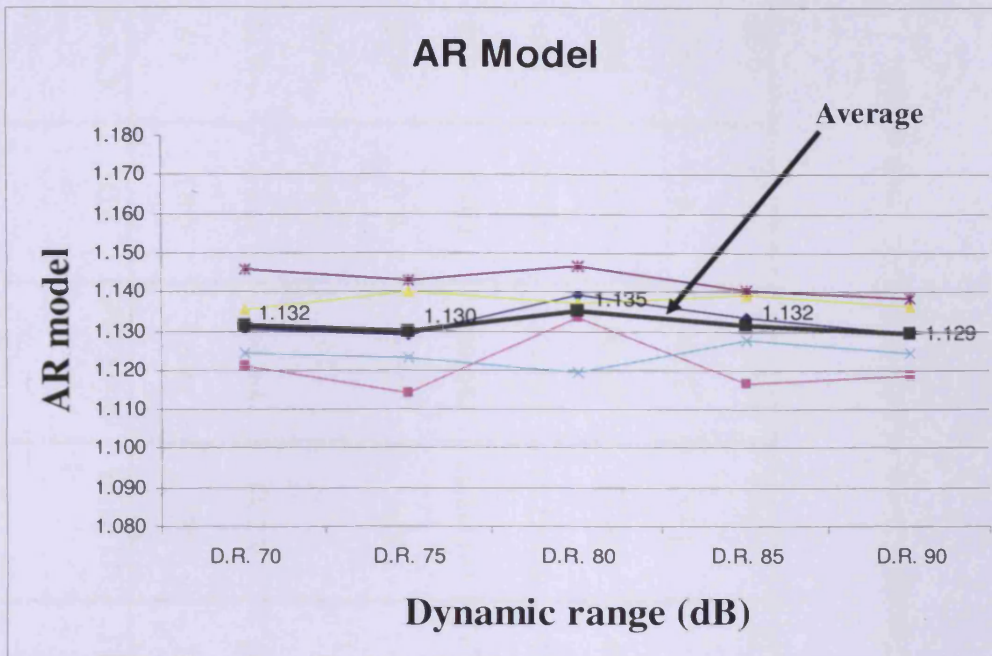
Figure 5.17 Line graph shows the effect of different dynamic range setting on auto-regressive model (5 subjects and average)
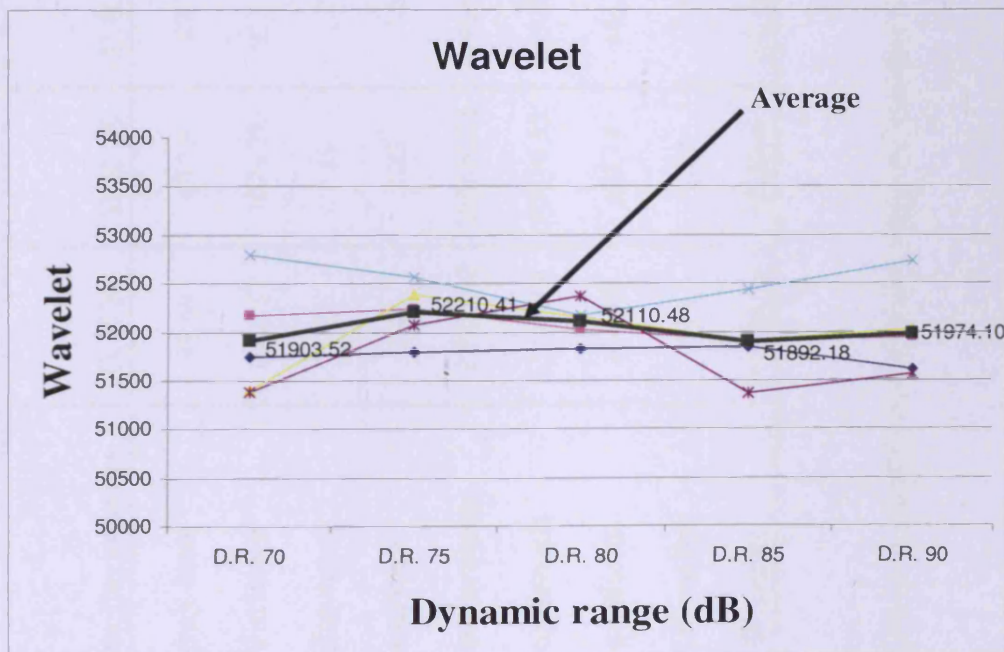
Figure 5.18 Line graph shows the effect of different dynamic range setting on wavelet transform (5 subjects and the average)

Texture Parameters	D.R 70	D.R 75	D.R 80	D.R 85	D.R 90	Average	SD	CV %
gray level	49.69	49.39	47.35	49.35	48.9	48.93	0.93	1.9
Variance	1066.37	1020.27	953.53	956.96	991.35	997.69	47.11	4.72
Skewness	1.28	1.19	1.24	1.18	1.17	1.21	0.04	3.56
kurtosis	2.48	2.23	2.63	2.57	2.31	2.44	0.17	6.98
co-occurrence	185029.62	185680.75	184546.18	183865.42	184718.52	184768.1	664.8	0.36
run length	63414.19	63114.55	63328.25	63079.64	62341.97	63055.72	423.16	0.67
gradient	446.39	422.14	443.74	411.69	401.25	425.04	19.73	4.64
AR model	1.13	1.13	1.14	1.13	1.13	1.13	0	0.2
Wavelet	51903.52	52210.41	52110.48	51892.18	51974.1	52018.14	138.24	0.27

Table 5.3 The mean, standard deviation and coefficient variation (CV %) for all texture parameters at different dynamic range setting.

All the texture parameters including first and second order statistics, AR model, and wavelet showed no significant difference (NS) when considering the dynamic range varying from 70 to 90.dB (70-75-80-85-90) indicating that dynamic range has no significant effect on texture features.

Texture Features	Dynamic range 70-75-80-85-90 dB (p value)
Gray level	0.999 (NS)
Variance	0.986 (NS)
Skewness	0.970 (NS)
Kurtosis	0.920 (NS)
Co-occurrence	0.903 (NS)
Rung length	0.947 (NS)
Gradient	0.748 (NS)
AR model	0.994 (NS)
Wavelet	0.939 (NS)

Table 5.4 Variation of parameters with dynamic ranges, p>0.05 no significant difference (NS = No significant difference)

5.4 Discussion

This study has shown that differential settings of the gain yield large variations on most of the first order statistics parameters and low variation for most of the second order statistics, AR model, and wavelet transform. Changing a system variable in the ultrasound machine alters the signal processing in ways which can change the echo amplitude relationships among structure seen an ultrasound image(Shung and Thieme 1993). The perception and interpretation of scattering interactions of sound in the body are greatly influenced by the operators control of system gain (Shung and Thieme 1993).The gain raises or lowers the overall amplification applied to the returning echo amplitude. As the system gain is increased, the mean gray level and variance increases but skewness and kurtosis remain virtually unchanged. It was shown that increasing the gain resulted in an approximate linear increase in the mean gray level and variance over the range of gains used (figure 5.1 and figure 5.2). The first order statistical parameters were highly affected by gain as they are computed from the intensity of pixels, without taking into consideration any spatial relations between the pixels within the image. On the other hand, the second order features were less affected by the gain compared. The second-order gray-level statistics describe the relationship between each pixel in the ROI and its neighbouring pixels. However, when considering gain ranging between 75 dB to 85 dB most of second order statistics parameters, AR model and wavelet resulted in no significant difference ($p > 0.05$) except for the run length matrix. Chan (1998) stated that co-occurrence matrix statistics have the advantage that they are less susceptible to variation in textures than first order statistics due to changes in image brightness and consequently the co-occurrence matrix method remain one of the most popular methods for quantitative ultrasonic tissue characterization. The dynamic range governs the

range of echoes, from the weakest to the highest amplitude that can be displayed (Rose 2004). Increasing dynamic range makes low amplitude echoes more distinguishable but decreases the contrast. Decreasing dynamic range will increase the contrast in the image and reduce the display of low amplitude echoes typical of noise (Rose 2004).However, all the texture parameters do not significantly change when the dynamic range is varied from 70 dB to 90 dB indicating that the dynamic range has no significant affect on texture feature over this range. Table (5.5)

Texture Parameters	Gain 75-85 (dB)	Dynamic range 70-90 (dB)
Gray level	Affected	Not affected
Variance	Affected	Not affected
Skewness	Not affected	Not affected
Kurtosis	Not affected	Not affected
Co-occurrence	Not affected	Not affected
Run length	Affected	Not affected
Gradient	Not affected	Not affected
AR model	Not affected	Not affected
wavelet	Not affected	Not affected

Table 5.5 The effect of gain (75-85 dB) and dynamic range (70-90 dB) on texture parameters

5.5 Conclusion

When in use the ultrasound scanner is constantly subjected to changes in setting according to their clinical applications. Settings such as gain can greatly influence the texture features and influence the automatic classification of the results. Hence, ultrasound settings should be considered and monitored. This preliminary study has shown that different gain settings of the ultrasound machine could yield significant variations in texture features, especially when looking at first order statistical methods involved in texture analysis and tissue characterization. Therefore, considering that gain setting is necessary for the classification of new cases it is important to ensure that the method is operator independent.

Chapter 6 Repeatability and Reproducibility

6.1 Introduction

The analysis of texture in medical applications provides a quantitative means to analyze and characterize properties of various tissues. The application of the analysis of texture to medical images provides highly advanced non -visible information advanced on tissues in the area of interest (Harrison et al. 2008). Despite the use of US in characterizing normal tissue, however, the texture characteristics of a tissue can be considered as accurate only when the sonographic measurement can be achieved consistently(Li et al. 2004). This is particularly important when a series of examinations need to be performed to monitor tissue feature changes over a period. Therefore, intra and inter operator repeatability and reproducibility are important variables that warrant investigation and examination (Li et al. 2004). This would potentially make US a robust quantitative method to characterize tissues. The B-mode ultrasound assessments are exposed to many confounders, which include instrumentation, scanning and reading protocols, and operators (Li et al. 1996). Therefore, validity and reliability of imaging assessments are very important attributes for use in routine clinical practice and research (Li et al. 1996).The aim of this study is to investigate and compare the short and long-term repeatability and reproducibility of the texture features extracted from the images. In the context of this work, short-term repeatability (within-operator reliability) is defined as the variation in measurements taken by a single observer on the same subjects, under the same conditions, on a single occasion. Long-term repeatability (within-operator reliability) is defined as the variation in sets of measurements taken by a single observer on the

same subjects, under the same conditions, but on different occasions. Reproducibility

(between-operator reliability) is defined as the variation in sets of measurements taken

by different observers on the same subjects, under the same conditions, on different

occasions (Bland and Altman 2000).

6.2 Subject and Method

6.2.1 Participants

The left gastrocnemius muscle of 5 healthy volunteers {5 males, with a mean age of

29 years (Range: 22-38 years)} were subjected to ultrasound scanning. All volunteers

had normal health with no history of any musculoskeletal disorder. Approval of the

local Ethics Committee was obtained and all participants were fully informed about

the protocol and procedure before obtaining their consent.

6.2.2 Image acquisitions and scanning protocol

A three dimensional ultrasound sweep was performed on the central region of the

muscle and four slices were extracted from the 3D set with a 10 mm distance between

them. Only one slice was chosen for the investigation of repeatability and

reproducibility as a previous study on 10 subjects (see chapter 4) has shown the

middle part of the gastrocnemius muscle is homogenous. Ultrasound scans were

performed according to a standard protocol for all the subjects (scanning protocol and

image acquisitions are described in chapter 3).

All system setting parameters such as gain (80 dB), dynamic range (80 dB), depth (4

cm), sweep angle (30 degrees) and TGC central, were kept constant throughout the

study. The settings of the ultrasound system were standardized for all participants and

kept constant during all scanning procedures to avoid potential variations in the

images due to different settings. To test short-term repeatability, each operator repeated the scanning 15 times on each subject; then 10 out of 15 scans were selected by an experienced ultrasound medical physicist at the Medical Physics and Clinical Engineering department, excluding images indicating artefacts or poor contact between the probe and the skin. To assess long-term repeatability, the subjects were invited to the study site to repeat the scans on two occasions, with an interval of one month; 2 subjects were unable to follow-up the scan.

To assess the reproducibility, all scanning procedures were performed by two operators. The first operator marked the scanning site and performed the scan.. After this was finished the second operator came to the room, marked the scanning sites from the beginning again, and performed another scan. Between each successive scan, the participants were allowed to move and the transducer was repositioned afresh

6.2.3 Image analysis

On each Ultrasound image slice, the largest possible rectangular shaped ROI with size of 250x80 pixels that encompassed the gastrocnemius muscle was defined. The size and shape of the ROI were kept constant for all subjects. The ROI was defined at the same level of depth for all subjects within the border of the gastrocnemius muscle, avoiding muscle boundaries, or neighbouring structures. Texture features were extracted from each ROI.

6.3 Statistical analysis

Repeatability and reproducibility were assessed for each texture parameter using a Coefficient variation (CV %) and Intra-class correlation (ICC). The coefficient variation (CV) is the ratio of the standard deviation and overall mean expressed as a percentage. Calculating the ICC involves splitting the total variation in the data into different sources. The variation due to each source is measured by a 'component of variance'. In a standard situation, each subject is measured once, resulting in two 'components of variance'. One of these measures the variability between subjects, and the other the variability between operators (or within-subjects). However, in this study there are 10 repeat trials for each operator and for each subject. This results in three components of variance , the variability between subjects and the variability between operators, but additionally the variability caused by repeat measurement of the same subjects. This is referred to as the within-operator variability

The first ICC is a measure of the variation between subjects relative to the differences between operators. This is calculated as:

ICC = Between subject variation / (Between subject variation + between operator variation)

The second ICC measures the variation between subjects relative to the variation between repeat measurements of the same subjects by the same operator. This is calculated as:

ICC = Between subject variation / (Between subject variation + within operator variation)   (Kirkwood and Sterne 2003)

These components of variance were used to calculate the standard deviation of the variability of each source, and from this, the coefficient variation (CV) could be found. The whole analysis was then repeated to consider the long-term repeatability of

operator 1 on the two occasions. For this analysis, results from operator 2 were omitted, and only the 3 subjects that were measured on two occasions were included. The overall strategy of the analysis was the same, but this time the between-operator variability was replaced by the between-occasion variability. Stata software   version 9.2 (StataCorp, College Station, Texas, USA) was the statistical package used for statistical analysis. The ICC value ranges from 0 to 1, with values closer to 1 representing stronger reproducibility. A high ICC with a value greater than 0.75 was interpreted as "excellent reproducibility"; an ICC value of 0.74–0.60 indicates "good reproducibility"; between 0.59–0.40 shows "fair reproducibility" and below 0.40 indicates "poor reproducibility" (Faul et al. 1999 , Fleiss 1986 , Rosner 2000).

6.4 Result

6.4.1 Short-term repeatability (intra-operator)

The CV was calculated for each texture parameter, subject, and operator. Figure (6.1) and figure (6.2) show the coefficient variation (CV) of texture parameters for operator 1 and operator 2. Generally, first order statistics parameters show a higher variation than the second order statistic parameters. The average CV percentages of the 5 subjects for each operator were: 2.3 % for operator 1 and 2.92 % for operator 2 for the co-occurrence matrix; 2.11 % for operator 1 and 2.44 % for operator 2 for the run length matrix; 7.83 % for operator 1 and 7.09 % for operator 2 for gradient; 0.52 5 % for operator 1 and 0.54 % for operator 2 for the AR model; and 0.634 % for operator 1 and 0.638 % for operator 2 for wavelet. On the other hand first order statistics showed higher variation gray level 5.88 % for operator 1 and 6.94 % for operator 2, variance 9.12 % for operator 1 and 10.92 % for operator 2, skewness 9.57 % for operator 1

and 15.21 % for operator 2and kurtosis 27.95 % for operator 1 and 44.62 % for operator 2.
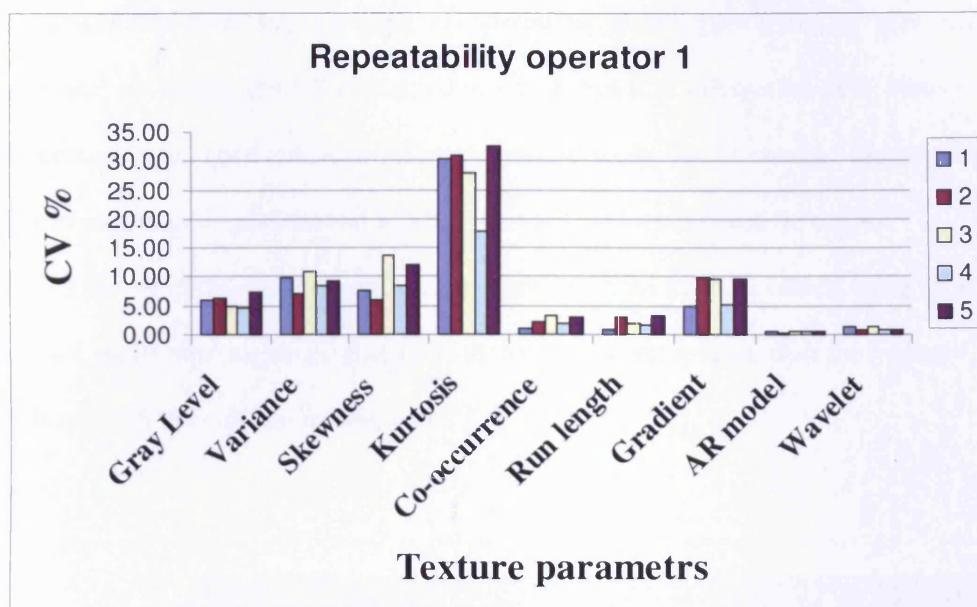
Figure 6.1 shows the short-term repeatability (CV %) of the texture parameters of operator 1(1 to 5 represents the subjects).
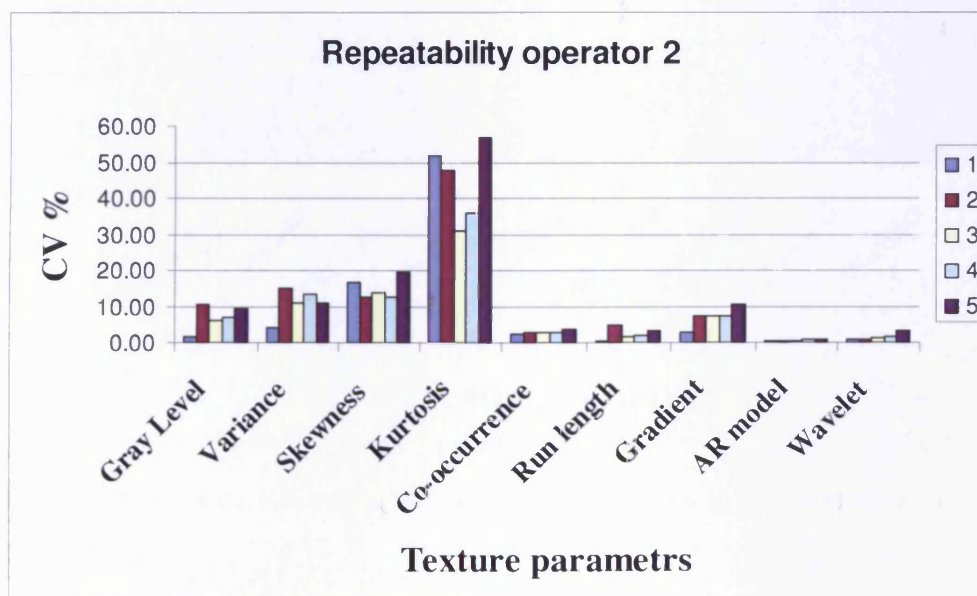
Figure 6.2 shows the short-term repeatability (CV %) of the texture parameters of operator 2 (1 to 5 represents the subjects).

When the within-operators ICC values were examined figure (6.3), the results suggested that there was excellent agreement between repeat trials for gray level, variance, run length and AR model, all of which had ICC values above 0.8. However, agreement was good and fair between repeat trials for skewness, kurtosis, co-occurrence matrix, gradient and wavelet with ICC values between 0.54-0.80

When the variation was measured as a proportion of the average values, using the CV values, the results suggested that kurtosis had the worst results, with the highest CV values 27.95 % as shown in table (6.1).
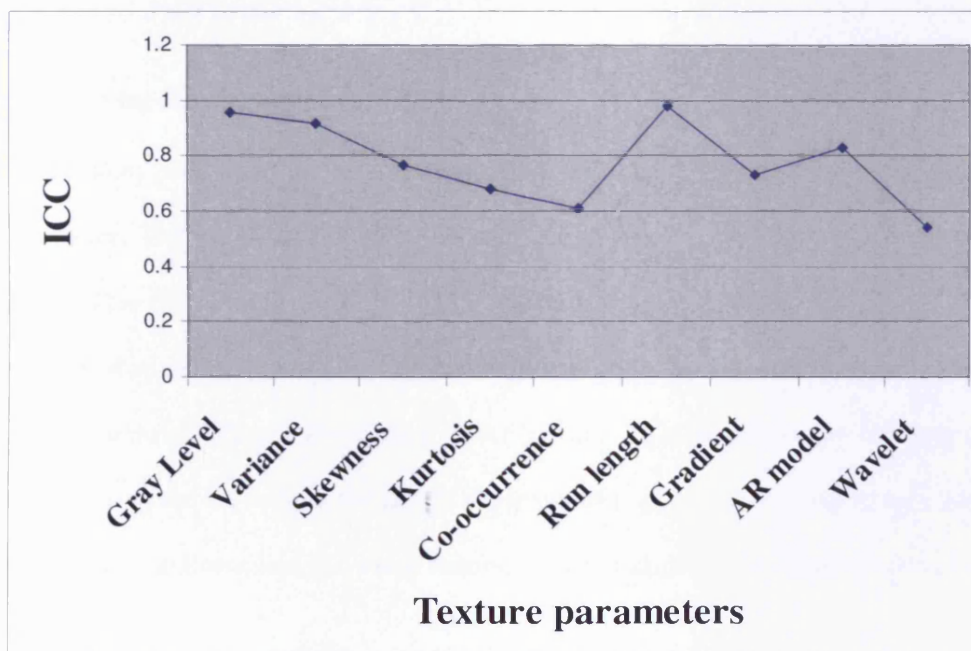
Figure 6.3 shows the ICC values for each texture parameter to test the short-term repeatability.

	Short-term repeatability	
	ICC	CV %
Gray Level	0.96	5.88
Variance	0.92	9.12
Skewness	0.77	9.57
Kurtosis	0.68	27.95
Co-occurrence	0.61	2.30
Run length	0.98	2.11
Gradient	0.73	7.83
AR model	0.83	0.53
Wavelet	0.54	0.63

Table 6.1 ICC and CV % of the texture parameters – short-term repeatability –

6.4.2 Long-term repeatability

Figure (6.4) and figure (6.5) show the CV % and the ICC values for each texture parameter. The variation between the same operators on different occasions was small. This is reflected by high ICC values for repeats between occasions. This suggests that, on average, there is little overall variability between intra-operator long-term variations. When the variation was measured as a proportion of the average values, using the CV values, the results suggested that gray level, variance, skewness, kurtosis and gradient had the worst results, with the highest CV values as shown in table (6.2).
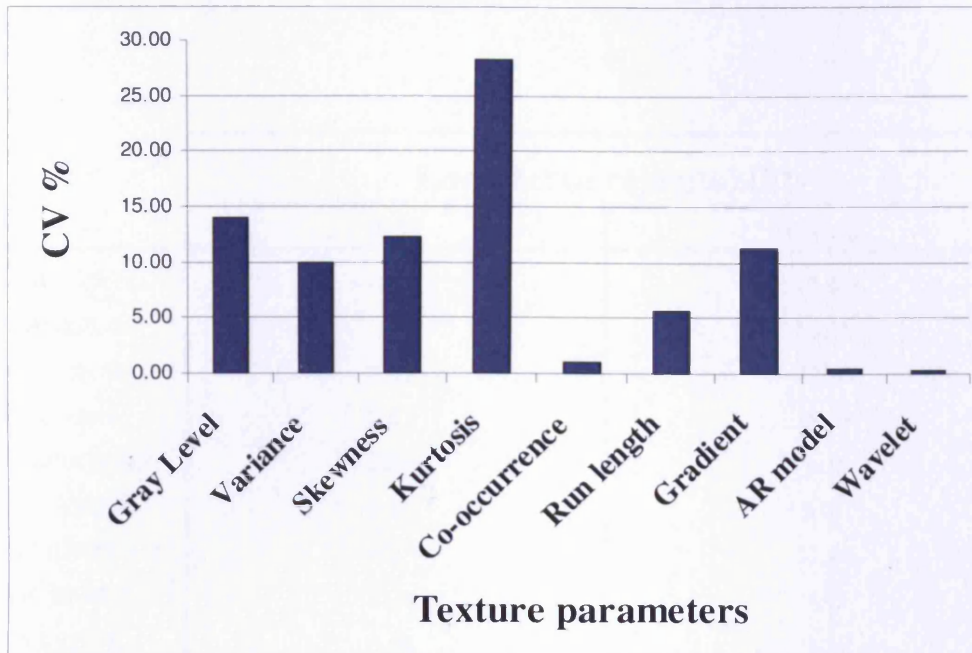
Figure 6.4 shows the long-term repeatability (CV %) of the texture parameters.
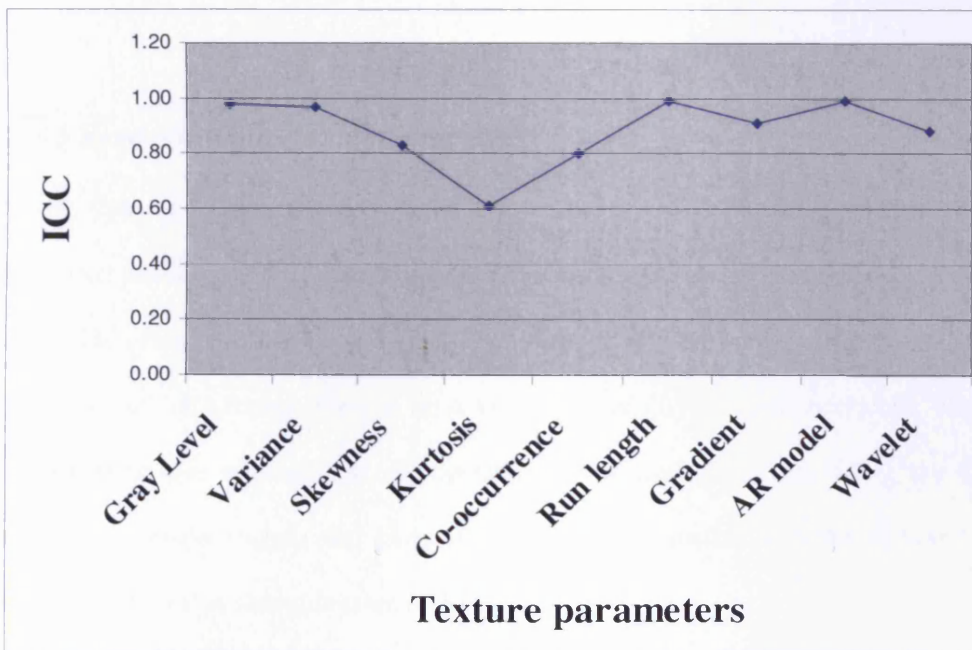
Figure 6.5 shows the ICC values for each texture parameter to test the long-term repeatability.

	Long term repeatability	
	ICC	CV %
Gray Level	0.98	13.94
Variance	0.97	10.01
Skewness	0.83	12.20
Kurtosis	0.61	28.23
Co-occurrence	0.80	1.04
Run length	0.99	5.57
Gradient	0.91	11.20
AR model	0.99	0.45
Wavelet	0.88	0.24

Table 6.2 ICC and CV % of the texture parameters long-term repeatability.

6.4.3 Reproducibility (Inter-operator)

Figure (6.6) and figure (6.7) show the CV % and the ICC values for each texture parameter and suggest that when compared, the variation between the two operators is negligible. This is reflected by high ICC values for repeats between operators. This suggests that, on average, there is little overall variability between operators. When the variation was measured as a proportion of the average values, using the CV values, the results suggest that kurtosis had the worst results, with the highest CV values (10.40%). as shown in table (6.3).
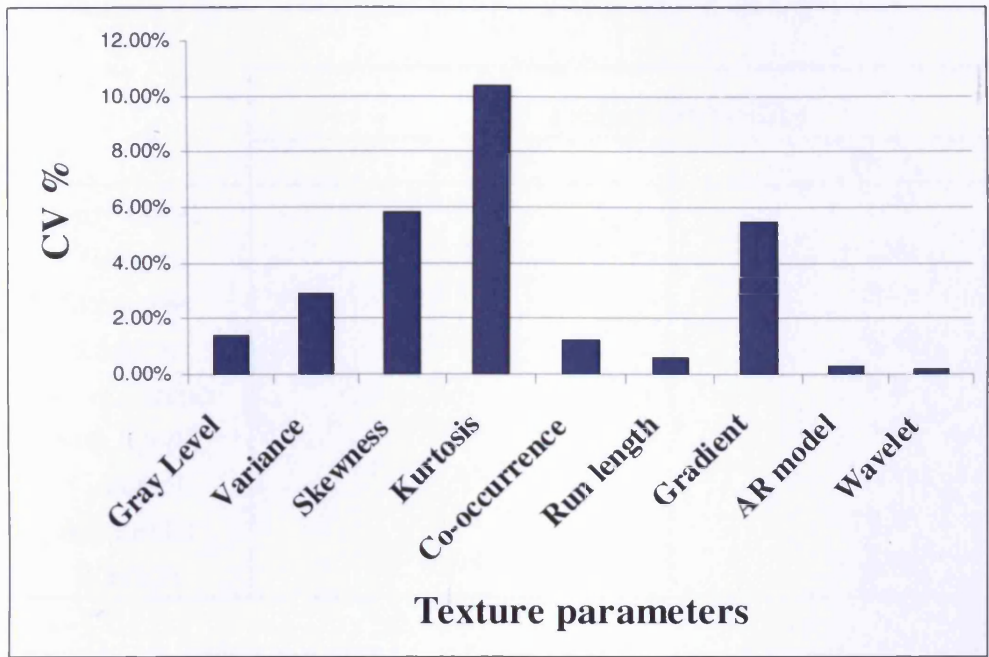
Figure 6.6 shows the reproducibility (CV %) of the texture parameters.
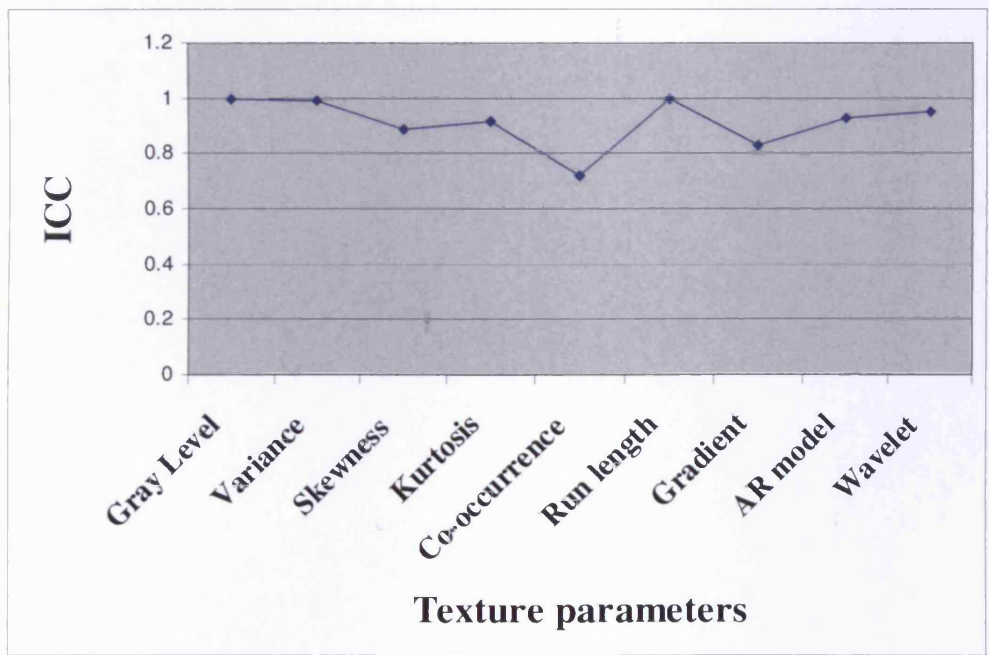
Figure 6.7 shows ICC values for each texture parameter to test the reproducibility.

	Reproducibility	
	ICC	**CV %**
Gray Level	0.99	1.40
Variance	0.99	2.90
Skewness	0.89	5.80
Kurtosis	0.92	10.40
Co-occurrence	0.72	1.20
Run length	0.99	0.60
Gradient	0.83	5.50
AR model	0.93	0.30
Wavelet	0.95	0.20

Table 6.3 ICC and CV % of the texture parameters reproducibility.

6.5 Discussion

For evaluating texture features of muscle, it is essential, to evaluate the repeatability and reproducibility of a given texture parameter since quantitative ultrasound tissue characterization is not a fully standardized procedure (Morales et al. 1996). The goal of this study was to test the accuracy of repeatability and reproducibility of the scanning method, and the changes, if any, in the texture parameters. In this study, calculation of the CV and ICC, showed that most of texture parameters, used to assess the characteristics of an echo image, are repeatable and reproducible, if all the ultrasonic settings are constant throughout the study. Each subject was scanned 10 times taking care to reposition the transducer each time. Low coefficients of variation (CV) were observed and good short-term and long-term repeatability for most of the texture parameters except kurtosis was encountered. When testing the reproducibility (inter-operators), all the texture parameters indicated high reproducibility with high ICC and low CV.

These results of short-term and long-term repeatability of first order statistical parameters agree with a study by Nielsen et al. (2000) and his colleagues. They investigated the repeatability of the first order statistics texture parameter by repeating the ultrasound scans 30 times on a subject. They found the coefficient variation (CV) of first order statistics to be gray level 5%, variance 15 %, skewness 16 % and kurtosis 35 %, which is similar to the results in this study as shown in table (6.4). When Nielsen et al. (2000) repeated the scanning at different days they found no statistically significant differences in the first order statistics parameters between the two different days. Nielsen et al. (2000) concluded that the results from the 30-repeated single measurement indicated a relatively high repeatability of the scanning

method, although the values of the coefficient variation emphasize the importance of using more than one measurement in order to increase the precision.

	Nielsen et al.(2000)	Current study
Gray level	5 %	5.88 %
Variance	15 %	9.12 %
Skewness	16 %	9.57 %
Kurtosis	35 %	27.95 %

Table 6.4 Comparison between the study by Nielsen et al.(2000) and the current study

The ICC and CV % for each texture parameter for short and long-term repeatability and reproducibility shown in table (6.5).

As mentioned earlier, quantitative ultrasound images are subject to variation from many sources. Since the ultrasound, scanning setting was fixed throughout the study and kept constant, variations due to human error and standard measurement errors could not be eliminated. For instance, the ultrasound probe had to manually positioned by the investigator and small movements and variations between two recordings could not be prevented, which may have a small influence on the echo intensity value in specific regions. In the other instance, movement of the subject during time of scanning could also be a reason for subtle variations in image and therefore texture features.

In realistic medical measurements, the limitations posed on repeatability and reproducibility due to errors of human handling and standard errors of measurement are inevitable and always present to a certain degree (Simaeys et al. 2000). Therefore, this study aims to provide an estimate of the minimum variation that may be

encountered in everyday clinical measurements rather than providing an estimate of the degree by which compensation of the texture features occurs due to human error, which in turn will affect repeatability and reproducibility. Another commonly encountered problem that causes variation in texture features is the presence of speckle noise, which seems to influence both visual interpretation of images and quantitative image analysis (Simaeys et al. 2000). The speckle noise reduces repeatability and reproducibility, especially when the ROI is small. The influence of speckle can be reduced or minimized by repeating the scans and taking the average of the texture values over large regions (Simaeys et al. 2000). This study adopted this method to minimize the influence of speckle noise. In the future, it would be useful to apply some method to suppress or filter speckle noise so scans that are more accurate can be performed.

	Short-term repeatability		Long-term repeatability		Reproducibility	
	ICC	CV %	ICC	CV %	ICC	CV %
Gray Level	0.96	5.88	0.98	13.94	0.99	1.40
Variance	0.92	9.12	0.97	10.01	0.99	2.90
Skewness	0.77	9.57	0.83	12.20	0.89	5.80
Kurtosis	0.68	27.95	0.61	28.23	0.92	10.40
Co-occurrence	0.61	2.30	0.80	1.04	0.72	1.20
Run length	0.98	2.11	0.99	5.57	0.99	0.60
Gradient	0.73	7.83	0.91	11.20	0.83	5.50
AR model	0.83	0.53	0.99	0.45	0.93	0.30
Wavelet	0.54	0.63	0.88	0.24	0.95	0.20

Table 6.5 Short-term and long-term repeatability and reproducibility for the texture parameters showing the ICC value and the coefficient variation (CV%) for each texture parameter

6.6 Conclusion

In conclusion, the results varied by the particular texture parameter examined, but overall the results suggested that there was a relatively good overall agreement between the two observers, between the measurements by the same observer on separate occasions and between repeat trials of the same subjects except for skewness and kurtosis.

Our resulted showed that second order statistics, AR model, and wavelet indicate higher repeatability and reproducibility than first orders statistics parameters.

CHAPTER 7

Reference set of normal gastrocnemius muscle

7.1 Introduction

To interpret abnormal or pathological features from US images, objective standardised normal data is required first to enable clinicians and researchers to distinguish normal from a pathological finding. The extracted statistical parameters of the ultrasound image give an understanding of the micro-structure of the organ or tissue (Wun and Chung 1998). Each organ and tissue type has unique characteristics and different texture features and when a single feature of the structure deviates from the normal the difference in texture is apparent (Wun and Chung 1998). When statistical parameters are extracted from specific region of interest of known structural components, the structure–plot for each feature conforms to a particular shape. Therefore, if every image is standardized i.e. to a particular property of gray level scale, the structure plot for each feature may share the same shape with images of the same organs. If this shape is consistent, a pathological state such as a malignant growth will change the characteristic or shape of the structure plot (Wun and Chung 1998). Many studies have shown that muscle pathologies alter the normal ultrasound image features. For instance, changes in muscle features (Heckmatt and Dubowitz 1985 , Reimers et al. 1996a , Schmidt and Voit 1993) and echo intensity (Heckmatt et al. 1988a , Kamala et al. 1985 , Zuberi et al. 1999) Therefore, a set of reference values for the different texture parameters are necessary to describe these changes quantitatively.

In order to define an objective parameter for tissue characterization, several factors have to be considered namely variation in diagnostic ultrasound equipment, different

tissue types, and the subjective interpretations of different investigators (Bamber and Hill 1981, Freese and Lyons 1977).

The variation of the texture features due to different levels of depth and variation of texture due to different size of ROI have to be considered. The table (7.1) summarises the findings from previous chapters and shows, which texture parameters that are not influenced by the factors mentioned above. The parameters that were not affected were the co-occurrence matrix, gradient, AR model and wavelet transform.

In this chapter, the main purpose was to investigate the texture features between medial gastrocnemius muscle in the right and left leg, the texture features between gastrocnemius and biceps muscle and to establish a normal range of values for muscle echo intensity using standardized real-time ultrasound examination in healthy subjects. Another goal was investigating texture parameters, in order to differentiate normal from injured muscle, which can be used as a tool to monitor the healing process. By combining several texture parameters in muscle US imaging may help in diagnosing muscle injury more accurately and help in monitoring the healing process ,which eventually could lead to finding the most effective treatment for muscle injury.

	Repeatability	Reproducibility	Depth	Size of ROI	Scanning sites	Gain (75-80-85)	Dynamic range
Gray level	√	√	X	√	√	X	√
Variance	√	√	X	√	√	X	√
Skewness	X	√	√	√	√	X	√
Kurtosis	X	√	√	√	√	X	√
Co-occurrence matrix	√	√	√	√	√	√	√
Run length matrix	√	√	X	X	√	X	√
Gradient	√	√	√	√	√	√	√
AR model	√	√	√	√	√	√	√
Wavelet	√	√	√	√	√	√	√

Table 7.1 Shows effect on the various texture parameters when different factors are altered

7.2 Participants

The right and left medial gastrocnemius muscle were scanned in 25 healthy subjects {21 males/4 females, with a mean age of 24 years (Range: 18-38 years)} 5 patients who had sustained injury to the gastrocnemius muscle were also scanned .In addition, the left biceps muscles was scanned in 4 male subjects out of the 25 subjects, with mean age of 28 years (range 25-38).All the subjects had normal health with no history of any musculoskeletal disorder or injury that required medical attention. Precautions were taken to ensure that none of the subjects had performed physical exercise prior to the scanning, which might have interfered with scan results due to increase in blood flow to the muscle. Approval of the local Ethics Committee was obtained and all participants were fully informed about the protocol and procedure before obtaining their consent. A three dimensional Ultrasound sweep was performed on the central region of the gastrocnemius and biceps muscles and four slices were extracted from the 3D set with 10 mm distance between them. The ultrasound scans were performed according to the standard protocol and image acquisitions for all the subjects described in chapter 3. All the system setting parameters such as gain (80 dB), dynamic range (80 dB), depth (4 cm), sweep angle (30 degrees), and TGC central, was kept constant throughout the study.

7.3 Comparing right to left leg

7.3.1 Method

For comparing between the medial gastrocnemius in the right and left leg , only one slice was chosen for the investigation as a previous study on 10 subjects (see chapter 4) has shown the middle part of the gastrocnemius muscle is homogenous. On each Ultrasound image slice, the largest possible rectangular ROI that encompassed the gastrocnemius muscle with a size of 280x70 pixels was defined. The size and shape of the ROI were kept constant for all slices in all subjects. The ROI was defined within the border of the medial gastrocnemius muscle of legs, avoiding muscle boundaries, or neighbouring structures

7.3.2 Statistical analysis

The Shapiro-Wilk test was used to test the normality of the data due to the small sample size of the study (<50).All texture parameters were found to be approximately normally distributed (P > 0.05). Therefore, paired t-test was used to test for significant differences between the right and left leg (the P value was set to 0.05 which was considered to be statistically significant).SPSS for Windows version 16 (SPSS inc., Chicago, II, USA) was the statistical package used for the statistical analysis

140

7.3.3 Result

Figure (7.1) to figure (7.4) shows the values of co-occurrence matrix, gradient, autoregressive model and wavelet transforms for the medial gastrocnemius muscle of the left and right legs. The trends in those parameters are similar in both legs. The mean value for each texture parameter in each leg with upper and lower 95 % interval confidence is shown on table (7.1). No significant differences in the texture features between the right and left medial gastrocnemius muscle were found (Table 7.2) indicating that the medial gastrocnemius muscles of the left leg have similar texture features to the medial gastrocnemius of the right leg
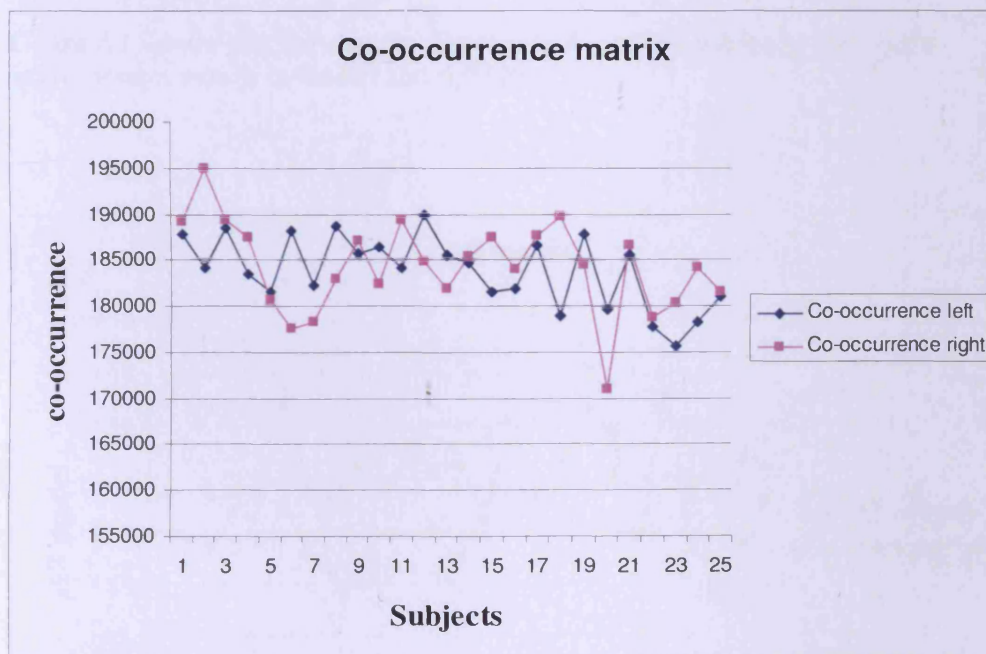
Figure 7.1 Scatter plot showing the dispersion of co-occurrence matrix values for the medial gastrocnemius muscle in the left and right legs.
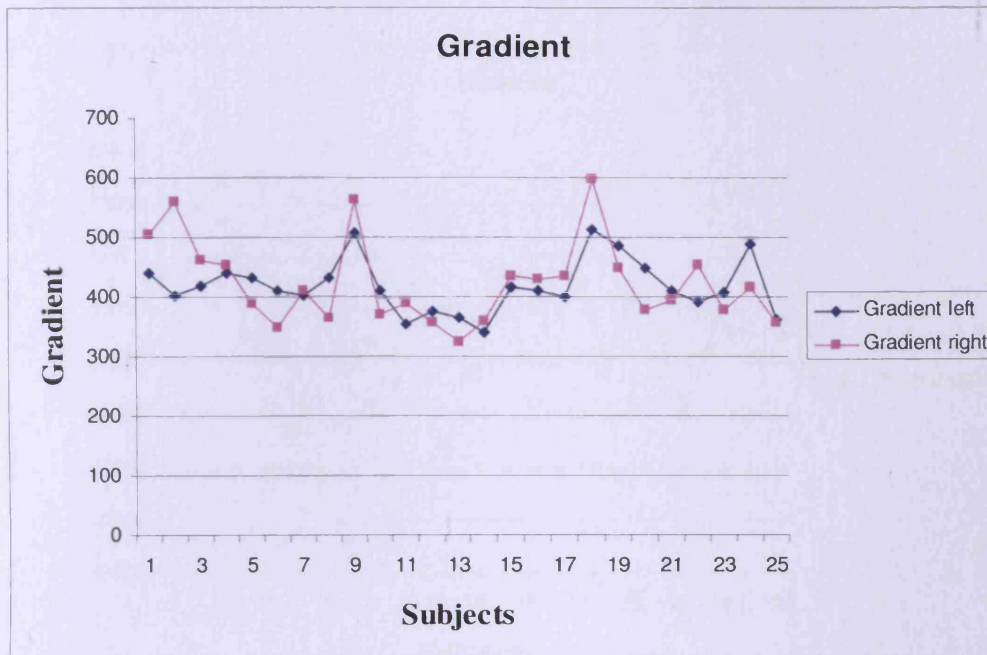
Figure 7.2 Scatter plot showing the dispersion of gradient values for the medial gastrocnemius muscle in the left and right legs.
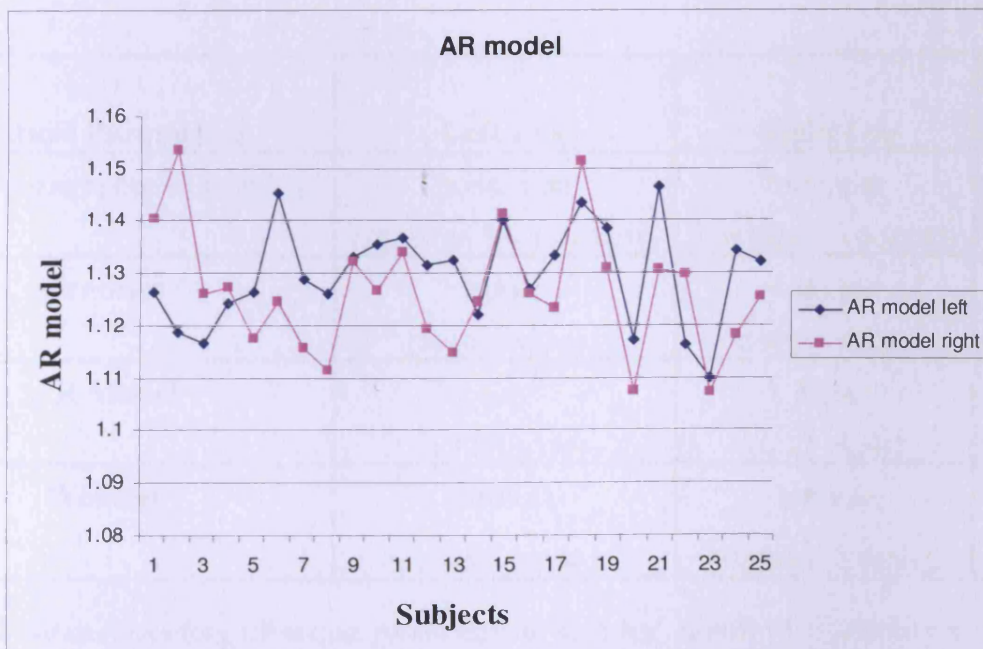
Figure 7.3 Scatter plot showing the dispersion of autoregressive model values for the medial gastrocnemius muscle in the left and right legs.
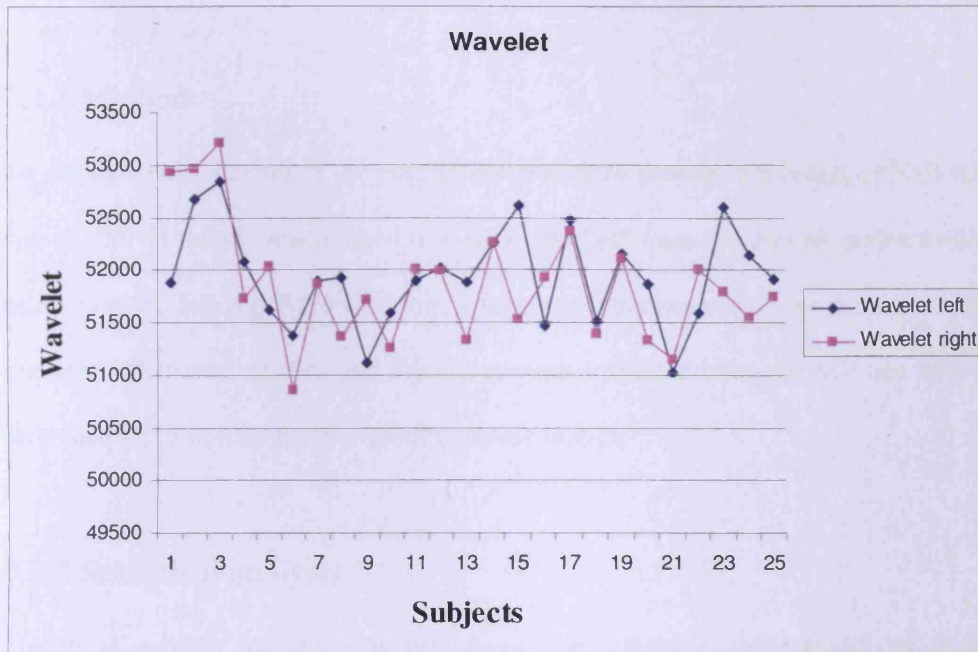
Figure 7.4 Scatter plot showing the dispersion of wavelet values for the medial gastrocnemius muscle in the left and right legs.

Texture Parameters	Left Leg	Right Leg	p-value
Co-occurrence matrix	183855.7381	184316.98	
	(182257.16.56 - 185454.31)	(182249.35 - 186384.62)	0.720
Gradient	418.62	423.36	
	(400.06 - 437.17)	(394.09 - 452.63)	0.839
AR Model	1.13	1.126	
	(1.126 - 1.134)	(1.122 - 1.131)	0.154
Wavelet	51939.53	51858.39	
	(51744.93 - 52134.13)	(51620.84 - 52095.93)	0.399

Table 7.2 Mean values for each texture parameters for each leg , (lower 95 % interval confidence of the mean , upper 95 % interval confidence of the mean) and p value (p>0.05) not significant difference

7.4 Reference set of normal gastrocnemius muscle

7.4.1 Method

To obtain a reference set of the normal gastronomies muscle, a rectangular ROI with size of 280*70 pixels was defined in a slice obtained from the medial gastrocnemius muscle on the left leg. Following this, four-texture parameters co-occurrence matrix, gradient, AR model and wavelet transform were extracted from the ROI and used as reference set of normal healthy gastrocnemius muscle.

7.4.2 Statistical analysis

Statistical analysis was done by calculating the reference range based on normal subjects only. A 95% reference range was calculated, giving the interval into which it would be expected that 95% of all normal subjects would fall. This was calculated using the following formula:

95% reference range = Mean ± 1.96 standard deviation

Stata software version 9.2 (StataCorp, College Station, Texas, USA) was the statistical package used for statistical analysis

7.4.3 Result

Figure (7.5) to figure (7.8) shows the reference ranges for each of the four textures parameters co-occurrence matrix, gradient, autoregressive model and wavelet transforms. The values shown are of the medial gastrocnemius muscle of the left leg and are based on the normal subjects only. The figures show the mean, standard deviation and 95% reference range for each texture parameter. Table (7.3) shows the mean, SD, CV and the 95 % upper and lower for each of texture parameters.
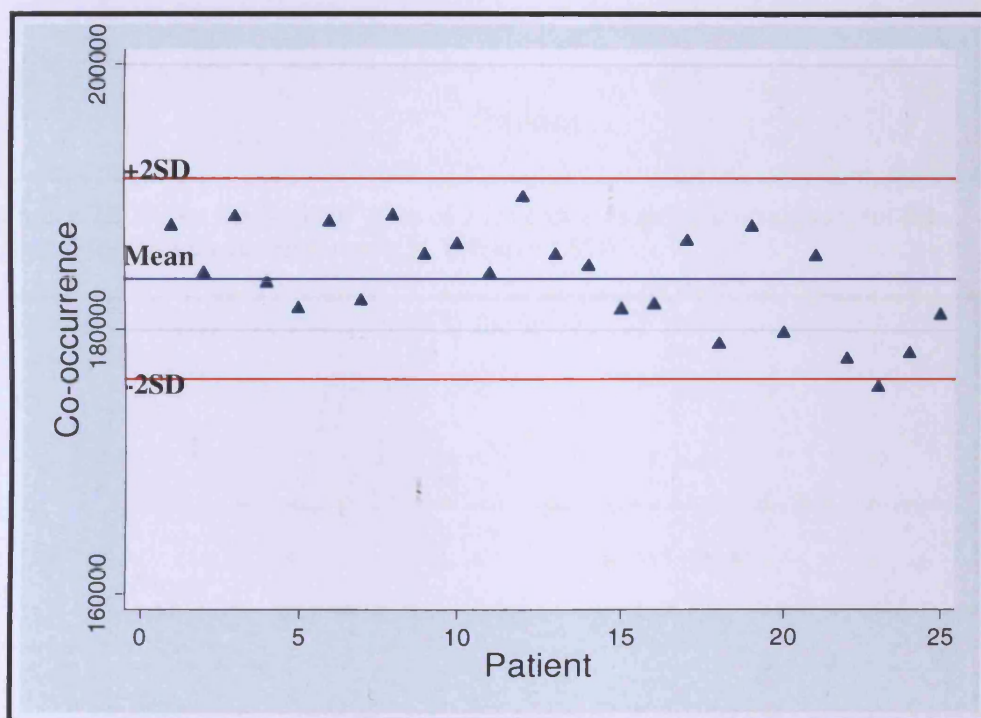
Figure 7.5 Shows the co-occurrence matrix value of 25 subjects as reference value set for normal medial gastrocnemius muscle. (Mean ±2 SD)
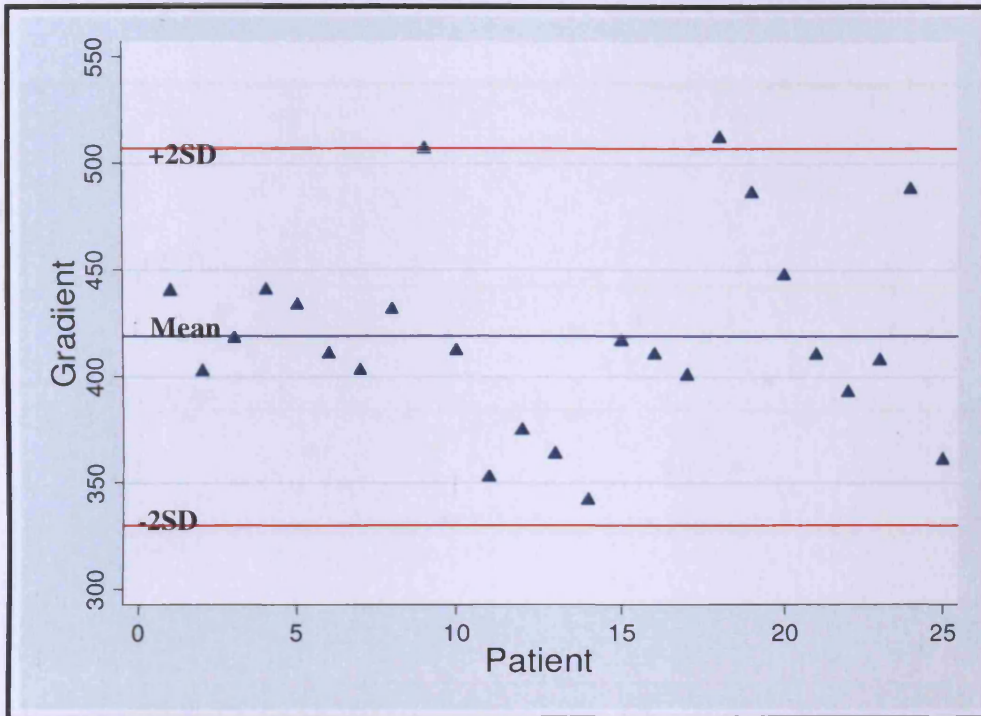
Figure 7.6 Shows the gradient value of 25 subjects as reference value set for the normal medial gastrocnemius muscle. (Mean ±2 SD)
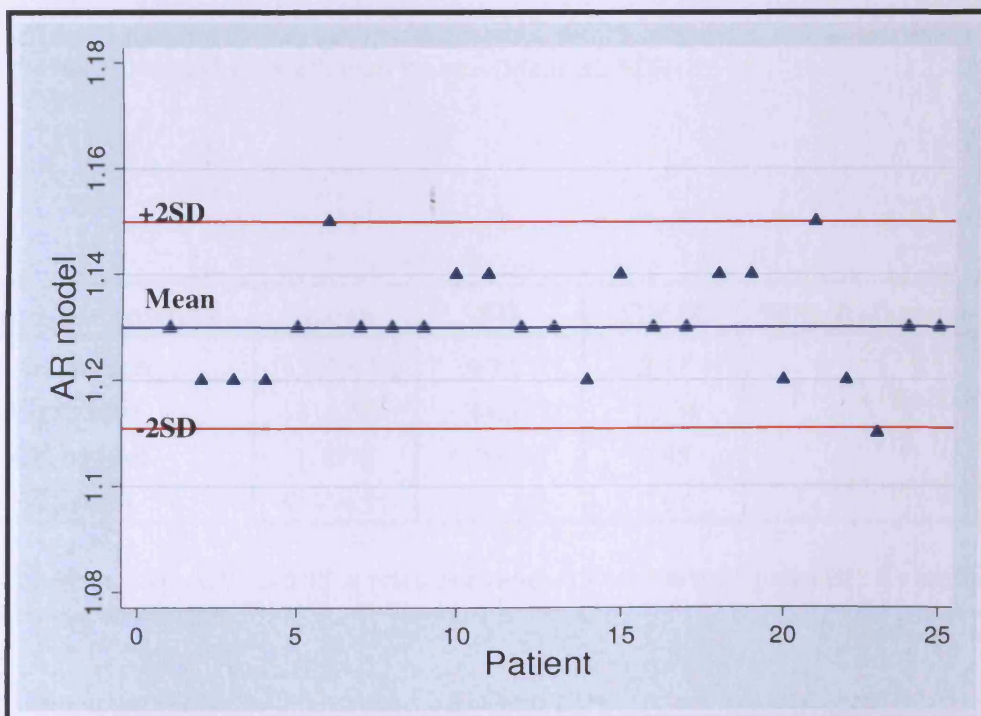
Figure 7.7 Shows the auto-regressive model value of 25 subjects as reference value of normal medial gastrocnemius muscle. (Mean ±2 SD)
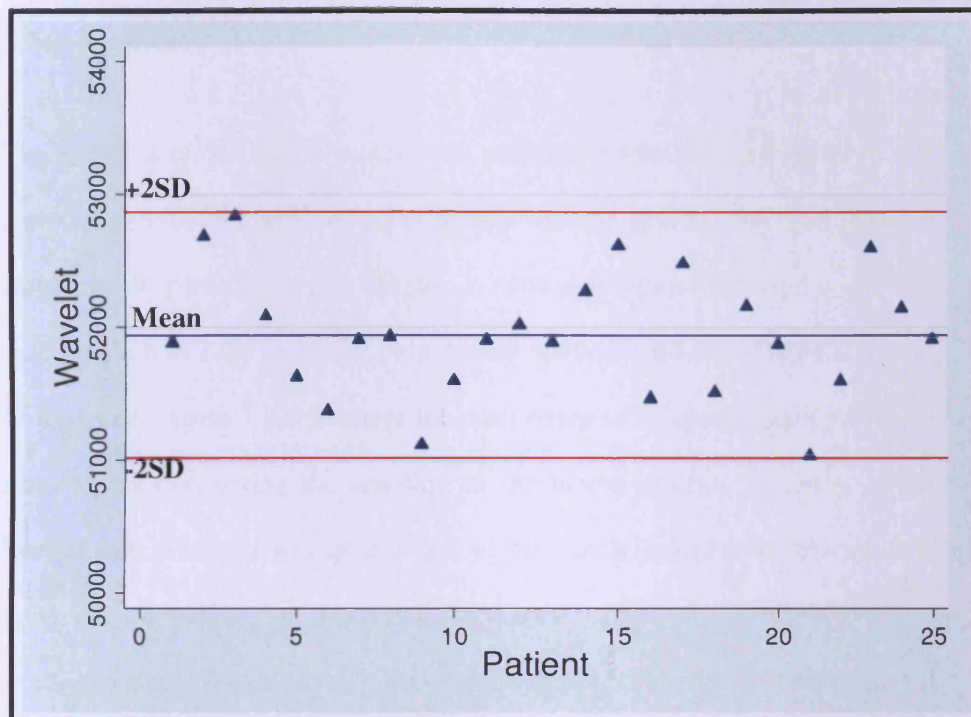
Figure 7.8 shows the wavelet transform value for 25 subjects as reference value set for normal medial gastrocnemius muscle (Mean ±2 SD)

Texture parameters	Mean	SD	CV %	95% Reference Range
Co-occurrence	183855.733	3872.7	2.11	(176265, 191446)
Gradient	418.62	44.95	10.74	(330, 507)
AR model	1.1298	0.00955	0.85	(1.111, 1.150)
Wavelet	51939.53	471.44	0.91	(51016, 52864)

Table 7.3 Mean , SD , CV and 95 % reference range for each texture parameter for medial gastrocnemius muscle (n=25).

7.5 Normal gastrocnemius muscle versus Biceps muscle

7.5.1 Method

The scanning of the biceps muscle was performed with the application of a similar protocol used for the gastrocnemius muscle and the process was kept standard with respect to all participants (see chapter 3). The participants lay supine on the couch, with their elbow fully extended, palm facing upwards and arm parallel to the midline of the trunk. Figure 7.10 illustrates the positioning of the participants and the images from four slices, during the scanning of the biceps muscle. To locate the area of interest, a skin marker was used to define the muscle's origin, insertion and the mid point was located through measuring the muscle using a measuring tape. The middle of the probe was placed in the middle of the muscle. Four slices were extracted from the 3D set along the length of the biceps muscle with distance 10 mm between them. One slice was considered sufficient in this study based on the assumption that the middle region of the muscle is homogenous (see chapter 4). A cross sectional 2D ultrasound set of images of the biceps muscle was obtained (figure 7.9). The participants were allowed to move and relax between each scan and the probe was repositioned to the standard position anew each time.

Fascia

Biceps muscle

Humerus
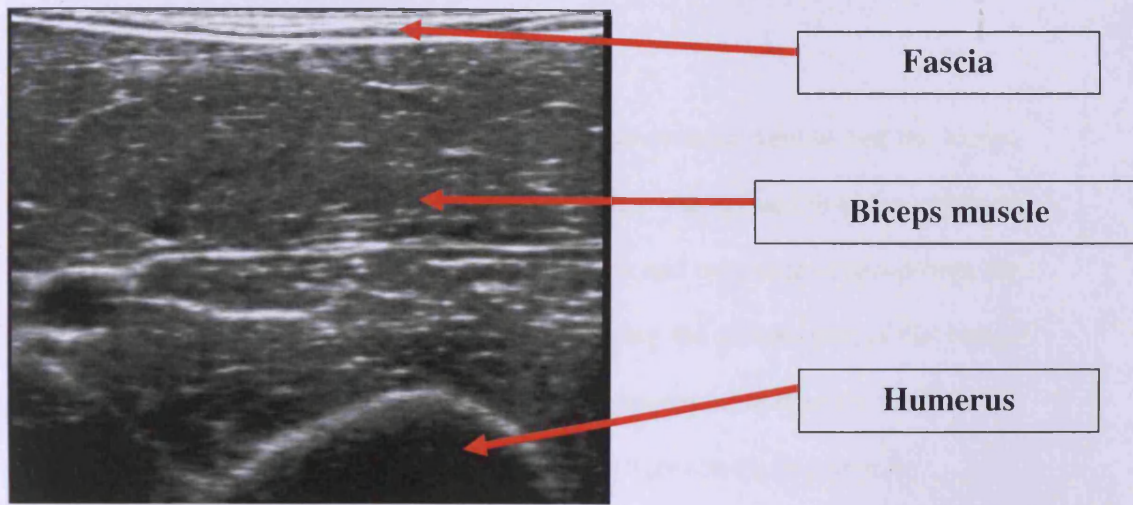
Figure 7.9 Ultrasound scans showing cross section of biceps muscle

Slice 1

Slice 2

Slice 3

Slice 4
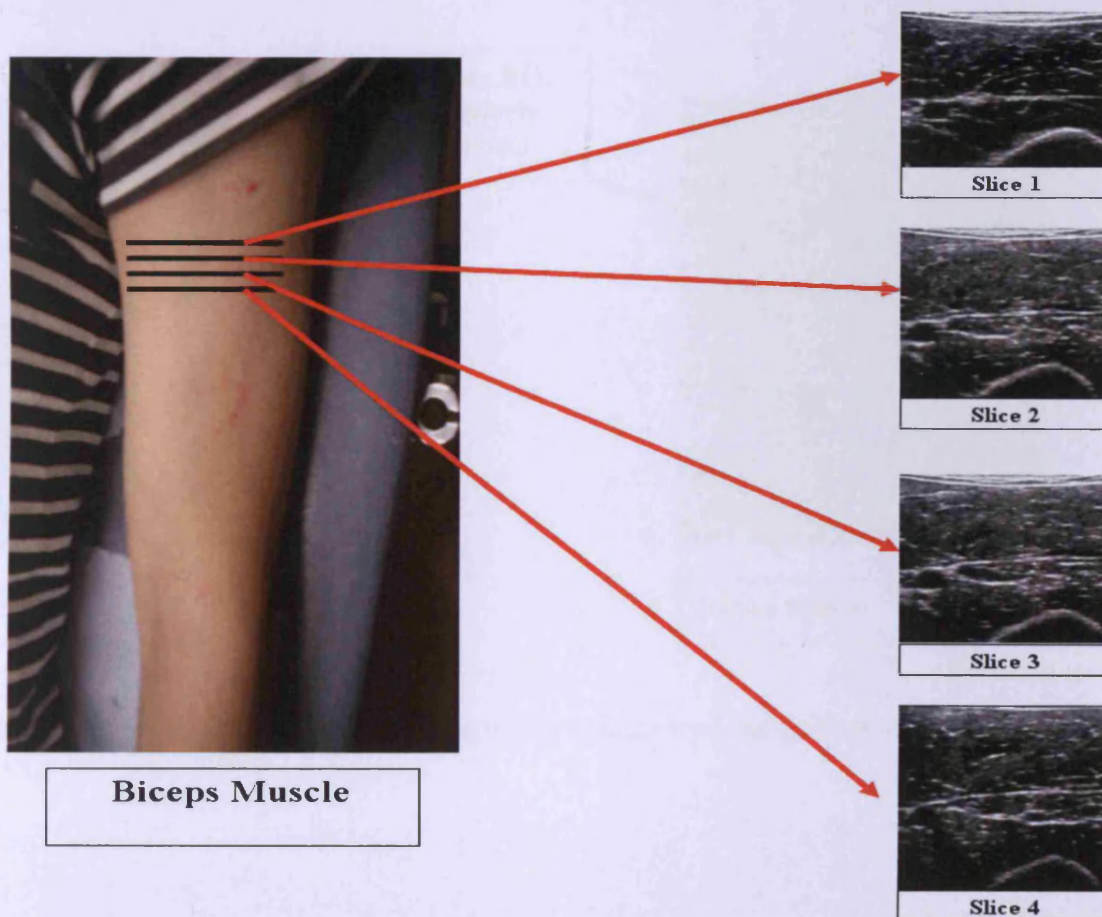
Biceps Muscle

Figure 7.10 Positioning of participants for scanning and example of the images extracted from 4 slices at the points shown on the participant.

To compare the texture features between the gastrocnemius muscle and the biceps muscle. A rectangular ROI with size of 280*70 pixels was defined in a slice obtained from the medial gastrocnemius muscle on the left leg and on a slice obtained from the middle of the biceps muscle on the left arm assuming the middle part of the biceps muscle is homogenous figure (7.11). Four texture parameters were extracted from the ROI and a suitable statistics was applied to compare between the two muscles.
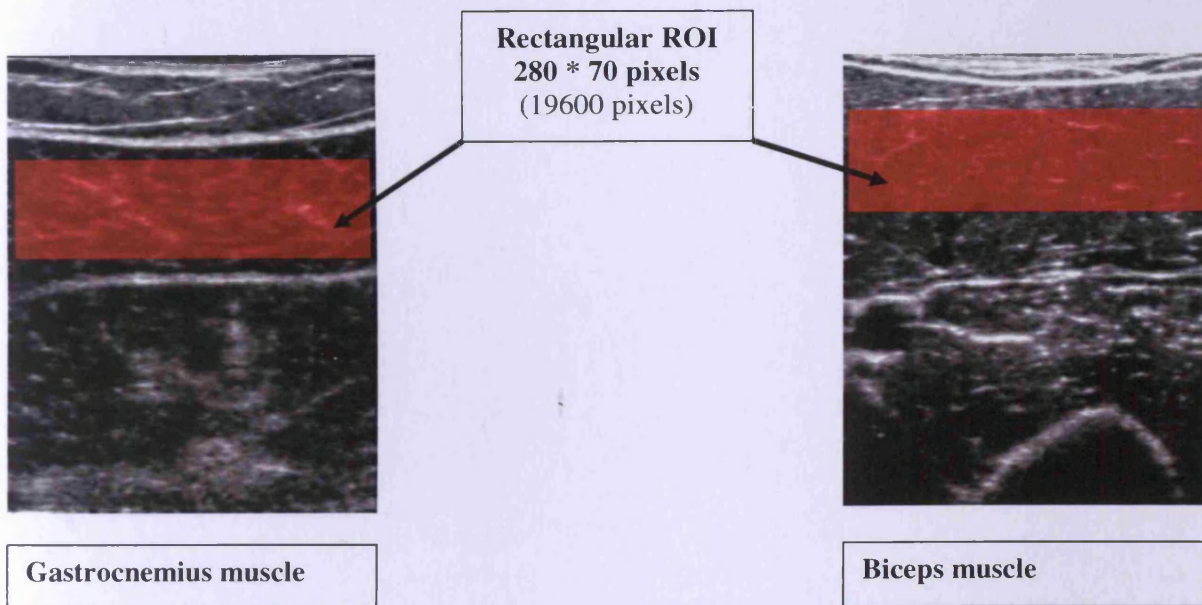
Figure 7.11 Image with red area shows the region of interest on the gastrocnemius muscle and biceps muscle

7.5.2 Statistical analysis

The Shapiro- Wilk test was used to test the normality of the data due to the small sample size of the study (<50).All texture parameters were found to be approximately normally distributed (P > 0.05). Therefore, paired t-test was used to test significant difference in each texture parameter between gastrocnemius muscle and biceps muscle. (The P value was set to 0.05, which was considered statistically significant) SPSS for Windows version 16 (SPSS inc., Chicago, II, USA) was the statistical package used for statistical analysis

7.5.3 Result

Significant differences in the average values of the co-occurrence matrix, gradient,
and AR model were found between the gastrocnemius muscle and the biceps muscle
as shown in figure (7.12) to figure (7.14). Wavelet transform shows no significant
difference between the gastrocnemius muscle and the biceps muscles fig (7.15). The
average values and SD for each of the texture parameters are shown in table (7.4).
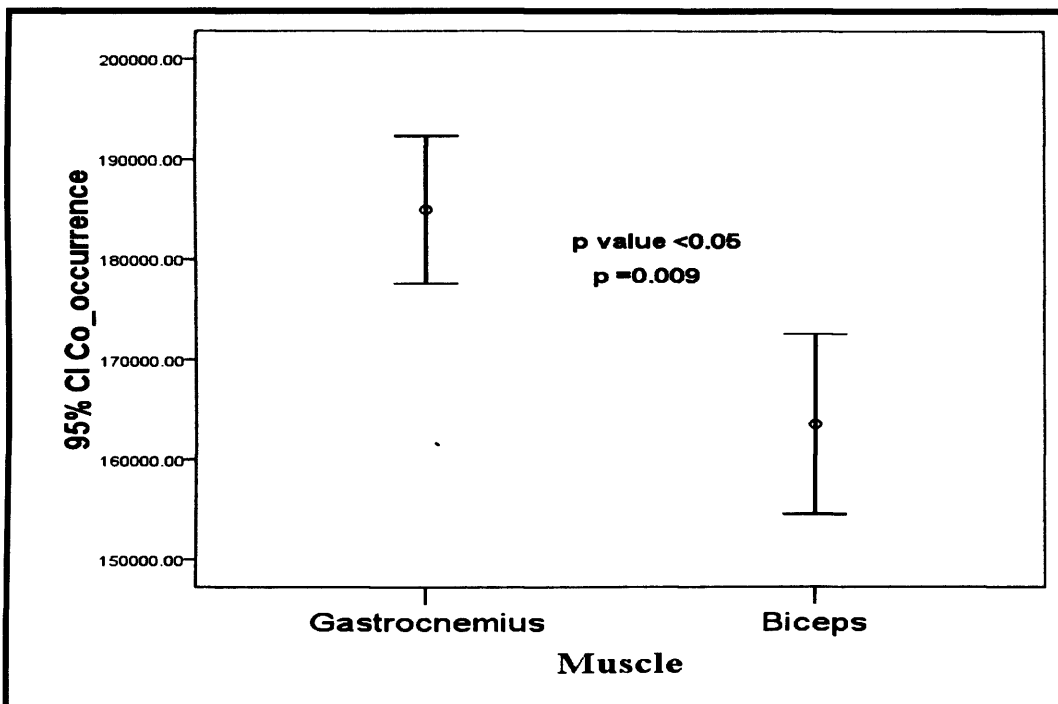
Figure 7.12 Error bar plot showing mean and SD of co-occurrence matrix of normal
gastrocnemius muscle and normal biceps muscle, error bar with 95 % confidence
interval. P > 0 .05(no significant difference)
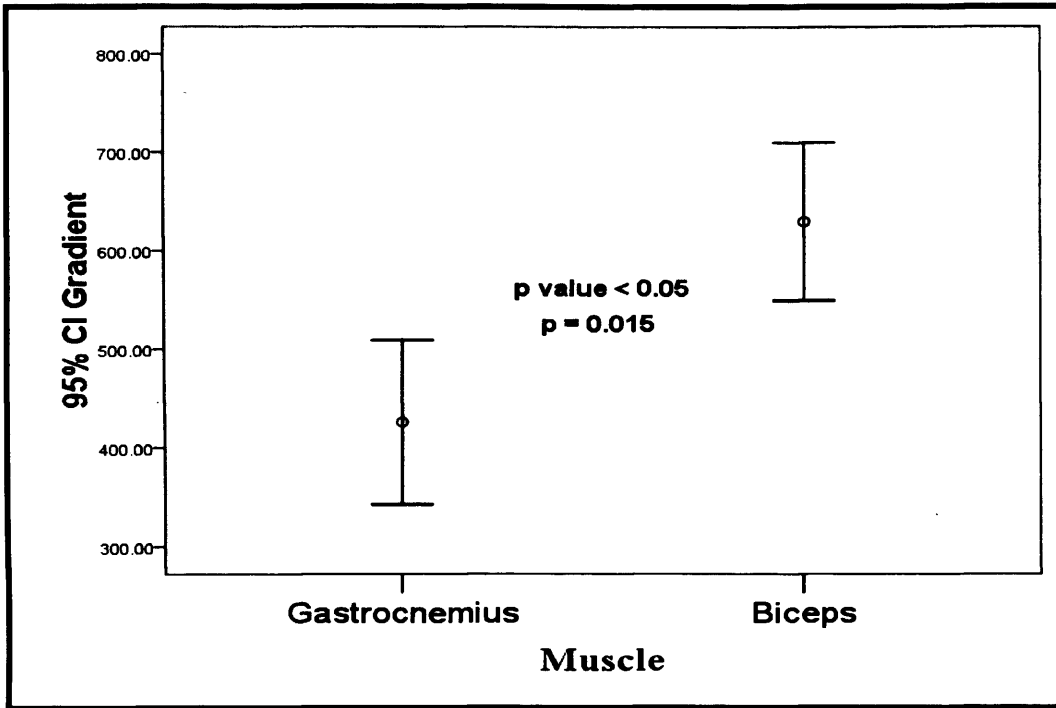
Figure 7.13 Error bar plot showing mean and SD for gradient values of normal gastrocnemius muscle and normal biceps muscle, error bar with 95 % confidence interval. P > 0 .05(no significant difference)
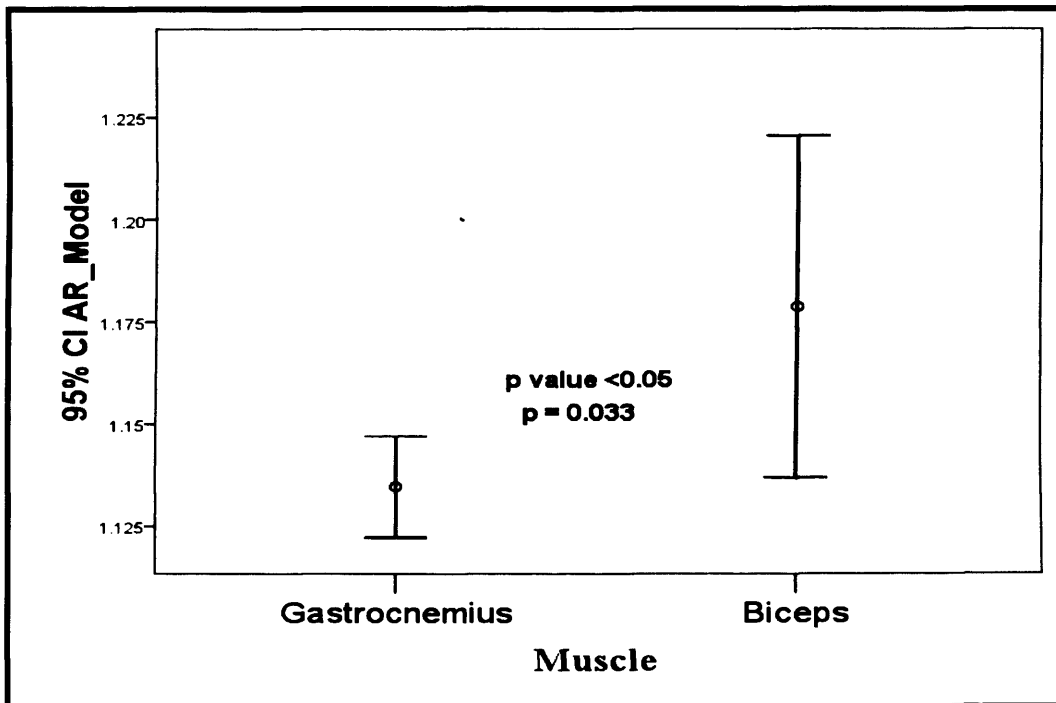
Figure 7.14 Error bar plot showing mean and SD of auto-regressive model values for normal gastrocnemius muscle and normal biceps muscle, error bar with 95 % confidence interval. P > 0 .05(no significant difference)
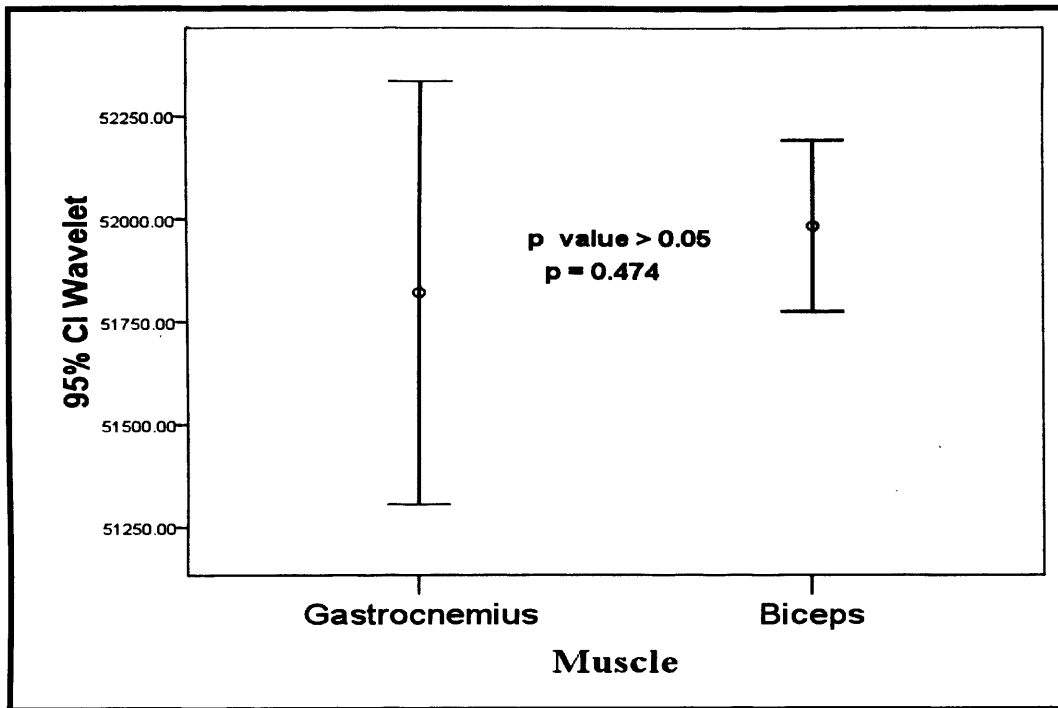
Figure 7.15 Error bar plot showing mean and SD for wavelet transform of normal gastrocnemius muscle and normal biceps muscle, error bar with 95 % confidence interval. P > 0 .05(no significant difference)

Parameter	Gastrocnemius Mean (SD)	Biceps Mean (SD)	P-value
Co-occurrence	184967 (46273)	163540 (5560)	0.009
Gradient	425 (52)	630 (50)	0.015
AR model	1.13 (0.01)	1.18 (0.03)	0.033
Wavelet	51821 (324)	51984 (131)	0.474

Table 7.4 Mean, SD, and p -value for each texture parameter extracted from medial gastrocnemius muscle images and biceps muscle n = 4 subjects. P<0.05 significant difference

7.6 Normal gastrocnemius muscle versus injured muscle

7.6.1 Method

For patient with the injured muscle the scan was repeated 5 times in order to quantify muscle rupture, a big ROI defined on each slice, the average of the five scans were obtained to minimize the variation. An example of injured muscle with the ROI defined is shown in figure (7.16). The size of the ROI of 5 subjects was varying from 48598 pixels to 98272   pixels.

Procedure for selecting ROI on the injured muscle were

- To include as much as possible of the muscle

- Defining the ROI within the border of the gastrocnemius muscle

- Avoiding inclusion of muscle boundaries

- To ensure the ROI includes the ruptured area.
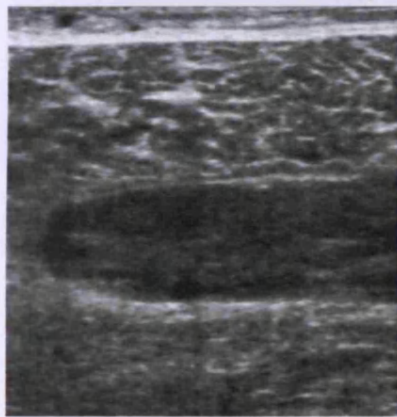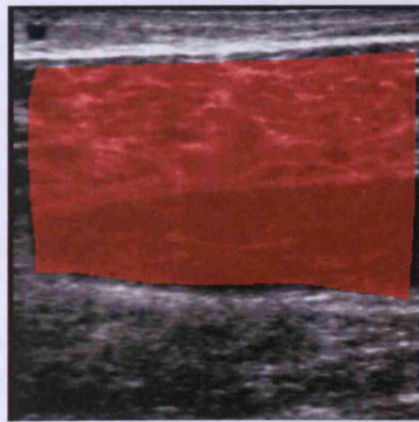
A   B

Figure 7.16 A: showing the bruising on the muscle **B:** ROI defined within the border of the muscle

7.6.2 Statistical analysis

The Shapiro- Wilk test was used to test the normality of the data due to the small sample size of the study (<50).All texture parameters were found to be approximately normally distributed (P>0.05). Therefore an unpaired t-test was used to test for any significant difference in each texture parameter between normal gastrocnemius muscles and injured muscle (the P value was set to 0.05 which was considered to be statistically significant). A 95% reference range was calculated, giving the interval into which it would be expected that 95% of all normal patients would fall. This was calculated using the following formula:

95% reference range = Mean ± 1.96 standard deviation

Stata software version 9.2 (StataCorp, College Station, Texas, USA) was the statistical package used for statistical analysis.

7.6.3 Results

The results of normal features of the gastrocnemius muscle when compared to the injured muscle showed significant differences in the average values of gradient, AR model, and wavelet. These differences are shown in figures 7.17 to figure 7.20. The average value of gradient (419) in the gastrocnemius muscle was higher than of injured muscle (219). The average value of AR model (1.13) in the gastrocnemius muscle was higher than the value in injured muscle (1.09). The value of the wavelet transform (51940) in the gastrocnemius muscle was lower than the value in injured muscle (52912) as shown in table 7.5.
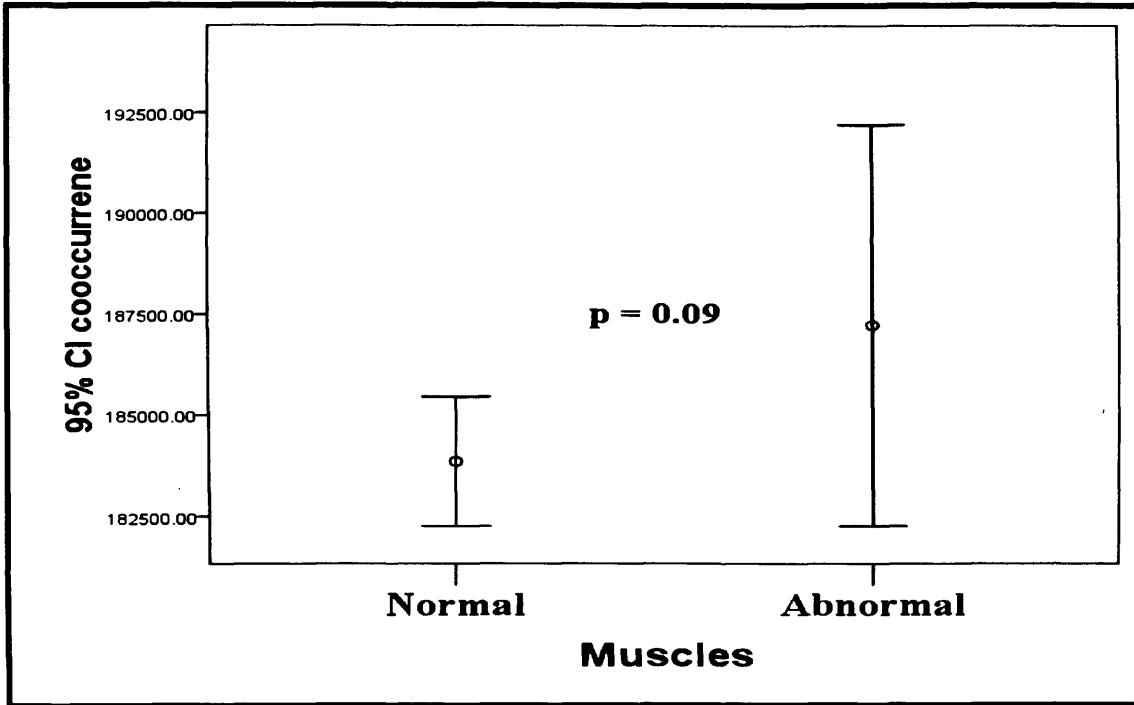
Figure 7.17 Error bar plot showing mean and SD for co-occurrence matrix values for normal and injured gastrocnemius muscle, error bar with 95 % confidence interval (p > 0 .05 : no significant difference)
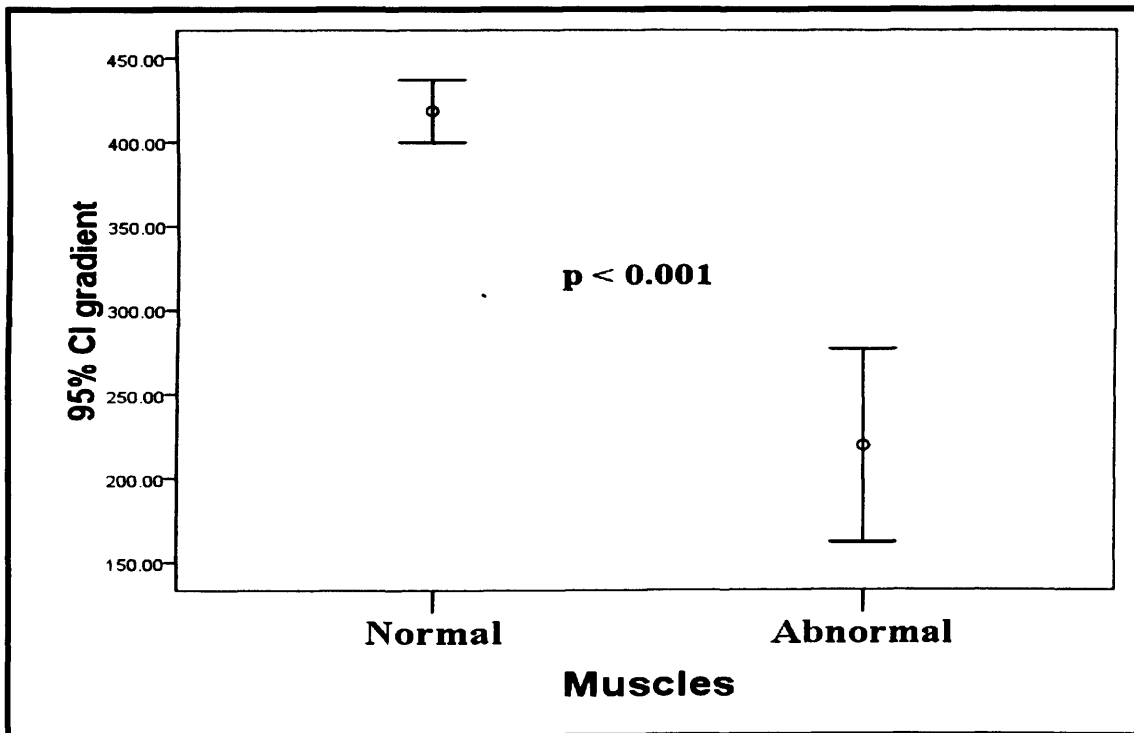
Figure 7.18 Error bar plot showing mean and SD of gradient values of normal gastrocnemius and abnormal muscle, error bar with 95 % confidence interval (p < 0 .05 : significant difference)
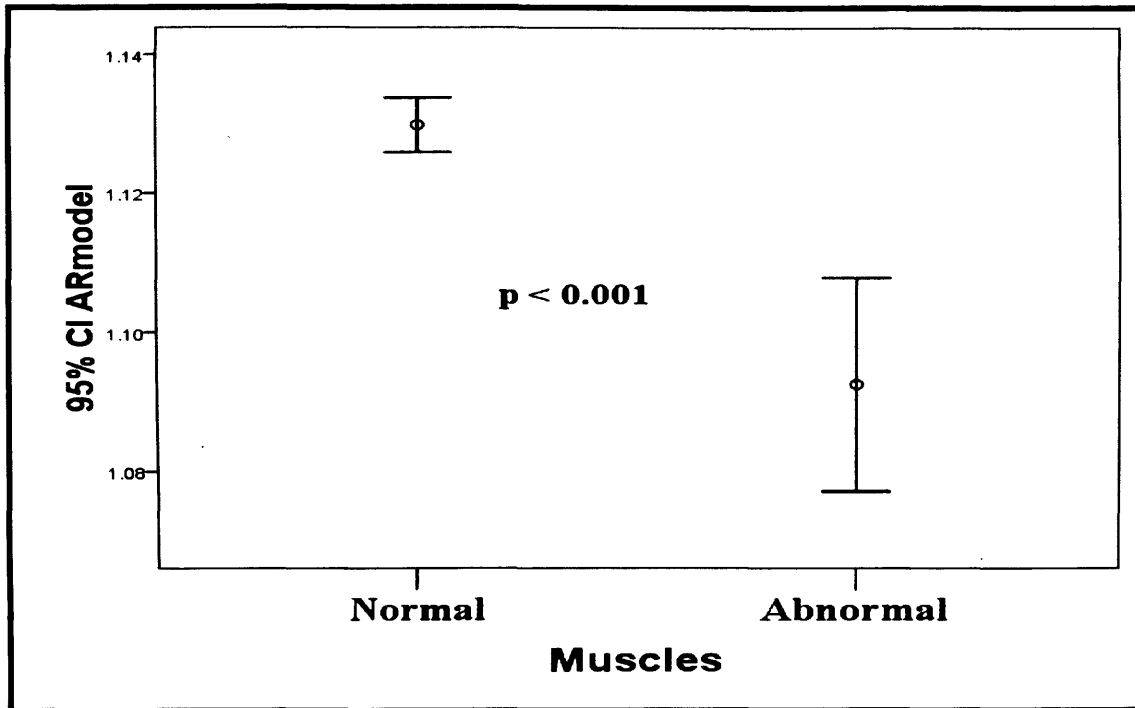
Figure 7.19 Error bar plot showing mean and SD of auto-regressive model values for normal and abnormal gastrocnemius muscle, error bar with 95 % confidence interval. (p < 0 .05 : significant difference)
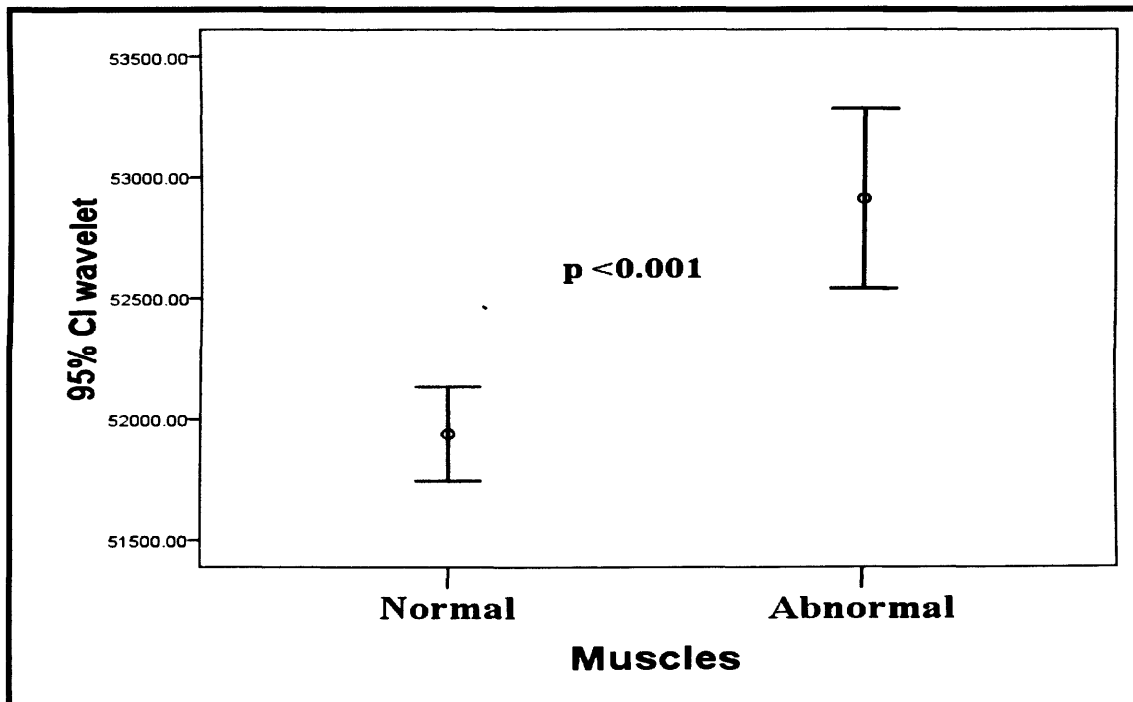
Figure 7.20 Error bar plot showing mean and SD of wavelet transform values of normal and abnormal gastrocnemius muscle, error bar with 95 % confidence interval. (p < 0 .05 : significant difference)

Parameter	Normal Mean (SD)	Abnormal Mean (SD)	P-value
Co-occurrence	183856 (3873)	187234 (4005)	0.09
Gradient	419 (45)	219 (46)	<0.001
AR model	1.13 (0.01)	1.09 (0.01)	<0.001
Wavelet	51940 (471)	52912 (299)	<0.001

Table 7.5 Mean, SD, and p -value for each texture parameter extracted from normal medial gastrocnemius muscle (n=25) and abnormal muscle (n=5)

Figures (7.21) to (7.24) show the results for the normal subjects for each of texture parameters plotted against the subjects with injured muscle. The horizontal lines in the graphs indicate the mean value for normal subjects (in blue) and the 95% reference ranges (in red). Also plotted on the graphs, in a different colour, are the results for the abnormal subject (brown triangles).

The results indicated that gradient, AR model, and wavelet significantly varied between normal and abnormal patients. Gradient and AR model were significantly lower in abnormal patients than the normal patients were, whilst wavelet values were significantly higher in abnormal patients relative to normal patients. There was no evidence to suggest that co-occurrence values varied between normal and abnormal subjects.
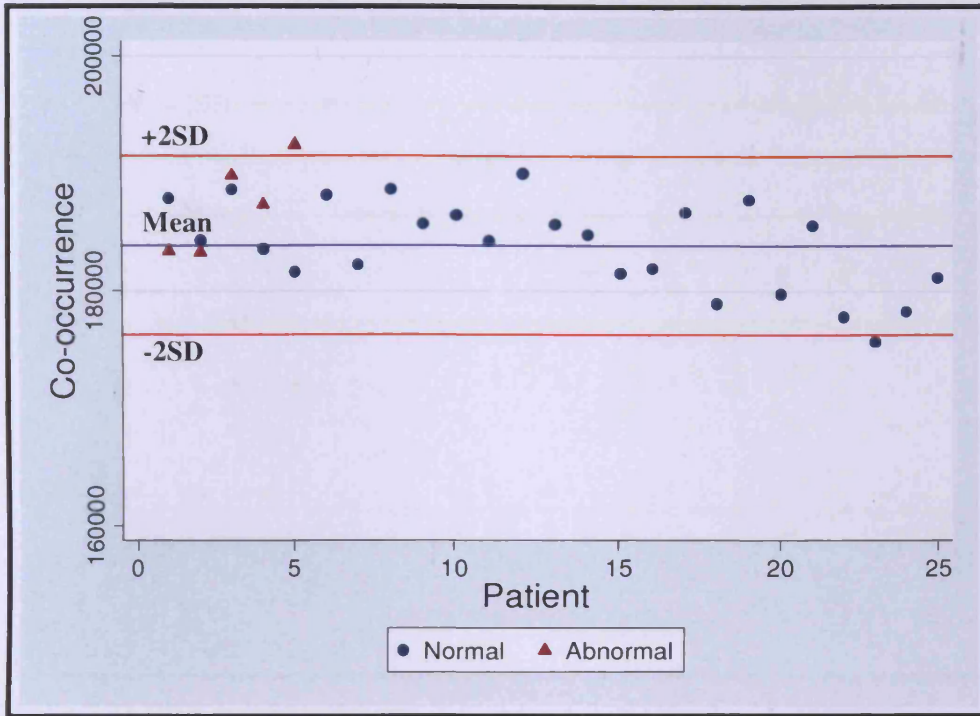
Figure 7.21 95% agreement of co-occurrence matrix (Mean ±2 SD) of normal medial and injured gastrocnemius muscle
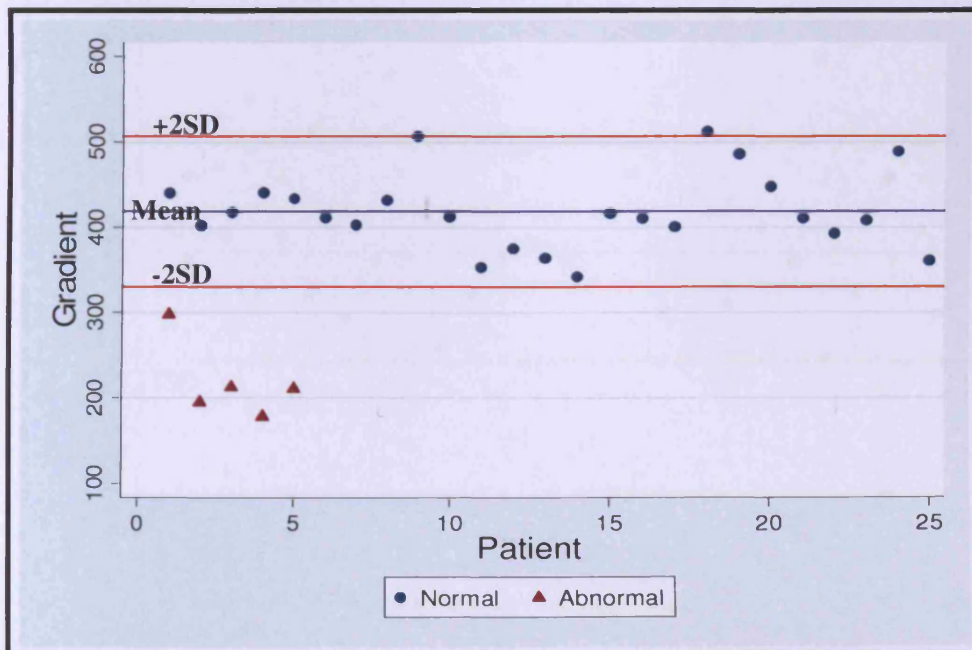
Figure 7.22 95% agreement of gradient (Mean ±2 SD) of normal medial and injured gastrocnemius muscle.
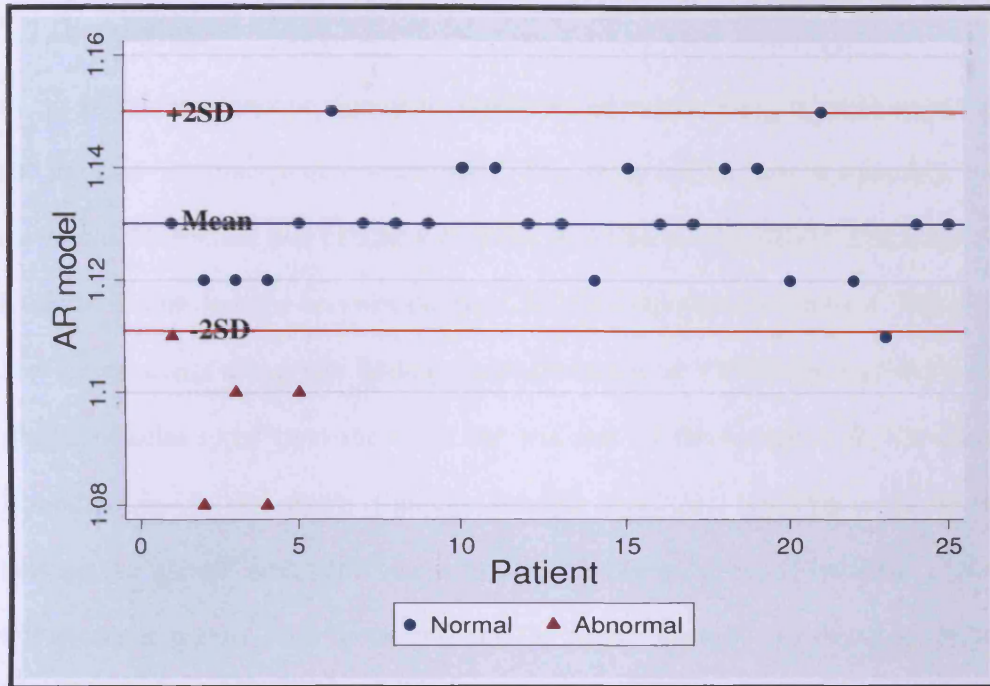
Figure 7.23 95% agreement of auto-regressive model (Mean ±2 SD) of normal medial and injured gastrocnemius muscle.
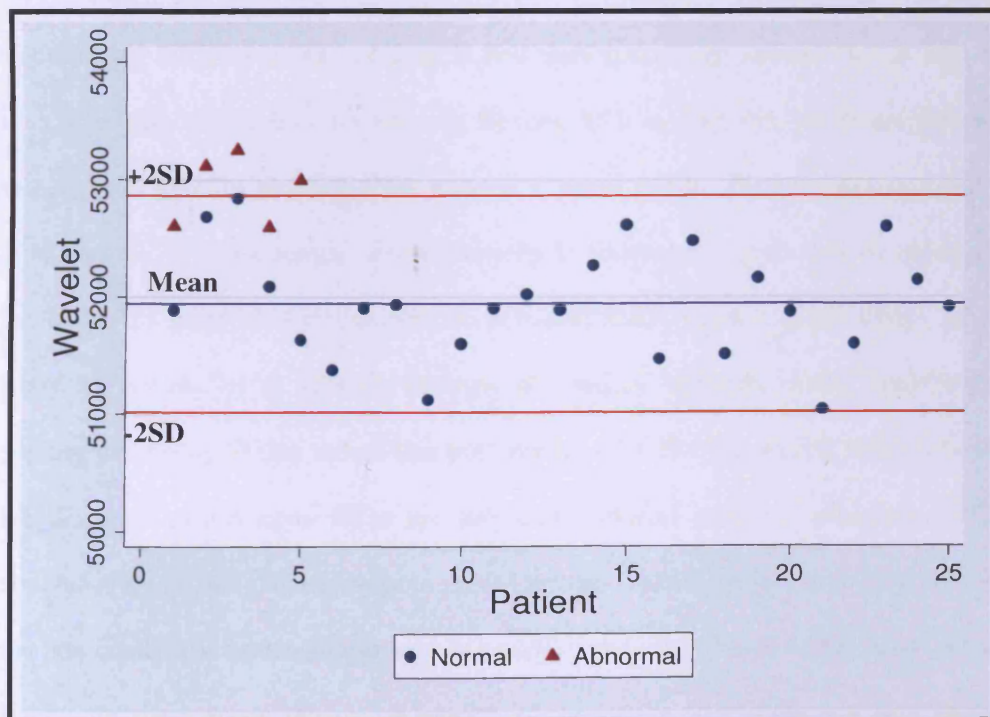
Figure 7.24 95% agreement of wavelet transform (Mean ±2 SD) of normal medial and injured gastrocnemius muscle.

161

7.7 Discussion

In this study component no significant difference in texture features between the right and left gastrocnemius muscle were found. Our study results were in consensus with the results by Nielsen and colleagues (2006) in which no significant difference was found in texture features between the right and left supraspinatus muscle. Therefore, our study findings along with findings from Nielsen et al. (2006) study postulate that similar muscles types from the right and left side of the human body are mainly homogeneous. In our study, findings showed significant differences in texture between the gastrocnemius and biceps muscle. In the study by Nielsen et al. (2006), differences in texture were found between the vastus lateralis and the supraspinatus muscle. They found the gray-scale intensity of the vastus lateralis muscle was higher than the intensity of the supraspinatus muscle. Therefore, different muscles have different gray values. A study by Scholten and colleagues (2003) measured the echo intensity for different groups of muscle and they found the values 39.7 ± 7.94 for biceps brachii, 43.9 ± 6.16 for forearm flexors, 35.3 ± 7.12 for quadriceps femoris, and 41.5 ± 9.07 for anterior tibial muscle (mean ± SD) . The muscle is a highly plastic tissue, in physiological terms plasticity in tissues or organs may be defined as the ability to adapt to circumstances or demands made upon it (Pette 2001). In the study by Nielsen et al. (2006), showing differences between vastus lateralis and supraspinatus may be due to fact that both the muscles are being used differently and the demands placed upon them are different. Nielsen and his colleagues (2006) concluded that the higher intensity in vastus lateralis muscle might have been because the non-contractile units were greater in number when compared to the supraspinatus muscle. In other words, the vastus lateralis is part of the quadriceps muscle, which is the main extensor of the knee and is a crucial muscle in walking and running. On the

other hand, the supraspinatus is a relatively smaller muscle and its action is initial abduction of the arm. Therefore, demands on the supraspinatus may be relatively less than the vastus lateralis which is a prime mover in walking, whereas abduction movements is more isolated and is carried out only by the supraspinatus in the initial arc of movement. Therefore, the comparison between the muscles in the study by Nielsen et al. (2006) comparing supraspinatus and vastus lateralis may not be appropriate for comparison due to difference in size, function and demands on the muscles. On the other hand, our study compared more commonly used muscles, biceps and gastrocnemius, where their function and demands are relatively similar (muscle bulk and size) in normal circumstances as flexing of elbow and walking occur several times during a day, whereas sideways lifting of arm may not be so common. However, since the muscle is such an adaptable tissue, changes in number of contractile units can depend on the way the muscle is used. For instance, if one used the biceps more and trained it regularly (placing increased demand, e.g. weight lifter) then the texture features can be different. Muscle plasticity and possible causes for change in fibre type will be discussed in the following chapter. Therefore, because of the differences in normal appearance of muscles and the inability to eliminate confounding variables (gain, etc) completely, the visual assessment of images alone is not an appropriate and robust method to define pathologies and objective reference sets play crucial role in standardising assessment grading systems

In this study component, a complete set of quantitative normal values for the gastrocnemius muscle was defined from 25 healthy adults using US imaging. The validity of reference set of normal values was investigated using it to distinguish normal from injured muscle. It was demonstrated that combined parameters can be

used to quantify muscle injury and changes in muscle appearance. These features could also be used to assess disease progression, monitoring prognosis, and tailoring therapy. In terms of clinical application, our technique has the ability to differentiate abnormal muscle from healthy/normal muscle tissue with just of three texture parameters namely gradient, AR model and wavelet transform. However, gradient and AR model are the most sensitive texture parameters for differentiating healthy muscle from injured muscle and may be used as a tool to monitor the healing process.

7.8 Conclusion

■ Texture analysis techniques are a useful method for characterizing muscle tissue.

■ No significant difference in texture parameters were found between medial gastrocnemius muscle in the right and left leg.

■ The gastrocnemius and the biceps muscle in the present study seemed to have different texture features, which seems to be in contrast to their macro anatomy.

■ Gradient and AR model are the most sensitive texture parameters for differentiating healthy muscle from injured muscle and may be used as a tool to monitor the healing process.

Chapter 8 General discussion and conclusion

Muscle rupture and injuries are a common presentation and more common in sporting activities. In addition, there is a range of treatment options available for every stage and grade of injury. However, there is dearth of robust clinical trials using objective outcome measures to gauge the efficacy of different treatments protocols and more importantly monitor the healing process with and without treatment.As mentioned before, the medial gastrocnemius muscle is known to be one of the most commonly injured muscles in sporting activities (Kwak et al. 2006a, Kwak et al. 2006b , Bianchi et al. 1998).This muscle was chosen to develop an objective method of injury evaluation and to monitor healing. Therefore, a novel study has been reported that aims to develop a reliable method to analyse muscle ultrasound image of the gastrocnemius muscle. As suggested earlier, previous studies evaluating muscle injuries mostly used subjective methods of visual inspection or the measurement of muscle thickness and only a few studies have used quantitative ultrasound to characterize different features of the muscle tissue. Moreover, the healing process of muscle injury is largely assessed by subjective evaluation of changes of echogenicity in repeated sonographic images.

The results from this thesis support the statement that quantitative Ultrasonography and computer image analysis is a useful and reliable method for studying the characteristics of muscle tissue. The method of visual inspection can be subjective and may not be sensitive enough to detect change as it often fails to acknowledge that the echo intensity for normal muscle is different for each muscle, and therefore can be

a less reproducible method. However, the sensitivity and reliability of this method was greatly improved by the quantification of muscle echo intensity. Muscle biopsies are usually not the method of choice due to their invasive nature and unsuitability for screening of larger groups. One of the finding of the study was that certain variables had to be kept constant during ultrasonographic imaging, as some variables seemed to affect measurement values. Therefore, keeping some variables constant will enable the investigator to compare measurements with one and another. Several studies (Heckmatt et al. 1980 , Heckmatt et al. 1988b , Heckmatt et al. 1989 , Reimers et al. 1996a , Zuberi et al. 1999) have found that age, site of measurement , position of subject , state of muscle(relaxed/stretched) , pressure exerted on the skin by transducer , position of the transducer and system settings are all potential confounders.

The major strength of this study was that the scanning sites, system settings, position of subject, position of transducer were all kept constant. The site of scanning was anatomically defined in the middle part of the gastrocnemius muscle. There was care taken to ensure that the subject was relaxed as much as possible and the transducer was repositioned between every scan giving the subject an opportunity to relax. The echo intensity of a muscle can change with muscle contraction (Heckmatt et al. 1988b, Heckmatt et al. 1980). Furthermore, it was ensured that there were no increased pressure applied on the tissue being imaged as the pressure from the transducer may influence the gray scale intensity of the pixels in the images due to the changes in the muscle shape and may result in changes in insonation angles (Nielsen et al. 2006). In the present study, excessive pressure on the muscle was also avoided by using extra conducting gel to avoid applying any pressure. It was observed that the

pressure exerted on the muscle by the transducer was not a significant confounder as the difference in parameters between the biceps and gastrocnemius and difference between normal and injured muscle was far greater than the small difference associated with increased pressure. Therefore, the difference in pressure due to human handling need not necessarily bias the results.

In this study, the age range was kept as narrow as possible (18-38). A study by Reimers et al. (1996a) showed that the echo intensity in adults (18-73 years) increased with age. The muscle fibres in a 20-week-old fetus (6 to 7 μm) increased to 38 to 42 μm at the age of 10 years (Engel and Banker 1986). Therefore, because of the enlargement of the muscle fibres, the distance between reflecting surfaces also increases and the number of reflections per cm^2 decreases, which causes reduced echo intensity. The large muscle fibres can also cause an increase in echo intensity, since large interfaces will cause less scattering of the US beam (Scholten et al. 2003).

It is very likely that there are other factors other than the muscle architecture that influence the echo intensity with increasing age like for instance the demands placed on the muscle as one gets older. Also in this study, all of our subjects were chosen to be untrained subjects because a study by Sipila and Suominen (1991) found US scans of the untrained men and the athletes were different. It was postulated that the scans of the untrained men, showed increased intramuscular echogenicity with decreased echoes, which were from larger connective tissue septa and the femur due to the likely increase of intramuscular connective tissue and fat (Bartrum and Crow 1977, Ferrucci 1979 , Hicks et al. 1984). The reasoning for this occurrence is readily understood as the passing of the US through multiple interfaces present in fat and collagen tissue reflects and refracts the wave. The US beam is weakened more rapidly

as there is loss of beam intensity on contact with each interface. Therefore, a decreased transmitted ultrasound beam results in decreased echoes reflected from deeper tissues like septum and bone(Sipila and Suominen 1991).

The results of the present study are in agreement with the results from another study (Nielsen et al. 2000) on the reliability of US imaging as a method for quantitative characterization of skeletal muscle .This study showed low variation in the coefficient of variation and intra-class correlation for texture parameters except skewness and kurtosis. Therefore, from findings for intra and inter operator correlation coefficients, this study mainly showed good reproducibility and repeatability.

The scanning session of the gastrocnemius muscles consisted of 10 scans over two different days, and showed no difference in texture features between the two different days. This suggests there was no significant change between the time intervals between scans suggesting a high long-term repeatability of the scanning method. Also in this study, the ultrasound system settings were standardized for all participants and were kept constant during all measurements to avoid any variation in images due to different settings of the ultrasound machine. The study demonstrated that different gain setting would highly influence the texture features. Therefore, for future studies using quantitative texture analysis, there is a need to standardise gain values and formulate a reference set to avoid variation in images due to setting of the system. Findings from the study also indicated that the varying gain from 75-85 dB did not produce any significant difference in the texture parameters. Nevertheless, it would be ideal to develop systems and methods for US imaging which is independent of the equipment and setting (Nielsen et al. 2006).Findings from this study, suggested that

the middle part of the gastrocnemius is homogenous. However, from the findings it is difficult to comment on the gastrocnemius muscle as a whole as several scanning sites throughout the muscle would be required to support the statement.

The result of this study showed that scanning conditions must be standardized for all the scans to ensure the fidelity of the tissue characterization procedure. Some of the inferences are as follows:

- Ultrasound machine settings – It was shown that varying the gain during the scanning procedure could greatly influence some of the first order statistic parameters. Therefore, it is important that standardised settings be used.

- ROI shape and size – It was found that the number of pixels in the ROI must be at least 5000 pixels for most of the texture features to obtain reliable statistical values. In addition, when the size of the ROI changes from one subject to the other, the run length matrix must be considered carefully as it was greatly affected by varying the size of ROI.

- Defining ROI at different depths – The results showed that parameters gray level, variance and run length matrix are highly influenced by depth. Therefore, when analysing these parameters it would be important to keep the ROI at the same level of depth.

As discussed earlier, muscle fibre size and architecture can change with age, activity and demands placed upon it. This study has shown that texture parameters can change from one muscle to the other. In the previous chapter parameters co-occurrence

matrix, gradient and AR model extracted from middle part the gastrocnemius muscle differed significantly when compared to the middle part of the biceps muscle.

Therefore, muscles can appear more or less echogenic due to composition of fibres and proportion of fat tissue. For instance, the triceps muscles are typically less echogenic than the biceps (Walker et al. 2004). Walker and Jackson (1997) suggested that the muscles that were hypertrophied due to exercise and training might appear hypoechoic due to the volume effect, which is due to the increase in myocyte size relative to fibrous tissue volume. Reimers and colleagues (1993a, 1993b) showed that excessive subcutaneous fat could reduce the echogenicity, by absorbing the excessive sound energy.

As stated earlier the muscle is an adaptable tissue. The muscle is known to adapt and condition itself depending on the demands placed on it. Pette (2001) reviewed numerous studies (for e.g. Howe et al. 1992 and Kernell 1998) and concluded that the muscle is an extremely adaptable tissue. Although, the biceps and the gastrocnemius are typical skeletal muscles, there can be differences in fibre types. In addition, although the main components of muscle tissue are present in infants, the composition of muscle fibre type and the proportion of slow to fast fibres in a given muscle is dependent on the neural input and the way in which the muscle is used. There are have been many nerve studies in animals since the work by Buller et al. (1960) showing that slow- contracting fibres can be induced to become fast- acting fibres and fast acting fibres can become slow- contracting fibres(Vrbrova et al. 1985, Pette 2001).

For instance, Thayer et al. (2000) postulated that aerobic training leads to an increase in type I (fatigue resistant) fibres at the expense of decrease of type II fibres (non-fatigue resistant , but can provide short burst of strong muscular contraction). Furthermore, loading also appears to be essential for the maintenance of type I fibres in antigravity muscles (Burnham et al. 1997, Anderson et al. 1999). Therefore, if one does not have enough loading standing etc or one has more standing to do for long periods the gastrocnemius may then have more type I fibres as compared to someone who stands and walks less. The gastrocnemius typically has more type II fibres to enable quick acts such as jumping, sprinting, and power lifting but with the available evidence the selective increase in type I fibres with lot or aerobic activity or training is very likely. This theory can also be used as explanation for differences found by Sipila and Suominen.(1991) which showed differences in muscle image between trained and untrained men. In addition, the biceps is a strong supinator (twisting – using a screwdriver) of the forearm and flexor of the elbow. For instance, persons who use the biceps a lot, for example using a screwdriver (electrician or mechanic) may have more type I (fatigue resistant) fibres and more endurance when compared to someone only doing weight lifting with few repetitions of the movement.

Therefore, both the biceps and gastrocnemius have an equal chance of fibre change than the supraspinatus and vastus lateralis used in the study by Nielsen (2006) where the supraspinatus performs a more isolated movement and can have more contractile units due to the nature of the movement. This makes selection of muscles in our study slightly more appropriate than the study by Nielsen (2006) although there was a similar agreement in the results.

One of the hypothesis of this thesis was that computer-assisted gray-scale analysis might detect subtle changes on an ultrasound image, which would not be detected by visual assessment. In this thesis, the texture features, which are normally used in medical image analysis, have been applied. The co-occurrence matrix is the texture feature which is the most widely used for discriminating between normal and abnormal tissue. In this thesis, there was no evidence to suggest that co-occurrence matrix values are able to differentiate between normal and injured muscles. The reason behind this could be because the sum of the co-occurrence matrices was used rather than individual matrices which are used in other reported work. Another reason could be the criteria of defining the ROI used. In this thesis, the whole muscle including the bruised area was selected as ROI rather than selecting the region of the bruising only. It was necessary to perform it in this way because of the difficulty of identifying the bruising boundaries in the beginning of the formation of the haematoma and also in the last stage of the healing, as the blood spreads out within the tissue. Also when monitoring the healing of haematoma, it would be necessary to know when the muscle has completely healed, so the whole ROI would need to be included from the start of the process. On the other hand, gradient and AR model were the most significant texture' parameters differentiating between normal and injured muscle in this study, suggesting that more studies are warranted to investigating these two texture parameters.

The conclusion from this thesis is that texture analysis techniques can be used as a tool to monitor the healing process and can be used to assess the effectiveness of treatments and how the injured tissue responds to different treatment techniques. The sum of the co-occurrence matrix parameters was not sensitive and could not

differentiate textures between normal and injured muscle. Therefore, the sum of the co-occurrence matrix is not a useful parameter in assessing muscle injury.

Summary

● A quantitative non-invasive method to describe the muscle tissue composition has been developed

● Quantitative ultrasound imaging analysis of the gastrocnemius muscle can be used as a tool to monitor the healing process of the injured muscle.

● No significant difference in texture features were found between scanning sites on the middle part of the gastrocnemius muscle.

● Gray level, variance, and run length matrix were found to be depth dependant variables.

● ROI size has a significant effect on the computed value of run length matrix.

● No significant difference was noted when the ROI size was varied from 5000 pixels and above for co-occurrence matrix, gradient, AR model, and wavelet.

● Choosing bigger ROI size seemed to give consistent results with low variation.

● Four texture parameters co-occurrence matrix, gradient, AR model and wavelet were used to obtain reference set of normal muscle as those parameters have no influence by varying depth or size of ROI and they showed a high level of repeatability and reproducibility.

● The ultrasound machine setting variables such as gain can greatly influence the texture features and influence the classification of the results.

● Varying the dynamic range on ultrasound machine had no influence on texture features.

• The use of constant settings for an ultrasonic scanner is necessary, especially for those who apply first order statistics to extract texture features from images.

• Texture parameters used to assess the characteristics of ultrasound image of the gastrocnemius muscle are repeatable and reproducible.

• No significant difference in texture parameters were found between medial gastrocnemius muscle in the right and left leg.

• A Quantitative ultrasound image analysis is able to differentiate between different muscle structures compositions. The gastrocnemius and biceps muscle were seen to have different muscle tissue texture.

• The texture parameters, AR model and gradient were found to be the most sensitive parameters in differentiating normal muscle from injured muscle. These parameters can be used as a reliable tool to monitor the healing process and study the response of injured muscles to different treatment protocol.

Implications for future research

A future goal would be to validate and use the ultrasound image analysis to monitor the healing process of muscle injury. This study aims to serve as a pilot and highlights the possibilities of using US image analysis. However, a clinical trial monitoring subjects who have had muscle injuries is necessary to validate findings for the application used in this thesis in the management of musculoskeletal injuries. In the study a reference set for the normal gastrocnemius muscle where specific texture parameters showed low variation between subjects was presented. Using this reference set , one can not only use it to differentiate between normal and injured muscle but also use it for comparison muscle changes seen in neuromuscular disorders such as muscular dystrophies and polyneuropathies. Also further studies looking at larger and whole muscle complexes are needed as our study only focussed on the middle part of the gastrocnemius muscle. Furthermore, it would be beneficial to carry out an in-depth analysis of each texture category rather than summing second order statistic parameters, AR model and wavelet transform. Finally, it must be stressed that there is a dearth of robust evidence to support common interventions used to treat muscle injuries and hope further research in this area will be carried out that is so urgently needed.

References

Allison J W, Barr L L, Massoth R J, Berg G P, Krasner B H and Garra B S (1994) Understanding the process of quantitative ultrasonic tissue characterization. *Radiographics*. 14(5)1099-1108

Anderson J, Almeida-Silveira M I and Perot C (1999) Reflex and muscular adaptations in rat soleus muscle after hindlimb suspension. *J Exp Biol.* 202 (Pt 19) 2701-2707.

Angelsen B A J (2000) *Ultrasound Imaging. Waves, Signals, and Signal Processing.* Emantec AS, Trondheim, Norway.

Bamber J C and Hill C R (1981) Acoustic properties of normal and cancerous human liver-I. Dependence on pathological condition. *Ultrasound Med Biol.* 7 (2) 121-133.

Bartrum R J and Crow H C (1977) *Gray Scale Ultrasound: A Manual for Physictans and Technical Personnel.* Philadelphia: W.B. Saunders.

Basset O, Buquet B, Abouelkaram S, Delachartre P and Culioli J (2000) Application of texture image analysis for the classification of bovine meat. *Food Chemistry* 69 (4) 437-445.

Basset O, Ramiaramanana V, Chirossel P, Hernandez A and Gimenez G (1994) Characterisation of muscle tissue during an effort by texture analysis of ultrasonic images. In *IEEE Ultrasonics Symposium Proceedings.* 3, 1455-1458.

Basset O, Sun Z, Mestas J L and Gimenez G (1993) Texture analysis of ultrasonic images of the prostate by means of co-occurrence matrices. *Ultrason Imaging.* 15 (3) 218-237.

Beekman R and Visser L H (2004) High-resolution sonography of the peripheral nervous system -- a review of the literature. *Eur J Neurol.* 11 (5) 305-314.

Beiner J M and Jokl P (2001) Muscle contusion injuries: current treatment options. *J Am Acad Orthop Surg.* 9 (4) 227-237.

Best T and Garrett W (1994) *Muscle and tendon.* Philadelphia, PA Orthopaedic sports medicine.

Bharati M H, Liu J J and MacGregor J F (2004) Image texture analysis: methods and comparisons. *Chemometrics and Intelligent Laboratory Systems* 72 (1) 57-71.

Bianchi S, Martinoli C, Abdelwahab I F, Derchi L E and Damiani S (1998) Sonographic evaluation of tears of the gastrocnemius medial head ("tennis leg"). *J Ultrasound Med.* 17 (3) 157-162.

Bland J M and Altman D G (2000) *An Introduction to Medical Statistics*. Oxford: Medical Publications.

Blankenbaker D G and De Smet A A (2004) MR imaging of muscle injuries. *Applied Radiology* 33 (4) 14-26.

Boutin R D, Fritz R C and Steinbach L S (2002) Imaging of sports-related muscle injuries. *Radiol Clin North Am.* 40 (2) 333-362

Bovik A C, Clark M and Geisler W S (1990) Multichannel texture analysis using localized spatial filters. *Pattern Analysis and Machine Intelligence, IEEE Transactions on* 12 (1) 55-73.

Brooke-Wavell K, Jones P R and Pye D W (1995) Ultrasound and dual X-ray absorptiometry measurement of the calcaneus: influence of region of interest location. *Calcif Tissue Int.* 57 (1) 20-24.

Buller A J, Eccles J C and Eccles R (1960) Interactions between motorneurons and muscles in respect of the characteristics speeds of their response. *Journal of Physiology* (150) 417-439.

Burnham R, Martin T, Stein R, Bell G, MacLean I and Steadward R (1997) Skeletal muscle fibre type transformation following spinal cord injury. *Spinal Cord.* 35 (2) 86-91.

Cady E B, Gardener J E and Edwards R H (1983) Ultrasonic tissue characterisation of skeletal muscle. *Eur J Clin Invest.* 13 (6) 469-473.

Campbell R S D and Wood J (2002) Ultrasound of muscle. *Imaging* 14 (3) 229-240.

Castellano G, Bonilha L, Li L M and Cendes F (2004) Texture analysis of medical images. *Clin Radiol.* 59 (12) 1061-1069.

Chan K L (1998) Adaptation of ultrasound image texture characterization parameters. In *Engineering in Medicine and Biology Society, 1998. Proceedings of the 20th Annual International Conference of the IEEE* (Vol. 2, pp. 804-807 vol.802).

Chan K L and McCarty K (1990) Aspects of the statistical texture analysis of medical ultrasound images. In *Ultrasound Instrumentation, IEE Colloquium on* (pp. 3/1-3/3).

Chen C P, Tang S F, Hsu C C, Chen R L, Hsu R, Wu C W and Chen M J (2009) A novel approach to sonographic examination in a patient with a calf muscle tear: a case report. *J Med Case Reports.* 3,7291

Clague J E, Roberts N, Gibson H and Edwards R H (1995) Muscle imaging in health and disease. *Neuromuscul Disord.* 5 (3) 171-178.

Cloostermans M J, Mol H, Verhoef W A, Thijssen J M and Kubat K (1986) In vitro estimation of acoustic parameters of the liver and correlations with histology. *Ultrasound Med Biol.* 12 (1) 39-51.

Cloostermans M J and Thijssen J M (1983) A beam corrected estimation of the frequency dependent attenuation of biological tissues from backscattered ultrasound. *Ultrason Imaging.* 5 (2) 136-147.

Cohen L (1989) Time-frequency distributions-a review. *Proceedings of the IEEE* 77 (7) 941-981.

Crisco J J, Jokl P, Heinen G T, Connell M D and Panjabi M M (1994) A muscle contusion injury model. Biomechanics, physiology, and histology. *Am J Sports Med.* 22 (5) 702-710.

Damilakis J, Perisinakis K, Vagios E, Tsinikas D and Gourtsoyiannis N (1998) Effect of region of interest location on ultrasound measurements of the calcaneus. *Calcif Tissue Int.* 63 (4) 300-305.

Darke R, Vogl A and Mitchel A (2009) *Gray's Anatomy for Students.* Churchill Livingstone; 2 edition

Daugman J G (1985) Uncertainty relation for resolution in space, spatial frequency, and orientation optimized by two-dimensional visual cortical filters. *J Opt Soc Am A.* 2 (7) 1160-1169.

Daugman J G (1988) Complete discrete 2-D Gabor transforms by neural networks for image analysis and compression. *Acoustics, Speech and Signal Processing, IEEE Transactions on* 36 (7) 1169-1179.

De Smet A A and Best T M (2000) MR imaging of the distribution and location of acute hamstring injuries in athletes. *AJR Am J Roentgenol.* 174 (2) 393-399.

Delgado G J, Chung C B, Lektrakul N, Azocar P, Botte M J, Coria D, Bosch E and Resnick D (2002) Tennis leg: clinical US study of 141 patients and anatomic investigation of four cadavers with MR imaging and US. *Radiology.* 224 (1) 112-119.

Deutsch A L and Mink J H (1989) Magnetic resonance imaging of musculoskeletal injuries. *Radiol Clin North Am.* 27 (5) 983-1002.

Dixon K J, Vince D G, Cothren R M and Cornhill J F (1997) Characterization of coronary plaque in intravascular ultrasound using histological correlation. In *Engineering in Medicine and Biology Society, 1997. Proceedings of the 19th Annual International Conference of the IEEE* (Vol. 2, pp. 530-533 vol.532).

Dreinhöfer K E, Reichel H and Käfer W (2007) Lower limb pain. *Best Practice & Research Clinical Rheumatology* 21 (1) 135-152.

Donohue K D, Huang L, Burks T, Forsberg F and Piccoli C W (2001) Tissue classification with generalized spectrum parameters. *Ultrasound Med Biol.* 27 (11) 1505-1514.

Ehman R L and Berquist T H (1986) Magnetic resonance imaging of musculoskeletal trauma. *Radiol Clin North Am.* 24 (2) 291-319.

Eisele R, Schmid R, Kinzl L, Kramer M, Katzmaier P and Hartwig E (1998) Soft tissue texture analysis by B-mode-ultrasound in the evaluation of impairment in chronic low back pain. *Eur J Ultrasound.* 8 (3) 167-175.

El-Khoury G Y, Brandser E A, Kathol M H, Tearse D S and Callaghan J J (1996) Imaging of muscle injuries. *Skeletal Radiol.* 25 (1) 3-11.

Elliot T L, Downey D B, Tong S, McLean C A and Fenster A (1996) Accuracy of prostate volume measurements in vitro using three-dimensional ultrasound. *Acad Radiol.* 3 (5) 401-406.

Engel A G and Banker B Q (1986) *Myology.* New York: McGraw-Hill , p 851.

Fatemi M and Kak A C (1980) Ultrasonic B-scan imaging: theory of image formation and a technique for restoration. *Ultrason Imaging.* 2 (1) 1-47.

Faul J L, Demers E A, Burke C M and Poulter L W (1999) The reproducibility of repeat measures of airway inflammation in stable atopic asthma. *Am J Respir Crit Care Med.* 160 (5 Pt 1) 1457-1461.

Fenster A and Downey D B (1996) 3-D ultrasound imaging: a review. *Engineering in Medicine and Biology Magazine, IEEE* 15 (6) 41-51.

Ferrucci J T, Jr. (1979) Body ultrasonography (first of two parts). *N Engl J Med.* 300 (10) 538-542.

Ferrell W, Crowe N, Walker F, Donofrio P and Williams D (1989) Force/diameter relationships in human muscle: an EMG and sonographic study. *Muscle Nerve* 12, 759.

Fink M A and Cardoso J F (1984) Diffraction Effects in Pulse-Echo Measurement. *Sonics and Ultrasonics, IEEE Transactions on* 31 (4) 313-329.

Fischer A Q, Carpenter D W, Hartlage P L, Carroll J E and Stephens S (1988) Muscle imaging in neuromuscular disease using computerized real-time sonography. *Muscle Nerve.* 11 (3) 270-275.

Flecca D, Tomei A, Ravazzolo N, Martinelli M and Giovagnorio F (2007) US evaluation and diagnosis of rupture of the medial head of the gastrocnemius (tennis leg). *Journal of Ultrasound* 10 (4) 194-198.

Flessi J L (1986) *The design and analysis of clinical experiments.* New York: John Wiley & Sons ,.

Fornage B (1995) *Muscular trauma.* New York, NY: Musculoskeletal ultrasound ,Churchill Livingstone.

Fornage B D (1999) Sonographically guided needle biopsy of nonpalpable breast lesions. *J Clin Ultrasound.* 27 (7) 385-398.

Fournier B, Chappard C, Roux C, Berger G and Laugier P (1997) Quantitative ultrasound imaging at the calcaneus using an automatic region of interest. *Osteoporos Int.* 7 (4) 363-369.

Freese M and Lyons E A (1977) Ultrasonic backscatter from human liver tissue: its dependence on frequency and protein/lipid composition. *J Clin Ultrasound.* 5 (5) 307-312.

Froimson A I (1969) Tennis leg. *Jama.* 209 (3) 415-416.

Garra B S, Insana M F, Shawker T H, Wagner R F, Bradford M and Russell M (1989) Quantitative ultrasonic detection and classification of diffuse liver disease. Comparison with human observer performance. *Invest Radiol.* 24 (3) 196-203.

Garra B S, Krasner B H, Horii S C, Ascher S, Mun S K and Zeman R K (1993) Improving the distinction between benign and malignant breast lesions: the value of sonographic texture analysis. *Ultrason Imaging.* 15 (4) 267-285.

Garrett W E, Jr. (1996) Muscle strain injuries. *Am J Sports Med.* 24 (6 Suppl) S2-8.

Gates C and Huard J (2005) Management of Skeletal Muscle Injuries in Military Personnel. *Operative Techniques in Sports Medicine* 13 (4) 247-256.

Genovese R L, Rantanen N W, Simpson B S and Simpson D M (1990) Clinical experience with quantitative analysis of superficial digital flexor tendon injuries in Thoroughbred and Standardbred racehorses. *Vet Clin North Am Equine Pract.* 6 (1) 129-145.

Gilbert T J, Jr., Bullis B R and Griffiths H J (1996) Tennis calf or tennis leg. *Orthopedics.* 19 (2) 179-184.

Ginther O (1995) *Ultrasound Imaging and Animal Reproduction: Fundamentals.* USA: Equiservices Publishing

Goldstein A and Madrazo B L (1981) Slice-thickness artifacts in gray-scale ultrasound. *J Clin Ultrasound.* 9 (7) 365-375.

Goldberg V, Manduca A, Ewert D L, Gisvold J J and Greenleaf J F (1992) Improvement in specificity of ultrasonography for diagnosis of breast tumors by means of artificial intelligence. *Med Phys.* 19 (6) 1475-1481.

Hamper U M, Trapanotto V, DeJong M R, Sheth S and Caskey C I (1999) Three-dimensional US of the prostate: early experience. *Radiology.* 212 (3) 719-723.

Haralick R M (1979) Statistical and structural approaches to texture. *Proceedings of the IEEE* 67 (5) 786-804.

Haralick R M, Shanmugam K and Dinstein I H (1973) Textural Features for Image Classification. *Systems, Man and Cybernetics, IEEE Transactions on* 3 (6) 610-621.

Harrison L, Dastidar P, Eskola H, Jarvenpaa R, Pertovaara H, Luukkaala T, Kellokumpu-Lehtinen P L and Soimakallio S (2008) Texture analysis on MRI images of non-Hodgkin lymphoma. *Comput Biol Med.* 38 (4) 519-524.

Hicks J E, Shawker T H, Jones B L, Linzer M and Gerber L H (1984) Diagnostic ultrasound: its use in the evaluation of muscle. *Arch Phys Med Rehabil.* 65 (3) 129-131.

Heckmatt J, Rodillo E, Doherty M, Willson K and Leeman S (1989) Quantitative sonography of muscle. *J Child Neurol.* 4 (Suppl) S101-106.

Heckmatt J Z and Dubowitz V (1985) Diagnostic advantage of needle muscle biopsy and ultrasound imaging in the detection of focal pathology in a girl with limb girdle dystrophy. *Muscle Nerve.* 8 (8) 705-709.

Heckmatt J Z, Dubowitz V and Leeman S (1980) Detection of pathological change in dystrophic muscle with B-scan ultrasound imaging. *Lancet.* 1 (8183) 1389-1390.

Heckmatt J Z, Leeman S and Dubowitz V (1982) Ultrasound imaging in the diagnosis of muscle disease. *J Pediatr.* 101 (5) 656-660.

Heckmatt J Z, Pier N and Dubowitz V (1988a) Assessment of quadriceps femoris muscle atrophy and hypertrophy in neuromuscular disease in children. *J Clin Ultrasound.* 16 (3) 177-181.

Heckmatt J Z, Pier N and Dubowitz V (1988b) Measurement of quadriceps muscle thickness and subcutaneous tissue thickness in normal children by real-time ultrasound imaging. *J Clin Ultrasound.* 16 (3) 171-176.

Heckmatt J Z, Pier N and Dubowitz V (1988c) Real-time ultrasound imaging of muscles. *Muscle Nerve.* 11 (1) 56-65.

Herzog W, Leonard T R and Guimàraes A C (1993) Forces in gastrocnemius, soleus, and plantaris tendons of the freely moving cat. *J Biomech.* 26 (8) 945-953.

Herlidou S, Rolland Y, Bansard J Y, Le Rumeur E and de Certaines J D (1999) Comparison of automated and visual texture analysis in MRI: characterization of normal and diseased skeletal muscle. *Magn Reson Imaging.* 17 (9) 1393-1397.

Hirning T, Zuna I, Schlaps D, Lorenz D, Meybier H, Tschahargane C and van Kaick G (1989) Quantification and classification of echographic findings in the thyroid gland by computerized B-mode texture analysis. *Eur J Radiol.* 9 (4) 244-247.

Holsbeeck M V and Introcaso J (2001) *Sonography of muscle* St Louis: Musculoskeletal ultrasound , 2nd edition.

Holli K K, Harrison L, Dastidar P, Waljas M, Liimatainen S, Luukkaala T, Ohman J, Soimakallio S and Eskola H (2010) Texture analysis of MR images of patients with Mild Traumatic Brain Injury. *BMC Med Imaging.* 10 (1) 8.

Howe T, Petterson T and Oldham J (1992) Making muscles grow as they are told. *Physiotherapy* 78 (10) 745-746.

Huard J, Li Y and Fu F H (2002) Muscle injuries and repair: current trends in research. *J Bone Joint Surg Am.* 84-A (5) 822-832.

Hurme T, Kalimo H, Lehto M and Jarvinen M (1991) Healing of skeletal muscle injury: an ultrastructural and immunohistochemical study. *Med Sci Sports Exerc.* 23 (7) 801-810.

Hyatt J P, Roy R R, Baldwin K M, Wernig A and Edgerton V R (2006) Activity-unrelated neural control of myogenic factors in a slow muscle. *Muscle Nerve.* 33 (1) 49-60.

Huynen A L, Giesen R J, de la Rosette J J, Aarnink R G, Debruyne F M and Wijkstra H (1994) Analysis of ultrasonographic prostate images for the detection of prostatic carcinoma: the automated urologic diagnostic expert system. *Ultrasound Med Biol.* 20 (1) 1-10.

Insana M, Zagzebski J and Madsen E (1983) Improvements in the spectral difference method for measuring ultrasonic attenuation. *Ultrason Imaging.* 5 (4) 331-345.

Jarvinen T A, Jarvinen T L, Kaariainen M, Aarimaa V, Vaittinen S, Kalimo H and Jarvinen M (2007) Muscle injuries: optimising recovery. *Best Pract Res Clin Rheumatol.* 21 (2) 317-331.

Jarvinen T A, Jarvinen T L, Kaariainen M, Kalimo H and Jarvinen M (2005) Muscle injuries: biology and treatment. *Am J Sports Med.* 33 (5) 745-764.

Jarvinen T A, Kaariainen M, Jarvinen M and Kalimo H (2000) Muscle strain injuries. *Curr Opin Rheumatol.* 12 (2) 155-161.

Julesz B (1975) Experiments in the visual perception of texture. *Sci Am.* 232 (4) 34-43.

Kadah Y M, Farag A A, Zurada J M, Badawi A M and Youssef A M (1996) Classification algorithms for quantitative tissue characterization of diffuse liver disease from ultrasound images. *IEEE Trans Med Imaging.* 15 (4) 466-478.

Kalimo H, Rantanen J and Järvinen M (1997) Muscle injuries in sports. *Baillieres Clinical Orthop* 2,1-24.

Kamala D, Suresh S and Githa K (1985) Real-time ultrasonography in neuromuscular problems in children. *J Clin Ultrasound.* 13 (7) 465-468.

Kasemkijwattana C, Menetrey J, Bosch P, Somogyi G, Moreland M S, Fu F H, Buranapanitkit B, Watkins S S and Huard J (2000) Use of growth factors to improve muscle healing after strain injury. *Clin Orthop Relat Res.* (370) 272-285.

Kawakami Y, Ichinose Y and Fukunaga T (1998) Architectural and functional features of human triceps surae muscles during contraction. *J Appl Physiol.* 85 (2) 398-404.

Kernell D (1998) The final common pathway in postural control--developmental perspective. *Neurosci Biobehav Rev.* 22 (4) 479-484.

Kiliaridis S, Engvall M and Tzakis M G (1995) Ultrasound imaging of the masseter muscle in myotonic dystrophy patients. *J Oral Rehabil.* 22 (8) 619-625.

Kim S and Choi B (2007) Three-dimensional (3D) and four-dimensional (4D) ultrasound: Techniques and abdominal applications. *J Med Ultrasound* 15, 228-242.

Kirkwood B R and Sterne A C (2003) *Essential Medical Statistics.* 2nd Edn,Blackwell Science.

Klein J H (1990) Muscular hematomas: diagnosis and management. *J Manipulative Physiol Ther.* 13 (2) 96-100.

Kociołek M, Materka A, Strzelecki M and Szczypiński P (2001) Discrete Wavelet Transform Derived Features for Digital Image Texture Analysis. In *Proc. Int. Conf. Signals and Electronic Systems.* Lodz, Poland ,111-116.

Kneeland J P (1997) MR imaging of muscle and tendon injury. *Eur J Radiol.* 25 (3) 198-208.

Krupinski E A (2004) Computer-aided detection in clinical environment: benefits and challenges for radiologists. *Radiology.* 231 (1) 7-9.

Kwak H S, Han Y M, Lee S Y, Kim K N and Chung G H (2006a) Diagnosis and follow-up US evaluation of ruptures of the medial head of the gastrocnemius ("tennis leg"). *Korean J Radiol.* 7 (3) 193-198.

Kwak H S, Lee K B and Han Y M (2006b) Ruptures of the medial head of the gastrocnemius ("tennis leg"): clinical outcome and compression effect. *Clin Imaging.* 30 (1) 48-53.

Kremkau F W (2002) *Diagnostic Ultrasound: Principles and Instruments.* 6th edition .Philadelphia: W.B. Saunders Company.

Lee H J, Choi B I, Han J K, Kim A Y, Kim K W, Park S H, Jeong J Y and Kang J W (2002) Three-dimensional ultrasonography using the minimum transparent mode in obstructive biliary diseases: early experience. *J Ultrasound Med.* 21 (4) 443-453.

Lee J C and Healy J (2004) Sonography of lower limb muscle injury. *AJR Am J Roentgenol.* 182 (2) 341-351.

Lefebvre F, Meunier M, Thibault F, Laugier P and Berger G (2000) Computerized ultrasound B-scan characterization of breast nodules. *Ultrasound Med Biol.* 26 (9) 1421-1428.

Levangie P K and Norkin C C (2001) *Joint Structure and Function: A comprehensive analysis.* F A Davis and Company. Philadelphia. 3rd edition.

Levine W N, Bergfeld J A, Tessendorf W and Moorman C T, 3rd (2000) Intramuscular corticosteroid injection for hamstring injuries. A 13-year experience in the National Football League. *Am J Sports Med.* 28 (3) 297-300.

Lerski R A, Straughan K, Schad L R, Boyce D, Bluml S and Zuna I (1993) MR image texture analysis--an approach to tissue characterization. *Magn Reson Imaging.* 11 (6) 873-887.

Lieber R L and Friden J (1999) Mechanisms of muscle injury after eccentric contraction. *J Sci Med Sport.* 2 (3) 253-265.

Li P S, Ying M, Chan K H, Chan P W and Chu K L (2004) The reproducibility and short-term and long-term repeatability of sonographic measurement of splenic length. *Ultrasound Med Biol.* 30 (7) 861-866.

Li R, Cai J, Tegeler C, Sorlie P, Metcalf P A and Heiss G (1996) Reproducibility of extracranial carotid atherosclerotic lesions assessed by B-mode ultrasound: the Atherosclerosis Risk in Communities Study. *Ultrasound Med Biol.* 22 (7) 791-799.

Liu S H and Chen W S (1989) Medial gastrocnemius hematoma mimicking deep vein thrombosis: report of a case. *Taiwan Yi Xue Hui Za Zhi.* 88 (6) 624-627.

Lizzi F L, Feleppa E J, Kaisar Alam S and Deng C X (2003) Ultrasonic spectrum analysis for tissue evaluation. *Pattern Recognition Letters* 24 (4-5) 637-658.

Lu R S, Tian G Y, Gledhill D and Ward S (2006) Grinding surface roughness measurement based on the co-occurrence matrix of speckle pattern texture. *Appl Opt.* 45 (35) 8839-8847.

Maganaris C N, Baltzopoulos V and Sargeant A J (1998) In vivo measurements of the triceps surae complex architecture in man: implications for muscle function. *J Physiol.* 512 (Pt 2) 603-614.

Mailloux G, Bertrand M, Stampfler R and Ethier S (1986) Computer analysis of echographic textures in Hashimoto disease of the thyroid. *J Clin Ultrasound.* 14 (7) 521-527.

Manjunath B S and Chellappa R (1991) Unsupervised texture segmentation using Markov random field models. *Pattern Analysis and Machine Intelligence, IEEE Transactions on* 13 (5) 478-482.

Mass L C (1994) *Statistical methods in ultrasonic tissue characterization.* MSc thesis.

Materka A and Strzelecki M (1998) Texture Analysis Methods - A Review. *Technical University of Lodz, Institute of Electronics, COST B11 Report, Brussels*

Maurits N M, Beenakker E A, van Schaik D E, Fock J M and van der Hoeven J H (2004) Muscle ultrasound in children: normal values and application to neuromuscular disorders. *Ultrasound Med Biol.* 30 (8) 1017-1027.

Maurits N M, Bollen A E, Windhausen A, De Jager A E and Van Der Hoeven J H (2003) Muscle ultrasound analysis: normal values and differentiation between myopathies and neuropathies. *Ultrasound Med Biol.* 29 (2) 215-225.

McClure J G (1984) Gastrocnemius musculotendinous rupture: a condition confused with thrombophlebitis. *South Med J.* 77 (9) 1143-1145.

Micklethwaite L, Wood A K, Sehgal C M, Polansky M, Dowling B A, Dart A J, Rose R J and Hodgson D R (2001) Use of quantitative analysis of sonographic brightness for detection of early healing of tendon injury in horses. *Am J Vet Res.* 62 (8) 1320-1327.

Miller W A (1977) Rupture of the musculotendinous juncture of the medial head of the gastrocnemius muscle. *Am J Sports Med.* 5 (5) 191-193.

Morales M A, Ferdeghini E M, Piacenti M, Pelosi G, Cerrai T, Maggiore Q and Distante A (1996) Videorecording or direct computer acquisition for videodensitometric analysis of 2-D echo images: what agreement?.*Computers in Cardiology* ,705-708.

Morris D T (1988) An evaluation of the use of texture measurements for the tissue characterisation of ultrasonic images of in vivo human placentae. *Ultrasound Med Biol.* 14 (5) 387-395.

Muzzolini R E (1996) *A Volumetric Approach to Segmentation and Texture Characterisation of Ultrasound Images. PhD thesis.*

Nguyen B, Brandser E and Rubin D A (2000) Pains, strains, and fasciculations: lower extremity muscle disorders. *Magn Reson Imaging Clin N Am.* 8 (2) 391-408.

Nielsen P K, Jensen B R, Darvann T, Jorgensen K and Bakke M (2000) Quantitative ultrasound image analysis of the supraspinatus muscle. *Clin Biomech (Bristol, Avon).* 15 (Suppl 1) S13-16.

Nielsen P K, Jensen B R, Darvann T, Jorgensen K and Bakke M (2006) Quantitative ultrasound tissue characterization in shoulder and thigh muscles--a new approach. *BMC Musculoskelet Disord.* 7 2.

Nicoll R G, Wood A K and Rothwell T L (1992) Ultrasonographical and pathological studies of equine superficial digital flexor tendons; initial observations, including tissue characterisation by analysis of image grey scale, in a thoroughbred gelding. *Equine Vet J.* 24 (4) 318-320.

Nicholas D, Nassiri D K, Garbutt P and Hill C R (1986) Tissue characterization from ultrasound B-scan data. *Ultrasound Med Biol.* 12 (2) 135-143.

Orchard J (2002) Biomechanics of muscle strain injury. *J Sports Med.* 30(4)92–98.

Orchard J W (2001) Intrinsic and extrinsic risk factors for muscle strains in Australian football. *Am J Sports Med.* 29 (3) 300-303.

Ojala T and Pietikäinen M (2004) Texture Classification. In *Machine Vision and Media Processing Unit, University of Oulu, Finland.*

Oosterveld B J, Thijssen J M, Hartman P C, Romijn R L and Rosenbusch G J (1991) Ultrasound attenuation and texture analysis of diffuse liver disease: methods and preliminary results. *Phys Med Biol.* 36 (8) 1039-1064.

Palmer W E, Kuong S J and Elmadbouh H M (1999) MR imaging of myotendinous strain. *AJR Am J Roentgenol.* 173 (3) 703-709.

Peetrons P (2002) Ultrasound of muscles. *Eur Radiol.* 12 (1) 35-43. Epub 2001 Oct 2019.

Pette D (2001) Historic Perspectives: Plasticity of mammalian skeletal muscle. *Journal of Applied Physiology* 90 (3) 1119-1124

Pillen S, Scholten R R, Zwarts M J and Verrips A (2003) Quantitative skeletal muscle ultrasonography in children with suspected neuromuscular disease. *Muscle Nerve.* 27 (6) 699-705.

Pillen S, van Dijk J P, Weijers G, Raijmann W, de Korte C L and Zwarts M J (2009) Quantitative gray-scale analysis in skeletal muscle ultrasound: a comparison study of two ultrasound devices. *Muscle Nerve.* 39 (6) 781-786.

Pillen S, Arts I M and Zwarts M J (2008) Muscle ultrasound in neuromuscular disorders. *Muscle Nerve.* 37 (6) 679-693.

Pillen S, van Keimpema M, Nievelstein R A, Verrips A, van Kruijsbergen-Raijmann W and Zwarts M J (2006) Skeletal muscle ultrasonography: Visual versus quantitative evaluation. *Ultrasound Med Biol.* 32 (9) 1315-1321.

Pierson R A and Adams G P (1995) Computer-assisted image analysis, diagnostic ultrasonography and ovulation induction: Strange bedfellows. *Theriogenology* 43 (1) 105-112.

Powell R W (1883) *Lawn tennis leg.* Lancet; 2,44.

Powis R and Powis W (1984) *A Thinker's Guide to Ultrasonic Imaging.* Urban and Schwartzenberg inc., Baltiomore , Maryland.

Pohle R, Rohden L v and Fisher D (1997) Skeletal muscle sonography with texture analysis. *In Proc Medical Imaging* (3034) 772-778.

Prager R W, Ijaz U Z, Gee A H and Treece G M (2010) Three-dimensional ultrasound imaging. *Proc Inst Mech Eng H.* 224 (2) 193-223.

Raeth U, Schlaps D, Limberg B, Zuna I, Lorenz A, van Kaick G, Lorenz W J and Kommerell B (1985) Diagnostic accuracy of computerized B-scan texture analysis and conventional ultrasonography in diffuse parenchymal and malignant liver disease. *J Clin Ultrasound.* 13 (2) 87-99.

Rankin R N, Fenster A, Downey D B, Munk P L, Levin M F and Vellet A D (1993) Three-dimensional sonographic reconstruction: techniques and diagnostic applications. *AJR Am J Roentgenol.* 161 (4) 695-702.

Reef V, Martin B and Elser A (1993) Types of tendon and ligament injuries detected with diagnostic ultrasound: description and follow-up. *Proc Am Assoc Equine Pract* 35, 245-248.

Reimers C D, Fleckenstein J L, Witt T N, Muller-Felber W and Pongratz D E (1993a) Muscular ultrasound in idiopathic inflammatory myopathies of adults. *J Neurol Sci.* 116 (1) 82-92.

Reimers K, Reimers C D, Wagner S, Paetzke I and Pongratz D E (1993b) Skeletal muscle sonography: a correlative study of echogenicity and morphology. *J Ultrasound Med.* 12 (2) 73-77.

Reimers C D, Schlotter B, Eicke B M and Witt T N (1996a) Calf enlargement in neuromuscular diseases: a quantitative ultrasound study in 350 patients and review of the literature. *J Neurol Sci.* 143 (1-2) 46-56.

Reimers C D, Ziemann U, Scheel A, Rieckmann P, Kunkel M and Kurth C (1996b) Fasciculations: clinical, electromyographic, and ultrasonographic assessment. *J Neurol.* 243 (8) 579-584.

Riley W A (1996) *Ultrasonic B-mode imaging systems.* New York: Neurosonology 1st edition.

Rothwell A G (1982) Quadriceps Hematoma. A prospective clinical study. *Clin Orthop Relat Res.* (171) 97-103.

Rose M (2004) When B Mode has an. Image Problem. *Advanced Applications and New Technology in Ultrasound, Visions 11.07,* 46-53.

Rosner B (2000) *Fundamentals of biostatistics* Pacific Grove, CA: Duxbury Press , 5th edition.

Romijn R L, Thijssen J M, Oosterveld B J and Verbeek A M (1991) Ultrasonic differentiation of intraocular melanomas: parameters and estimation methods. *Ultrason Imaging.* 13 (1) 27-55.

Rubin J M, Carson P L and Meyer C R (1988) Anisotropic ultrasonic backscatter from the renal cortex. *Ultrasound Med Biol.* 14 (6) 507-511.

Saglimbeni A J (2009) Medial Gastrocnemius Strain.*E-Medicine* (*http://emedicine.medscape.com/article/91687-overview*).

Schedel H, Reimers C D, Nagele M, Witt T N, Pongratz D E and Vogl T (1992) Imaging techniques in myotonic dystrophy. A comparative study of ultrasound, computed tomography and magnetic resonance imaging of skeletal muscles. *Eur J Radiol.* 15 (3) 230-238.

Schmidt R and Voit T (1993) Ultrasound measurement of quadriceps muscle in the first year of life. Normal values and application to spinal muscular atrophy. *Neuropediatrics.* 24 (1) 36-42.

Scholten R R, Pillen S, Verrips A and Zwarts M J (2003) Quantitative ultrasonography of skeletal muscles in children: normal values. *Muscle Nerve.* 27 (6) 693-698.

Sipila S and Suominen H (1996) Quantitative ultrasonography of muscle: detection of adaptations to training in elderly women. *Arch Phys Med Rehabil.* 77 (11) 1173-1178.

Sipila S and Suominen H (1991) Ultrasound imaging of the quadriceps muscle in elderly athletes and untrained men. *Muscle Nerve.* 14 (6) 527-533.

Shamir L, Wolkow C A and Goldberg I G (2009) Quantitative measurement of aging using image texture entropy. *Bioinformatics.* 25 (23) 3060-3063. Epub 2009 Oct 3066.

Shellock F, Mink J and Deutsch A (1994) MR imaging of muscle injuries. *Appl Radiol* (2) 11-16.

Shung K and Thieme G (1993) *Ultrasonic scattering in biological tissues.* CRC Press, Boca Raton.

Simaeys B, Philips W, Lemahieu I and Govaert P (2000) Quantitative analysis of the neonatal brain by ultrasound. *Comput Med Imaging Graph.* 24 (1) 11-18.

Singh J, Pierson R A and Adams G P (1997) Ultrasound image attributes of the bovine corpus luteum: structural and functional correlates. *J Reprod Fertil.* 109 (1) 35-44.

Smith R K, Jones R and Webbon P M (1994) The cross-sectional areas of normal equine digital flexor tendons determined ultrasonographically. *Equine Vet J.* 26 (6) 460-465.

Smith T O, Hunt N J and Wood S J (2006) The physiotherapy management of muscle haematomas. *Physical Therapy in Sport* 7 (4) 201-209.

Staron R S (1997) Human Skeletal Muscle fibre types: Delineation, development and distribution. *Canadian Journal of Applied Physiology* 22, 307-327.

Srinivasan G N and Shobha G (2008) Statistical Texture Analysis. In *Proceedings of World Academy of Science, Engineering and Technology.* 36, 1264 -1269.

Steinbach L, Fleckenstein J and Mink J (1997) MR imaging of muscle injuries. *Semin Musculoskelet Radiol* 1, 127-141.

Strzelecki M and Materka A (1997) Markov Random Fields as Models of Textured Biomedical Images. In *Proc. 20th National Conf. Circuit Theory and Electronic Networks.* Poland, 493-498

Szczypiński P, Kociołek M, Materka A and Strzelecki M (2001) Computer Program for Image Texture Analysis in PhD Students Laboratory. In *Proc. Int. Conf. Signals and Electronic Systems* ,Lodz, Poland. 255-261

Szczypinski P M, Strzelecki M and Materka A (2007) Mazda - a software for texture analysis. In *Information Technology Convergence, 2007. ISITC 2007. International Symposium on* (pp. 245-249).

Szczypinski P M, Strzelecki M, Materka A and Klepaczko A (2009) MaZda--A software package for image texture analysis. *Computer Methods and Programs in Biomedicine* 94 (1) 66-76.

Sun Y N, Horng M H, Lin X Z and Wang X Z (1996) Ultrasonic image analysis for liver diagnosis. A noninvasive alternative to determine liver disease. *IEEE Engineering in Medicine and Biology* 6, 93 - 101.

Temple H T, Kuklo T R, Sweet D E, Gibbons C L and Murphey M D (1998) Rectus femoris muscle tear appearing as a pseudotumor. *Am J Sports Med.* 26 (4) 544-548.

Thayer R, Collins J, Noble E G and Taylor A W (2000) A decade of aerobic endurance training: histological evidence for fibre type transformation. *J Sports Med Phys Fitness.* 40 (4) 284-289.

Van Schie H T, Bakker E M, Jonker A M and van Weeren P R (2001) Efficacy of computerized discrimination between structure-related and non-structure-related echoes in ultrasonographic images for the quantitative evaluation of the structural integrity of superficial digital flexor tendons in horses. *Am J Vet Res.* 62 (7) 1159-1166.

Varela J R, Rodriguez E, Soler R, Gonzalez J and Pombo S (2000) Complete rupture of the distal semimembranosus tendon with secondary hamstring muscles atrophy: MR findings in two cases. *Skeletal Radiol.* 29 (6) 362-364.

Verhoef W A, Cloostermans M J T M and Thijssen J M (1985) Diffraction and Dispersion Effects on the Estimation of Ultrasound Attenuation and Velocity in

Biological Tissues. *Biomedical Engineering, IEEE Transactions on* BME-32 (7) 521-529.

Vrbova G, Navarrete R and Lowrie M (1985) Matching of muscle properties and motoneurone firing patterns during early stages of development. *J Exp Biol.* 115, 113-123.

Walker F O (1996) *Normal neuromuscular sonography*. New York: Neurosonology, 1st edition.

Walker F O (1998) *Muscle ultrasound: an AAEM workshop*. Rochester, MN: American Association of Electrodiagnostic Medicine.

Walker F O, Cartwright M S, Wiesler E R and Caress J (2004) Ultrasound of nerve and muscle. *Clin Neurophysiol.* 115 (3) 495-507.

Walker F O and Jackson G H (1997) Shoot first, draw later peroneal nerve palsy: a sonographic study. *J Neuroimaging.* 7 (1) 54-55.

Walmsley B, Hodgson J A and Burke R E (1978) Forces produced by medial gastrocnemius and soleus muscles during locomotion in freely moving cats. *J Neurophysiol.* 41 (5) 1203-1216.

Wong L S (2005) Imaging of muscle injuries
J Hong Kong Coll Radio 8 (4) 191-201.

Won H J, Han J K, Do K H, Lee K H, Kim K W, Kim S H, Yoon C J, Kim Y J, Park C M and Choi B I (2003) Value of four-dimensional ultrasonography in ultrasonographically guided biopsy of hepatic masses. *J Ultrasound Med.* 22 (2) 215-220.

Wun Y T and Chung R (1998) Ultrasound characterization by stable statistical patterns. *Comput Methods Programs Biomed.* 55 (2) 117-126.

Yilmaz C, Orgenc Y, Ergenc R and Erkan N (2008) Rupture of the medial gastrocnemius muscle during namàz praying: an unusual cause of tennis leg. *Comput Med Imaging Graph.* 32 (8) 728-731.

Youssef A M and Sharawi A A (1990) KSODATA clustering analysis for diffuse liver diseases. In *Proc. IEEE Symp. Ultrasound*.

Zagzebski J A (1996) *Essentials of Ultrasound Physics*. St. Louise: Mosby Inc.

Zuberi S M, Matta N, Nawaz S, Stephenson J B, McWilliam R C and Hollman A (1999) Muscle ultrasound in the assessment of suspected neuromuscular disease in childhood. *Neuromuscul Disord.* 9 (4) 203-207.

Internet websites

www.biologycorner.com/anatomy/muscles/notes_muscles.html (access 04/2010)

www.nucleusinc.com(access 03/2007)

www.tomahawknation.com/2009/3/29/813817/in-the-treatment-room-a-di (access 03/2010)

APPENDIX A

Figure A 1 Coefficient of variation (CV %) of the first order statistic parameters for all sizes of ROI for group 2.

Figure A 2 Coefficient of variation (CV %) of the second order statistic parameters AR model and wavelet transforms for all sizes of ROI for group 2 (cut off point represent the minimum size of ROI to be used)
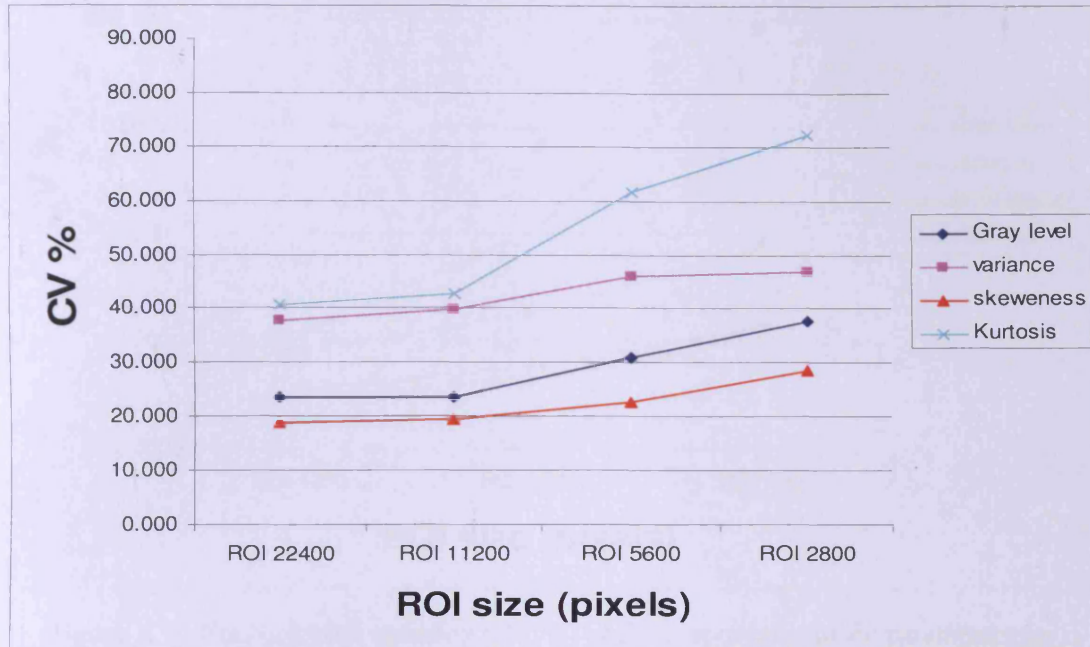
192

Figure A 3 Coefficient of variation (CV %) of the first order statistic parameters for all sizes of ROI for group 2
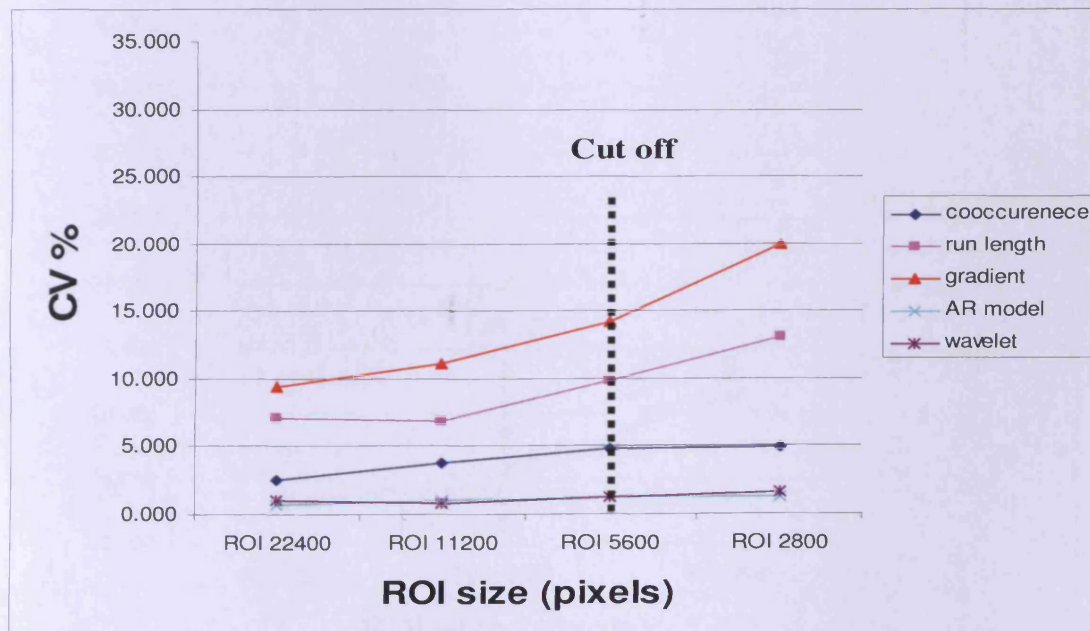

Figure A 4 Coefficient of variation (CV %) of the second order statistic parameters AR model and wavelet transforms for all sizes of ROI for group 2 (cut off point represent the minimum size of ROI to be used)
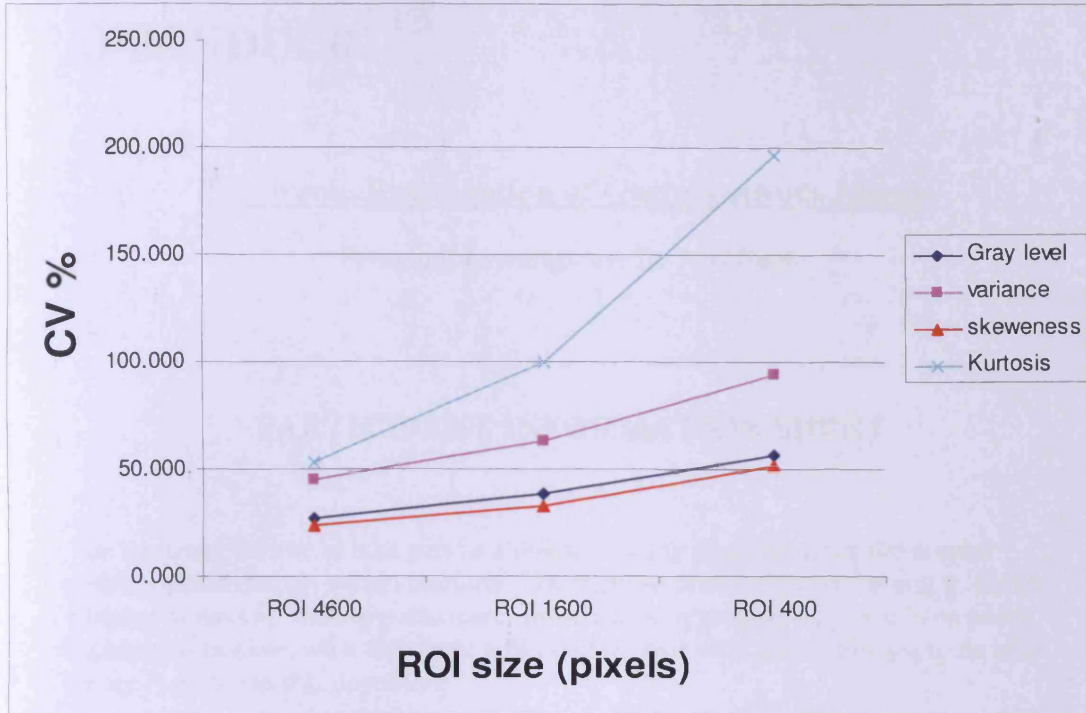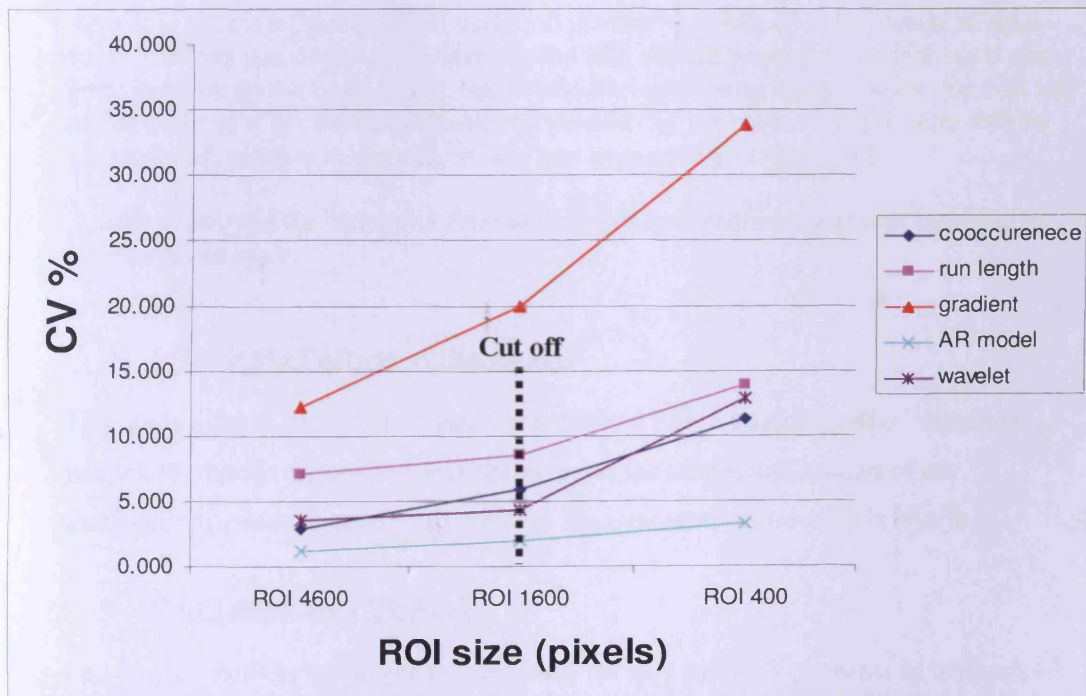
APPENDIX B

Ultrasonic Examination of Gastrocnemius Muscle

Principal Investigator: Dr Neil Pugh

PARTICIPANT INFORMATION SHEET

You are being invited to take part in a research study characterizing the normal gastrocnemius muscle within humans. The purpose of this form is for you to decide whether or not you wish to participate. Information regarding why you have been asked to participate, what the study will involve, and what the results are to be used for are included in this document.

It is important that you take time to read the following information and consider your decision carefully as to whether to participate – perhaps discuss it with friends or family if you think a second opinion would be useful.

Also, it is important that you feel under no pressure or obligation to partake in this study – indeed you do not even have to read this should you not wish. If there is any point that you do not understand, you would like more information on, or you feel has not be covered at all, then please ask any member of the research team, who will be glad to be of assistance. We will answer any questions you may have.

Finally, thank you for taking the time to read this information sheet and in taking an interest in our work.

- **What is the Purpose of this Study?**

This study aims to develop and validate a method based on quantitative ultrasound images, to objectively analyze and characterize the ultrasound images of the gastrocnemius muscle in order to improve the treatment of the muscle injuries.

- **Why have I been Chosen?**

As you are a healthy volunteer you are ideal for this study.. Volunteers of between 18-40 years of age are being asked to volunteer, as muscle injuries are common in this population.

- ## **Do I have to Take Part?**

No, you are under absolutely no obligation to take part. It is also important that you understand that if you do decide that you wish to take part, and then for whatever reason you decide that you do not want to take part – you can withdraw. You can do this at any time and you do not have to give any reason.

It is also important to understand that your current or future medical care will in no way be effected by your decision of whether to partake or not. Should you withdraw part-way through, again this will not in any way effect present or future medical care provided to you.

Once you have read this form, you will be asked to keep this and retire to consider your decision. Should you choose to participate, you will then be asked to sign a consent form. Once this form has been signed you are still completely free to withdraw without giving a reason.

- ## **What will happen to me if I Take Part?**

You will be asked to attend the Medical Physics department at the University Hospital Wales for approximately 1 hour. At this session, we will scan the gastrocnimus muscle within your body using ultrasound machine. An ultrasound scan is what expectant mothers have when the black & white images of their unborn child are produced – it is a painless, harmless method of seeing inside your body.

You will be asked to wear shorts, so making it more convenient to expose the relevant area of skin, as direct contact between the measuring equipment and your skin is required.

A gel will be applied to your skin to improve the contact between the equipment and your skin, though this is very easy to wipe off with some tissues afterwards.

Also present in the room may be Professor Len Nokes who will be overseeing the imaging, and
Dr Neil Pugh, Dr Declan Coleman and Mr Mahdi AlQahtani who will be studying and recording the images obtained.

- ## **Are there any Side-Effects?**

Ultrasound has no side-effects. In fact it is so safe that it used to scan the unborn children of expectant mothers.

- ## **What will Happen to the Results of the Research Study?**

The results that we obtain from your visit to the hospital will be in the form of ultrasound images. These images will be analysed, and should we find a trend in all the results collected, these results will be published in an international journal. This will allow the wider academic community access to these findings. Should you wish

to know the results of our findings, contact Professor Nokes using the contact details at the end of this form.

- **<u>Will my Taking Part in this Study be kept Confidential?</u>**

Yes, your participation in this study will be kept confidential, and you will not be identified by name in any results or images that we publish – you will be identified instead by your age and gender.

- **<u>Who is Organising and Funding the Research?</u>**

Members of the research team are drawn from the Medical Physics and Clinical Engineering Directorate at the University Hospital Wales (Dr Pugh ,Dr Coleman), and the Schools of Engineering (Professor Nokes, Mr.Alqahtani) at Cardiff University. Funding for the project is not required, as all staff involved are able to spend time researching as part of their contract.

- **<u>Who has Reviewed the Study?</u>**

To safeguard the welfare of volunteers, any study that requires voluntary participation has to be approved by the Local Research Ethics Committee. This study has been reviewed and its conduct approved.

- **<u>Contact Details and Further Information</u>**

If you want any further information please do not hesitate in contacting:

Dr Neil Pugh, Principal Investigator : <u>Neil.Pugh@Cardiffandvale.wales.nhs.uk</u>

Professor Len Nokes, Academic Supervisor : <u>Nokes@Cardiff.ac.uk</u>

Date : ....

Sex : ....

Age : ....

Q1: Do you have any pain in the lower leg?

---- Yes	----- No

Q2: Do you or have you had any injury to your calf muscle? if yes when?

---- Yes	----- No

Q3: Do you have any muscular weakness, spasticity/rigidity or loss of muscular control?

---- Yes	----- No

Q4: Do you do any sport activities?

---- Yes	----- No

If yes which type of sport? And how frequently?

....

Q5: Do you do any exercise to increase the calf muscle strength?

---- Yes	----- No

Q6: Have you had any operation surgery to the lower leg?

---- Yes	----- No

Ultrasonic Examination of gastrocnemius muscle

Principal Investigator: Dr Neil Pugh

CONSENT FORM

Participants Name: _____.

Please read the statements below and, if you agree to them, please tick the appropriate box. On completion, please sign the form to state your consent.

If there are any statements that you do not understand or require clarification on, then please ask one of the research team who will be more than happy to assist.

If you disagree with any of these statements, then feel free not to complete this form and opt out of the study.

1. I confirm that I have read and understand the information sheet entitled Ultrasonic Examination of gastrocnemius muscle, that I have had the opportunity to ask questions and I accept the answers received.

2. I understand that my participation is entirely voluntary and that I am free to withdraw at any time without giving any reason, and that neither my right to present or future medical care will be affected, nor my legal rights.

3. I agree to take part in the above study.

_____   _____   _____
Name of Subject   Date   Signature

_____   _____   _____
Name of Researcher   Date   Signature